

**Characterization of mAb charge heterogeneity by CE-based  
methods coupled to mass spectrometry**

**Dissertation**

in Partial Fulfilment of the Requirements for the Degree of

**“doctor rerum naturalium“ (Dr. rer. nat.)**

**Submitted to the Council of the Faculty of Biological Sciences  
of Friedrich Schiller University Jena**

**by Johannes Schlecht, M.Sc.**

**born on 24.09.1988 in Filderstadt**

**Reviewers:**

- 1) Prof. Dr. Gerhard K. E. Scriba  
Friedrich-Schiller-University Jena  
Institute of Pharmacy  
Department of Pharmaceutical and Medicinal Chemistry  
Philosophenweg 14  
07743 Jena
  
- 2) Prof. Dr. Christian Neusüß  
Aalen University  
Department of Chemistry  
Beethovenstraße 1  
73430 Aalen
  
- 3) Prof. Dr. Michael Lämmerhofer  
Eberhard-Karls-University Tuebingen  
Institute of Pharmaceutical Sciences  
Pharmaceutical (Bio-)Analysis  
Auf der Morgenstelle 8 (Haus B)  
72076 Tübingen

Date of public defense: 06.09.2023

## Acknowledgments

### **Acknowledgments**

First, I would like to express my deepest appreciation to Prof. Dr. Christian Neusüß for the opportunity to work on this topic. Thanks for the countless good discussions, ideas and especially the supervision throughout the years with patience and kindness.

Many thanks to Prof. Dr. Gerhard K. E. Scriba for the support throughout this thesis and the acceptance as a doctoral student.

I am also very thankful to Dr. Bernd Moritz und Dr. Steffen Kiessig for the long and fruitful collaboration, the good discussions and the support during this thesis. I would like to extend my sincere thanks to F. Hoffmann-La Roche Ltd. for funding this project.

My special thanks to all my colleagues and lab members at Aalen University. I remember with great pleasure the good discussions and the collaboration in the lab. Thanks to Kevin, Oli, Jenni, Alex and Lukas for the great time and the activities outside the lab.

Finally, I would like to thank everyone who contributed in any way to the creation of this work, as well as the continued support of my family and friends.

## Abbreviations

AD	Acrylamide derivative
AES	Advanced Electrophoresis Solutions Ltd.
Arg	Arginine
Asn	Asparagine
Asp	Aspartate
BGE	Background electrolyte
CA	Carrier ampholytes
CE	Capillary electrophoresis
CEX	Cation exchange chromatography
CGE	Capillary gel electrophoresis
CHO	Chinese hamster ovary
CIEF	Capillary isoelectric focusing
CMOS	Complementary metal oxide semiconductor
CZE	Capillary zone electrophoresis
DNA	Desoxyribonucleic acid
EACA	$\epsilon$ -aminocaproic acid
EMA	European medicine agency
EOF	Electroosmotic flow
ESI	Electrospray ionization
FA	Formic acid
Fab	Fragment antigen-binding
Fc	Fragment crystallizable
FC	Fluorocarbon
FDA	Food and Drug Administration
FEP	Fluorinated ethylene propylene
FS	Fused silica
H <sub>3</sub> PO <sub>4</sub>	Phosphoric acid
HAc	Acetic acid
HC	Heavy chain
HCl	Hydrochloric acid
HDX	Hydrogen deuterium exchange

## Abbreviations

HIC	Hydrophobic interaction chromatography
HILIC	Hydrophilic interaction chromatography
HPC	Hydroxypropyl cellulose
HPMC	Hydroxypropyl methylcellulose
HV	High voltage
iCIEF	Imaged capillary isoelectric focusing
ID	Inner diameter
IDA	Iminodiacetic acid
IEC	Ion exchange chromatography
IEF	Isoelectric focusing
IPA	2-propanol
LC	Light chain
LIF	Laser-induced fluorescence
Lys	Lysine
mAb	Monoclonal antibody
MeOH	Methanol
Met	Methionine
MS	Mass spectrometry
NaOH	Sodium hydroxide
OD	Outer diameter
PA	Polyacrylamide
PEEK	Polyether ether ketone
PTM	Posttranslational modification
RPLC	Reversed-phase liquid chromatography
SEC	Size exclusion chromatography
SL	Sheath liquid
TCEP	Tris(2-carboxyethyl)phosphine
TDLFP	Transverse diffusion of laminar flow profiles
TETA	Triethylenetetramine
UI	User interface
UV	Ultraviolet
VI	Virtual instrument
WCID	Whole column imaging detection

## Table of Content

1 Introduction .....	5
1.1 Therapeutic proteins and monoclonal antibodies .....	5
1.1.1 MAb heterogeneity and PTMs .....	6
1.1.2 Characterization of mAb heterogeneity .....	7
1.2 Capillary electrophoresis .....	8
1.3 Capillary isoelectric focusing .....	10
1.4 Charge heterogeneity analysis of proteins by CZE and CIEF .....	12
1.5 CE-MS of proteins and mAbs .....	13
1.5.1 Mass spectrometry interfacing .....	14
1.6 Two-dimensional capillary electrophoresis-mass spectrometry (CE-CE-MS) .	15
1.7 Objectives of the work .....	17
2 Overview manuscripts .....	19
2.1 Manuscript I .....	21
2.2 Manuscript II .....	28
2.3 Manuscript III .....	38
2.3 Manuscript IV .....	46
3 Discussion .....	55
3.1 nanoCEasy CE-MS interface .....	55
3.2 iCIEF-MS coupling .....	61
3.3 Two-dimensional capillary electrophoresis-mass spectrometry .....	68
4 Summary .....	76
5 Zusammenfassung .....	79
6 References .....	82
7 Ehrenwörtliche Erklärung .....	90
9 Supplementary information .....	XCI

## Table of Content

9.1 Supplementary information manuscript I.....	XCI
9.2 Supplementary information manuscript II.....	XCVIII
9.3 Supplementary Information manuscript IV .....	XCIX
9.4 Documentation of contribution .....	CXI
9.5 List of publications and presentations .....	CXV

# 1 Introduction

## 1.1 Therapeutic proteins and monoclonal antibodies

Protein-based therapeutics are an essential part of treatment options in current medicine. The first therapeutic protein administered was insulin in 1922, purified from animal pancreas.[1] Decades later, the development of recombinant DNA technology in 1979 enabled the manufacturing of protein pharmaceuticals on a larger scale, starting with insulin derived from *E.coli*. [2] The first monoclonal antibody approved by the United States Food and Drug Administration (FDA) in 1986 was Orthoclone OKT3 (Muronomab CD3) based on the murine hybridoma technology from Köhler and Milstein.[3, 4] Since then, more than 100 mAbs were approved by the FDA and the European Medicines Agency (EMA) until 2022, representing a broad spectrum of therapeutic applications including cancer, immune-mediated disorders, infectious diseases, cardiovascular/hemostasis disorders, neurological disorders, genetic diseases, ophthalmic disorders, and musculoskeletal disorders.[5, 6]

Antibodies are large proteins with a molecular weight typically around 150 kDa. The most common mAb is immunoglobulin G (IgG) composed of two heavy (2x HC with 50 kDa) and two light chains (2x LC with 25 kDa) (Figure 1).

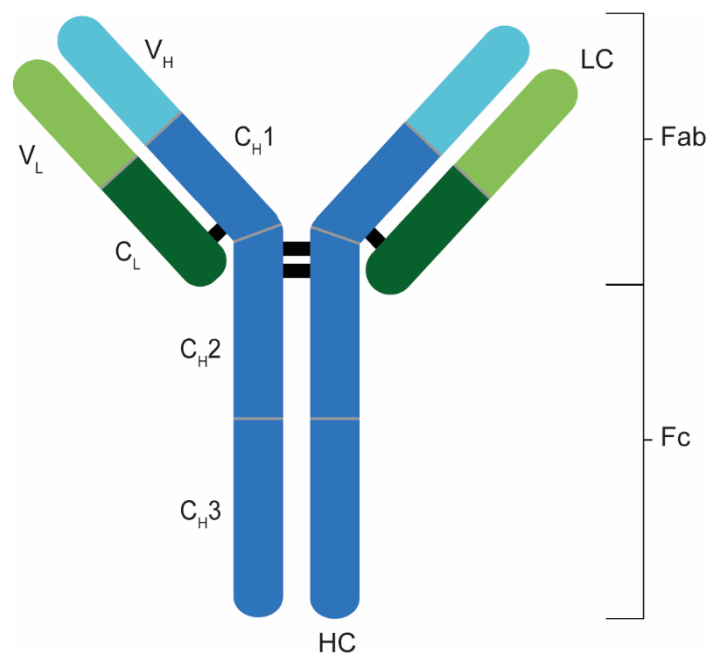


**Figure 1.** Scheme of an IgG structure. Two heavy chains (HC) and two light chains (LC) are connected via disulfide bonds. Both chains comprise variable (V<sub>x</sub>) and constant (C<sub>x</sub>) domains.



## Introduction

Both chains comprise variable ( $V_L$  and  $V_H$ ) and constant domains ( $C_L$ ,  $C_{H1-3}$ ), and are linked via 16 intra- and intermolecular disulfide bonds. A key attribute of mAbs is their high affinity toward target antigens determined by the complementary-determining region (CDR) in the variable domains  $V_L$  and  $V_H$  which are part of the fragment antigen binding (Fab). Another important attribute is the ability to recruit other immune cells to support the killing of the target cells. The latter is mediated by the C-terminal area of the heavy chain, the fragment crystallizable (Fc) part. The characteristic of high specificity makes mAbs exceptionally efficient for the treatment of autoimmune or cancer diseases.

Of the four existing subclasses of IgG (IgG1-4), the subclass IgG1 is frequently selected for the production of therapeutic mAbs using mammalian cells such as Chinese hamster ovary (CHO) cells. MAb produced by CHO cells contain glycosylation as a common posttranslational modification (PTM) at Asp 297 in each of the heavy chains. Glycosylation plays also an important role for the stability and the prevention of aggregation.[7] Combinations of multiple possible sugars form different glycoforms affecting among others the immune response by binding to Fcγ receptors.[8, 9]

Therapeutic mAbs undergo several processing steps during production, purification, and concentration leading to potential heterogeneities. These include filtration, protein A affinity chromatography, cation exchange chromatography, and anion exchange chromatography for the removal of impurities derived from the host cell, such as proteins, aggregates, DNA, or endotoxins.[10]

The characterization of occurring mAb variants is essential for the quality control and release testing of protein pharmaceuticals. Therefore, an important field of analytical research and development regarding product quality, safety, and stability has been implemented.

### 1.1.1 MAb heterogeneity and PTMs

Heterogeneity in therapeutic mAbs can occur from PTMs and physicochemical transformations either during manufacturing and subsequent processing or during storage. As the heterogeneity of a product defines the quality, it is an important surveillance parameter assuring lot-to-lot consistency.[11] The International

## Introduction

Conference on Harmonization (ICH) Q6B differentiates here between “product-related substances” and “product-related impurities”. The first mentioned “product-related substances” comprise variants with comparable activity, efficacy, and safety as the desired product but have nevertheless to be characterized thoroughly. The latter mentioned “product-related impurities” comprise precursors or degradation products not having comparable properties to the desired activity, efficacy, and safety.[11] Such undesired modifications can result in changes of mass, charge, or hydrophobicity which could have an impact on the safety of patients. Relevant examples include N-terminal modifications such as pyroGlu formation (mass and charge), Asn deamidation (mass and charge), Asp isomerization (charge and hydrophobicity), succinimide formation (mass, charge, and hydrophobicity), Met oxidation (mass and hydrophobicity), glycosylation (mass and charge) and C-terminal Lys clipping (mass, charge, and hydrophobicity).[12–14]

### **1.1.2 Characterization of mAb heterogeneity**

Several chromatographic techniques are established in the quality control for extended characterization of mAb heterogeneity.[15] These include reversed-phase liquid chromatography (RPLC) [16], size exclusion chromatography (SEC) [17], hydrophobic and hydrophilic interaction chromatography (HIC and HILIC) [18, 19], and ion exchange chromatography (IEC) [20]. Electrophoretic separation techniques are also an indispensable part of process development, quality control, and release testing of biopharmaceuticals.[21–26] These methods include capillary zone electrophoresis (CZE) and capillary isoelectric focusing (CIEF or imaged (i)CIEF) for charge heterogeneity analysis [27–29] as well as capillary gel electrophoresis (CGE) for the determination of size heterogeneity and size impurities.[30, 31]

Characterization of charge heterogeneity is an essential part of pharmaceutical development and quality control of therapeutic monoclonal antibodies (mAbs). The precise localization and identification via mass spectrometry (MS) of these modifications is an important aspect of biopharmaceutical quality control and the goal of various analytical techniques. One of the most common types of mAb heterogeneity is deamidation, usually linked with non-enzymatic irreversible degradation forming Asp or isoAsp via a succinimide intermediate [32–34] having a potential impact on the safety and efficacy of mAbs, as well as reduced potency.[12, 35] Deamidation

## Introduction

increases the molecular mass by only +0.984 Da making it challenging for mass spectrometric detection, especially on the intact protein level. At the same time, deamidation can be artificially induced by sample preparation steps, especially when elevated pH is involved. The characterization of mAb charge heterogeneity, in particular of deamidation, is therefore of high interest for the biopharmaceutical development and quality control units. IEC, CZE, and (i)CIEF are the analytical techniques of choice for this purpose and are frequently applied in the biopharmaceutical sector.

### 1.2 Capillary electrophoresis

Electrophoresis is the differential movement of ions by attraction or repulsion in an electric field and was introduced by Tiselius in 1937 for the separation of proteins in free solution.[36] However, the separation efficiency was limited due to high Joule heating and diffusion in free solutions. Jorgensen and Lukacs improved the technique during the 1980s and were the first to perform capillary electrophoresis (CE) in 75  $\mu\text{m}$  (ID) fused silica (FS) capillaries.[37] This approach led to much less generated heat and better separation efficiency. Today, CE is usually performed with 30–50  $\mu\text{m}$  ID capillaries or on microfluidic (glass) chips.[38] A basic CE system is shown in Figure 2.

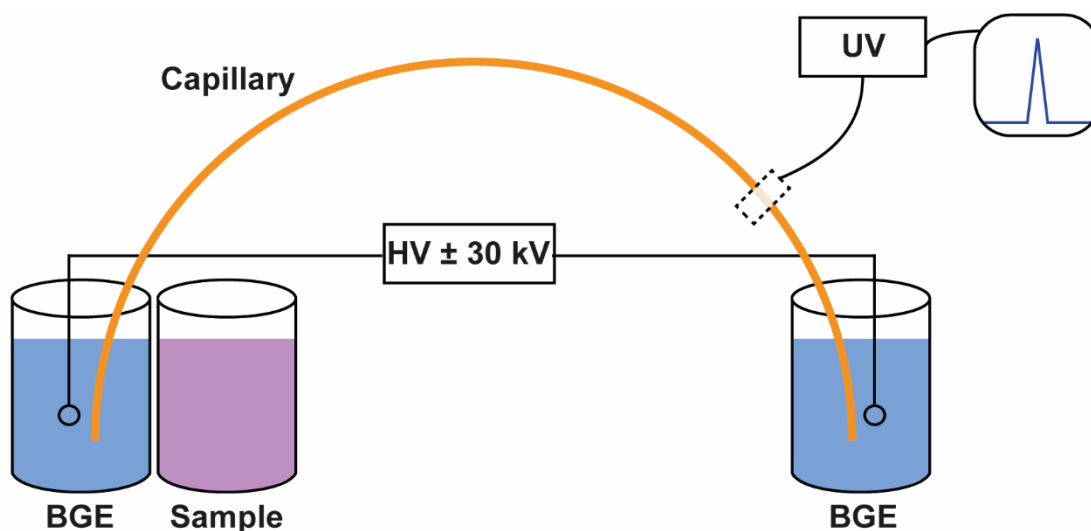


**Figure 2.** Basic scheme of a CE system with UV detection. The capillary is immersed in two vessels containing BGE. The capillary is filled with BGE. The sample is injected from the sample vial using pressure or voltage. Upon applying voltage, the sample migrates toward the detector.

## Introduction

Both ends of a fused silica capillary are immersed into two buffer reservoirs each containing conductive liquid (background electrolyte, BGE). Additionally, two electrodes are immersed in the BGE reservoirs and connected to a high voltage (HV) power supply capable to apply voltages up to  $\pm 30$  kV. Sample injection is performed by exchanging one of the buffer reservoirs with a sample vial and either by applying pressure or vacuum at one of the buffer reservoirs (hydrodynamic injection), by applying voltage (electrokinetic injection), or by elevating or lowering one of the reservoirs (siphoning injection). Electrokinetic injection is preferred when using viscous BGE systems. The amount of sample injected depends here strongly on the ion strength of the sample. Pressure-assisted injections are usually applied in non-viscous, aqueous systems. Detection can be done optically (absorbance of ultraviolet radiation, UV; laser-induced fluorescence, LIF) or by MS. The inner surface of FS capillaries comprise silanol groups. These silanol groups are deprotonated at a pH  $> \sim 4$  leading to a negative charge of the inner wall. Cations from the BGE can form then a fixed layer ("Stern layer"). When more cations start to attach to the wall, a second mobile layer is created. This second diffuse layer will start to move towards the cathode if high voltage is applied, creating an electroosmotic flow (EOF). The EOF has a stamp-like flow profile, unlike the laminar flow profile known from pressure-driven systems (e.g HPLC), and can be controlled or suppressed by adjusting the pH, ionic strength, or modifications to the surface (coatings).

CZE is the most commonly used separation mode in today's CE applications. In CZE, analytes migrate according to their respective charge and hydrodynamic radius in an electric field. The analyte migration velocity is determined by the electrophoretic mobility and the electric field strength (equation 1.1):

$$v = \mu_e \cdot E \quad (1.1)$$

$v$ : ion velocity

$\mu_e$ : electrophoretic mobility

$E$ : electric field strength

The electric field strength is a result of the applied voltage (V) and the capillary total

## Introduction

length (L), given in V/cm. The electrophoretic mobility depends on the ion charge, viscosity of the surrounding medium, and lastly on the ion's hydrodynamic radius (equation 1.2):

$$\mu_e = \frac{q}{6 \cdot \pi \cdot \eta \cdot r} \quad (1.2)$$

$q$ : ion charge

$\eta$ : viscosity of the surrounding medium

$r$ : hydrodynamic ion radius

The number of charges on analytes can be controlled by adapting the pH of the BGE. This is of particular interest, especially for charge heterogeneity analysis of proteins.

### 1.3 Capillary isoelectric focusing

Another frequently used CE technique for the determination of charge heterogeneity is capillary isoelectric focusing (CIEF). CIEF was introduced in 1985 and is based on a pH gradient formed by carrier ampholytes (CA) after applying an electric field.[39] CA are a complex mixture of many different zwitterionic molecules [40] and are injected together with the sample (proteins or peptides) in a capillary with one end immersed in an acidic, usually low pH solution (anolyte; e.g. H<sub>3</sub>PO<sub>4</sub> at pH 1) and the other end immersed in a basic, usually high pH solution (catholyte; e.g. NaOH at pH 14). Upon applying an electric field, the ampholytes form a pH gradient and proteins or peptides are focused according to their isoelectric point (pI). In CIEF, the focused analytes are usually detected via UV at 280 nm in the capillary window due to the high background absorption of ampholytes in the lower UV range. Anodic spacers such as iminodiacetic acid (IDA; pI 2.2) and cathodic spacers such as arginine (Arg, pI 10.7) are often applied to block the respective capillary length in front of the capillary window. After the focusing process has finished, a mobilization step is required. This can be done either pressure-mediated or by chemical mobilization.[41] For pressure-assisted mobilization, low pressure (< 20-30 mbar) is applied to the CE inlet side while high voltage is still being kept on and the focused zone is forced to move through the detection window. However, due to the applied pressure a laminar flow is induced leading to zone broadening (peak broadening) and potential loss of peak resolution.

## Introduction

During chemical mobilization, the outlet vial (usually catholyte) is exchanged for a chemical mobilizer, e.g. acidic acid (pH 4). The high voltage is kept on and the focused zone is mobilized toward the detector.

Chemical mobilization is often preferred over pressure-assisted mobilization due to less zone broadening. Prevention of protein adsorption to the capillary wall, protein aggregation, and precipitation is of special interest in CIEF methods, as the proteins are forced to their  $pI$  associated with low solubility. For this reason, often urea or equivalent substances are added to maintain protein solubility and in addition, effective neutral capillary coatings are applied to suppress a potential, undesired EOF.

The closely related technique imaged (i)CIEF was introduced in the 1990s, using whole column imaging detection (WCID) instead of the classical one-point detection [42, 43]. Nowadays, iCIEF is performed with specifically designed iCIEF cartridges and dedicated iCIEF instruments [44, 45]. Figure 3 shows the basic scheme of an iCIEF cartridge.

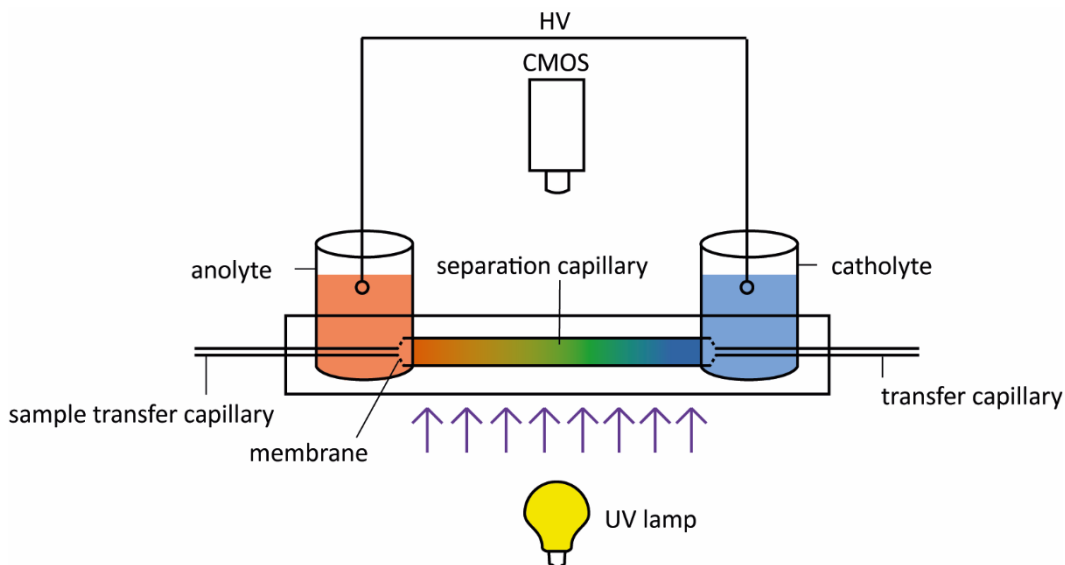


**Figure 3.** Basic scheme of an iCIEF cartridge. The sample mixture containing mAb and ampholytes is introduced from the autosampler via the sample transfer capillary. Focusing voltage is applied via electrodes immersed in anolyte and catholyte. UV detection occurs over the whole separation capillary (imaged). After the focusing process has finished, the focused zones can be mobilized by pressure via a syringe pump and the sample transfer capillary toward the transfer capillary while keeping constant voltage. Fraction collection or ESI-MS can be connected to the transfer capillary.

iCIEF cartridges comprise a separation capillary with a length of 50 mm between two vessels filled with anolyte and catholyte, respectively. The whole separation capillary is imaged by a CMOS camera at 280 nm. As the proteins are focused in the separation

## Introduction

capillary between the two vessels, no spacers are required in contrast to conventional CIEF. In addition, no mobilization is required and the whole focusing process can be monitored online and in real-time. Therefore, less time per analysis is needed and adverse mobilization effects (e.g. zone broadening) are avoided.

Depending on the manufacturer, different cartridges, cartridge coatings, and instrument configurations are available. In this work, an iCIEF instrument from Advanced Electrophoresis Solutions Ltd. (AES) was used providing the possibility for fraction collection or direct transfer of focused samples towards MS. iCIEF cartridges are available with IDs ranging from 100 to 320  $\mu\text{m}$  and different coatings preventing protein adsorption to the capillary wall (fluorocarbon (FC), polyacrylamide derivative (PA), and acrylamide derivative (AD) (<https://ceinfinite.com/product/shop-cartridges/>).

### **1.4 Charge heterogeneity analysis of proteins by CZE and CIEF**

A well-suited and frequently used method for fast charge heterogeneity analysis by CZE was introduced in 2011 using an  $\epsilon$ -amino-caproic acid (EACA) based BGE with a pH of 5.7.[47] At pH 5.7, proteins are present in a zwitterionic state due to deprotonated, negatively charged carboxyl groups ( $pK_a \sim 4-4.5$ ) and protonated, positively charged primary amino groups ( $pK_a \sim 10$ ). The high concentration of around 400 mM EACA reduces interaction with the capillary wall to prevent the adsorption of positively charged proteins with the negatively charged silanol groups of the capillary wall. In addition, 2 mM triethylenetetramine (TETA) and 0.05 % hydroxypropyl methylcellulose (HPMC) serve as dynamic coating and for electroosmotic flow (EOF) suppression. The charge-based separated proteins and mAbs are detected via UV at 214 nm. This particular method for charge heterogeneity testing is routinely applied in the development and quality control of biopharmaceuticals.[27] Figures 4A and B show the well-known and for a long time used mAb trastuzumab analyzed with two different charge-based CE techniques: (i) charge heterogeneity assay based on CZE with an EACA-based BGE (Figure 4A) (ii) the imaged UV profile after isoelectric focusing (Figure 4B).

## Introduction

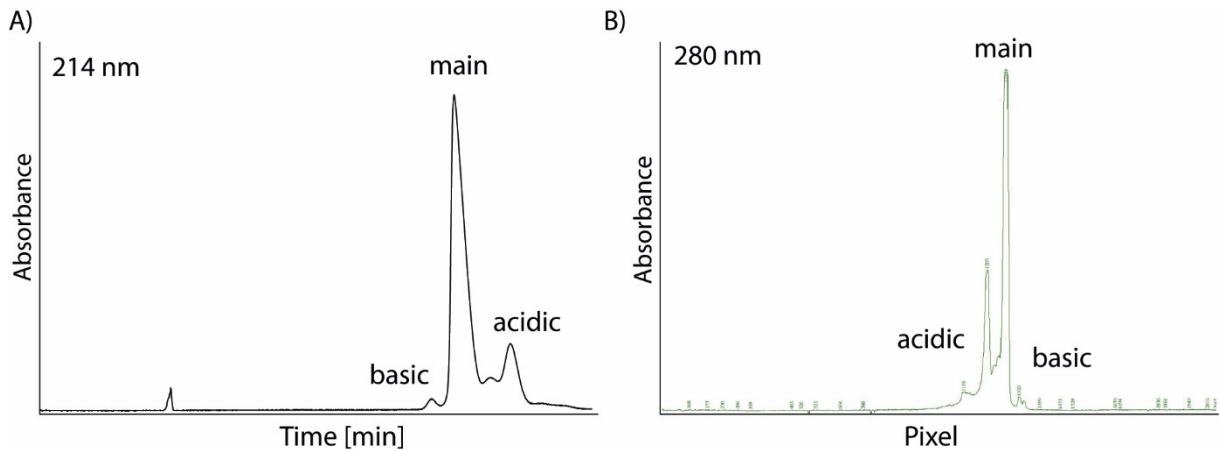


**Figure 4.** Comparison of Trastuzumab analyzed with CZE (EACA) and iCIEF **A)** CZE(EACA) of Trastuzumab (1 mg/mL). BGE: 400 mM EACA, 2 mM TETA, 0.05% HPC, pH 5.7) UV detection at 214 nm **B)** iCIEF-UV image of Trastuzumab (1 mg/mL), 1.5 % Pharmalyte 8-10.5 and 0.5% Pharmalyte 3-10.

Both techniques provide charge heterogeneity profiles and are utilized for the characterization and quality control of mAbs in the biopharmaceutical sector.[48] CZE is very fast (down to > 5 min/sample) providing a charge heterogeneity profile that is often used for the determination of the ratios of basic and acidic groups compared to the main variant. In contrast to CZE, CIEF provides the exact pI determination using pI markers and can provide greater charge variant separation resolution (small pI deviations < 0.01 detectable) but requires intensive method development and a longer time per sample. Though these two approaches provide great selectivity towards charge variants of mAbs, they are lacking any information about the occurring type of modification and their respective position in the protein sequence. Therefore, the identification of mAb charge variants and localization of (charge-related) PTMs based on MS is crucial for safety and efficacy. However, an EACA-based BGE, ampholytes and sample matrix applied in IEF interfere significantly with electrospray ionization (ESI) which is the most commonly applied ionization technique for proteins.

### 1.5 CE-MS of proteins and mAbs

Electrospray ionization-mass spectrometry (ESI-MS) is extensively used for the characterization of proteins and mAbs.[49] Electrospray ionization in positive mode is the state-of-the-art ionization technique for biomolecules such as proteins due to the availability of amino acid side chains that can be protonated. This results in multiply charged ions that are formed during the electrospray process enabling the detection of



## Introduction

proteins ranging from a few kDa up to a few hundred kDa, depending on the type of MS instrument. The analysis of intact and fragmented mAb species is here of special interest to identify and localize occurring PTMs within the protein sequence. The desire to reach sensitivity that allows the characterization of low-abundant protein species was one critical factor driving the development of more efficient CE-MS interfaces over the past two decades. Consequently, there is a high demand for sensitive CE-MS interfaces which can meet the requirements of the biopharmaceutical industry and other protein-related research fields.

### 1.5.1 Mass spectrometry interfacing

Several ways of CE-MS hyphenation exist, depending on the CE mode and the type of MS instrument. [50, 51] The two most frequently applied CE-MS interfaces are: (i) sheath flow interfaces, and (ii) sheathless interfaces. For a long time, the widely used co-axial sheath liquid interface (“triple tube sprayer”) was the state-of-the-art CE-MS interface providing simplicity, versatility, and robustness [52]. In this type of interface, a sheath flow of 2-10  $\mu\text{L}/\text{min}$  and a nebulizing gas are applied. The much higher sheath flow compared to the CE effluent (typically  $<100 \text{ nL}/\text{min}$ ) causes a significant dilution effect thereby reducing sensitivity. In addition, the applied nebulizing gas forms a “suction effect” at the capillary outlet creating a more parabolic-like flow profile that introduces additional zone broadening of the analytes.[53, 54]

Nanoflow sheath liquid interfaces and sheathless interfaces operate without a nebulizing gas flow and with a total ESI fluid consumption in the sub- $\mu\text{L}$  range (nanoESI). NanoESI is considered very efficient at ionization, reducing matrix effects, and increasing sensitivity.[55] The commercial introduction of a sheathless interface in 2007 (“CESI”)[56] and two nano sheath flow interfaces in 2010 (“EMASS-II” and a “flow-through microvial interface”)[57, 58] enabled access to nanoESI for a broad group of CE-MS users. Each commercially available interface has its characteristics and price, whereby the CESI interface being the most expensive. The gain of sensitivity depending on the type of interface and analyte has been demonstrated by Höcker et al.[59] However, occasional emitter clogging and bubble formation interfere with the measurement process. In addition, the usage and handling of these interfaces require considerable expertise. [60, 61] One approach to improve some of these issues with current nanoflow sheath liquid interfaces was shown by utilizing a two-capillary

approach. [62] Though this approach was beneficial in preventing emitter clogging and bubble formation, the set-up was still laborious and had a high risk to break the required etched capillaries, and had generally limited ease of use. Further optimization and potential commercialization would be necessary to make this type of sensitive CE-MS interface more accessible and convenient to use.

### **1.6 Two-dimensional capillary electrophoresis-mass spectrometry (CE-CE-MS)**

Certain CE modes are very challenging to hyphenate to MS regardless of the utilized interface as the respective electrolytes require highly ESI-interfering substances. These methods (CZE, CIEF, CGE) are exceptionally important for the characterization and quality control of biopharmaceuticals but cannot be directly coupled to MS, or only to a limited extent. In general, multi-dimensional separation systems are used to increase the peak capacity by choosing different selectivity for each dimension and therefore increase the separation power. The concept of two-dimensional CE-MS (CE-CE-MS) was introduced to allow MS-incompatible CE methods in the first dimension and an MS-compatible CE method in the second dimension for successful CE-CE-MS coupling.[63] The second dimension serves mostly as a clean-up step to transfer any peak or analyte towards interference-free MS detection with an MS-compatible BGE after a heart-cut procedure but can also provide separation power when underlying species are transferred. Our group around Prof. Neusüß has already shown many examples with various CE modes which were successfully coupled to MS via a mechanical valve: CZE-CZE-MS [64, 65], CIEF-CZE-MS [66, 67], iCIEF-CZE-MS [63], and CE(SDS)-CZE-MS [68–70]. Figure 5 shows the schematic set-up of two CE instruments coupled to a valve and hyphenated to MS. One CE instrument serves as the first dimension with an external UV detector and an external CE outlet vial. The second CE instrument serves as the second dimension and is hyphenated to MS via a (nano flow) sheath liquid interface. One major challenge in two-dimensional CE-CE coupling is the timing of the heart-cut procedure. There are different ways to tackle this depending on the CE mode, either via constant voltage or via applied pressure after the peak of interest has reached the detection point. Pressure-assisted positioning relies on constant backpressure of the system which can be difficult as many utilized BGE components from first dimensions (gel, high molar buffers) tend to precipitate and

## Introduction

clog capillaries or parts of the valve when getting in contact with boundary surfaces. Another challenge is the precise transfer of minimal peak volumes (4-20 nL) with as low dead volume as possible. Up to now, the second dimension was used for clean-up or complexing SDS (CGE-CZE-MS). Nevertheless, in one example it was possible to achieve a separation of two underlying species in the second dimension which were separated together in the first dimension.[68] The second dimension can thus be used for clean-up, additional separation power, and complexing reactions or other sample treatment options. One interesting approach is here in-capillary denaturing and digestion, providing fast incubation times while keeping high digestion efficiency and having a lower risk of induction of artificial modifications than in off-line reactions in solution.[71–73] The concept of in-capillary digestion was up to date not applied in a two-dimensional CE-CE system and would allow getting a deep insight into the PTM localization on the peptide level of charge-based separated therapeutic mAbs.

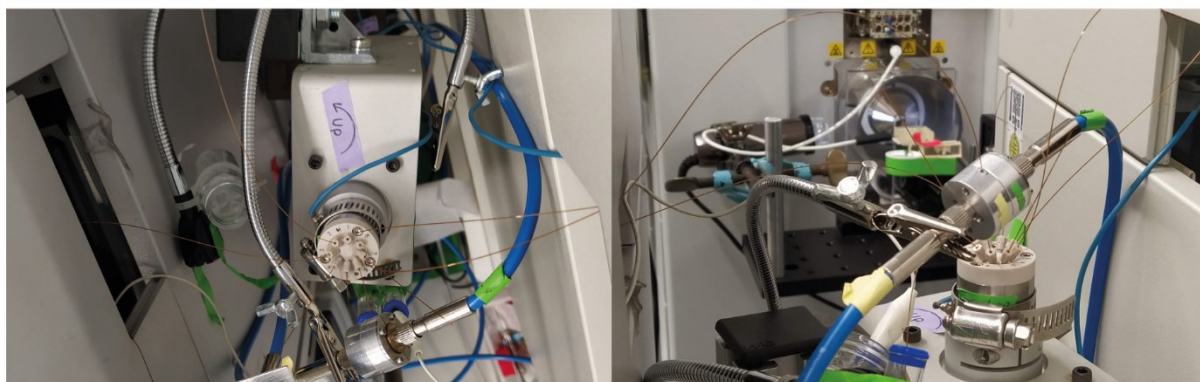
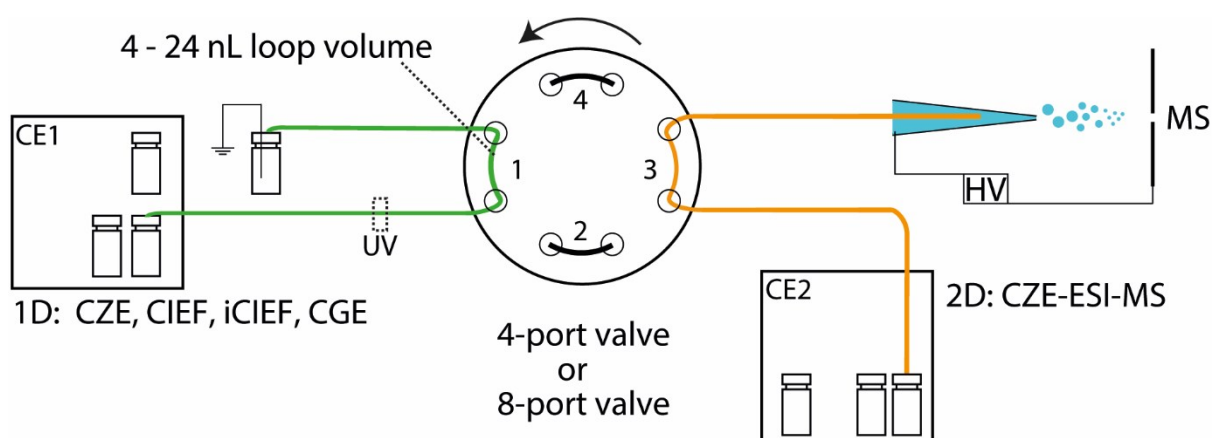


**Figure 5.** Schematic set-up of two CE instruments coupled via a nanoliter valve. The first dimension can be any CE mode with UV detection in front of the valve. The second CE dimension can be any volatile, MS-compatible BGE. Below the scheme are two pictures of a running CZE-CZE system hyphenated to MS via a nanoflow sheath liquid interface.

## 1.7 Objectives of the work

This thesis deals with the challenges and possibilities of ESI-MS coupling of charge-based CE separation techniques for the characterization of mAbs. CE method development and technical developments are supposed to enable direct (CE-MS) and two-dimensional (CE-CE-MS) hyphenation of electromigrative protein charge heterogeneity methods to MS. This should be accomplished by the development of suitable technical solutions, analytical methods, and example applications.

The application and development of commercialized and home-built nanoESI interfaces have grown strongly during the past decade providing a sensitive approach for CE-MS methods. Nevertheless, the ease of use, robustness, and lack of flexibility are still pain points for many potential users. Therefore, the first part of this thesis is dedicated to the development and characterization of a nanoflow sheath liquid ESI-MS interface for sensitive CE-MS coupling combined with ease of use (manuscript I).

In the next part of my thesis, the goal was to couple iCIEF directly to MS. In recent years, iCIEF has emerged as an important method for charge heterogeneity analysis of intact mAb drug products. In addition to the charge heterogeneity profile, characterization by MS is desired for quality control, efficacy, and safety of the drug. Coupling of IEF methods to MS is in general challenging due to the required chemicals, especially if low abundant charge variants are subject to focus. The CE-MS interface development (manuscript I) enables the direct iCIEF-MS coupling for the characterization of intact mAb charge variants (manuscript II).

In general, two-dimensional CE-MS coupling can be used to combine an ESI-interfering first dimension with a second ESI-MS compatible dimension (manuscript III). In the third part of my thesis, the goal was the development of a two-dimensional CZE-CZE-MS set-up and method for the characterization of mAb charge heterogeneity. In addition to the type of charge variant in intact mAb molecules, PTM localization on the peptide level is crucial for thorough characterization. The frequently applied CZE method containing an ESI-interfering buffer based on EACA is not compatible with the standard digestion enzyme trypsin. A two-dimensional CZE-CZE-

## Objectives of the work

MS system is therefore developed for charge-based CZE separation of intact mAbs in combination with a heart-cut of a specific charge variant peak, subsequent in-capillary digestion, and peptide mapping using the aspartate protease pepsin (manuscript IV).

## 2 Overview manuscripts

### **Manuscript I**

**Schlecht J, Stolz A, Hofmann A, Gerstung L, Neusüß C (2021)** nanoCEasy: An Easy, Flexible, and Robust Nanoflow Sheath Liquid Capillary Electrophoresis-Mass Spectrometry Interface Based on 3D Printed Parts. *Analytical Chemistry* 93(44):14593–14598

This manuscript describes the development, set-up, and characterization of a sensitive and flexible CE-MS interface. It consists of 3D-printed parts, provides a two-capillary set-up, and requires less handling expertise than in other commercially available interfaces.

### **Manuscript II**

**Schlecht J, Moritz B, Kiessig S, Neusüß C (2023)** Characterization of Therapeutic mAb Charge Heterogeneity by iCIEF Coupled to Mass Spectrometry (iCIEF-MS). *Electrophoresis* 44 (5-6):540–548

This manuscript describes the direct coupling of a preparative iCIEF instrument to a mass spectrometer using a sensitive and flexible CE-MS interface. Several parameters were investigated and specific parameters for iCIEF-MS characterization of two different mAbs could be determined.

### **Manuscript III**

**Schlecht J, Jooß K, Neusüß C (2018)** Two-dimensional capillary electrophoresis-mass spectrometry (CE-CE-MS): coupling MS-interfering capillary electromigration methods with mass spectrometry. *Analytical and Bioanalytical Chemistry* 410(25):6353–6359

## Overview manuscripts

This manuscript describes the possibilities and challenges of two-dimensional capillary electrophoresis coupled with mass spectrometry. It highlights advantages and possible fields of applications with a few examples, as well as technical requirements and limitations.

### **Manuscript IV**

**Schlecht J**, Jooß K, Moritz B, Kiessig S, Neusüß C (2023). Two-Dimensional Capillary Zone Electrophoresis-Mass Spectrometry: Intact mAb Charge Variant Separation Followed by Peptide Level Analysis Using In-Capillary Digestion. *Analytical Chemistry* 95(8):4059-4066

This manuscript describes a two-dimensional capillary electrophoresis set-up coupled to mass spectrometry applying a non-MS compatible method in the first dimension and an MS-compatible dimension in the second dimension. The first dimension separated intact charge variants of monoclonal antibodies and in the second dimension on-line reduction, digestion, and peptide mapping of these variants were performed.

## 2.1 Manuscript I

### FORM 1

**Manuscript No. I**

**Manuscript title:**

**nanoCEasy: An Easy, Flexible, and Robust Nanoflow Sheath Liquid Capillary Electrophoresis-Mass Spectrometry Interface Based on 3D Printed Parts**

**Authors:** Johannes Schlecht<sup>§</sup>, Alexander Stolz<sup>§</sup>, Lukas Gerstung, Adrian Hofmann, and Christian Neusüß

#### **Bibliographic Information:**

Schlecht J, Stolz A, Hofmann A, Gerstung L, Neusüß C, 2021 Analytical Chemistry 93(44):14593–14598. <https://doi.org/10.1021/acs.analchem.1c03213>

**The candidate is**

First author,  Co-first author,  Corresponding author,  Co-author.

#### **Authors' contributions (in %) to the given categories of the publication**

<b>Author</b>	<b>Conceptual</b>	<b>Data analysis</b>	<b>Experimental</b>	<b>Writing the manuscript</b>	<b>Provision of material</b>
Johannes Schlecht	40%	40%	40%	45%	
Alexander Stolz	40%	40%	40%	45%	
Lukas Gerstung		5%	10%		
Adrian Hofmann		5%	10%		
Christian Neusüß	20%	10%		10%	
Total:	100%	100%	100%	100%	



## nanoCEasy: An Easy, Flexible, and Robust Nanoflow Sheath Liquid Capillary Electrophoresis-Mass Spectrometry Interface Based on 3D Printed Parts

Johannes Schlecht,<sup>§</sup> Alexander Stolz,<sup>§</sup> Adrian Hofmann, Lukas Gerstung, and Christian Neusüß\*

Cite This: *Anal. Chem.* 2021, 93, 14593–14598

Read Online

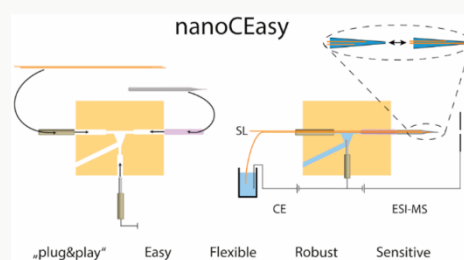
ACCESS |

Metrics & More

Article Recommendations

Supporting Information

**ABSTRACT:** Capillary electrophoresis-mass spectrometry (CE-MS) is a powerful tool in various fields including proteomics, metabolomics, and biopharmaceutical and environmental analysis. Nanoflow sheath liquid (SL) CE-MS interfaces provide sensitive ionization, required in these fields, but are still limited to a few research laboratories as handling is difficult and expertise is necessary. Here, we introduce nanoCEasy, a novel nanoflow SL interface based on 3D printed parts, including our previously reported two capillary approach. The customized plug-and-play design enables the introduction of capillaries and an emitter without any fittings in less than a minute. The transparency of the polymer enables visual inspection of the liquid flow inside the interface. Robust operation was systematically demonstrated regarding the electrospray voltage, the distance between the emitter and MS orifice, the distance between the separation capillary and emitter tip, and different individual emitters of the same type. For the first time, we evaluated the influence of high electroosmotic flow (EOF) separation conditions on a nanoflow SL interface. A high flow from the separation capillary can be outbalanced by increasing the electrospray voltage, leading to an overall increased electrospray flow, which enables stable operation under high-EOF conditions. Overall, the nanoCEasy interface allows easy, sensitive, and robust coupling of CE-MS. We aspire the use of this sensitive, easy-to-use interface in large-scale studies and by nonexperts.



### INTRODUCTION

Due to the increasing complexity of samples analyzed by mass spectrometry (MS), sophisticated separation techniques are necessary to fully exploit the capabilities of modern MS techniques. Capillary electrophoresis (CE) represents an attractive separation technique in these fields due to its unique features, such as high separation selectivity (charge/size ratio), high separation efficiency, and small sample/reagent consumption.<sup>1–3</sup>

Due to the high sheath liquid (SL) flow rates used with the widely applied coaxial sheath liquid interface and the resulting high dilution of the CE effluent,<sup>4</sup> research has been focused to find alternative, more sensitive approaches to couple CE and MS. To increase the sensitivity of CE-MS methods, operation in the nanoESI regime has been established as the leading concept in research.<sup>1,3–5</sup> Operation in the nanoESI regime at sub- $\mu\text{L}/\text{min}$  flow rates reduces dilution and increases the spray efficiency.<sup>6</sup> SL-based interfaces enable flexible selection of BGE and capillary dimensions while obtaining similar sensitivities as sheathless interfaces.<sup>7</sup>

In nanoflow SL interfaces, the separation capillary is introduced into a stainless steel or glass emitter which is filled with SL.<sup>8</sup> Some interfaces use separation capillaries with small

outer diameters (ODs) which allows protrusion of the capillary through the emitter to enable direct electrospray from the capillary tip.<sup>9–11</sup> Other interfaces employ electrospray from the tip of the stainless steel or glass emitter.<sup>7,12–14</sup>

The value of nanoflow SL interfaces to increase sensitivity in CE-MS has been proven several times recently,<sup>7,10,15,16</sup> and the commercialization of the interface developed by the Dovichi group as the EMASS-II interface (CMP Scientific) enabled access to this technique to a broader scientific community.<sup>13</sup> However, the setup and operation of these interfaces are laborious and need some experience and expertise.<sup>16,17</sup> Additionally, problems with bubble formation and emitter clogging hamper the analytical ruggedness.

Our group recently developed an in-house built nanoflow SL interface<sup>7</sup> which was already successfully used for the quantification and screening of anionic compounds in drinking

Received: July 29, 2021

Accepted: October 4, 2021

Published: November 1, 2021



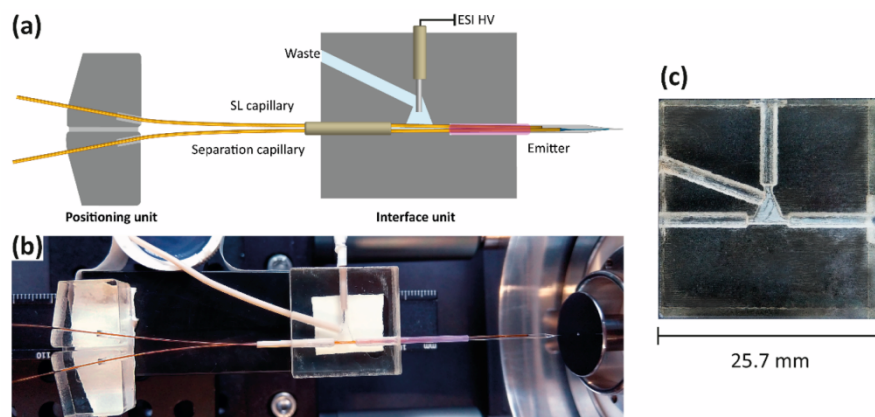


**Figure 1.** Setup of the nanoCEasy interface. (a) Schematic view of the interface with attached capillaries and electrodes (not to scale). (b) Image of the nanoCEasy interface mounted to a Bruker QTOF instrument. (c) Close-up image of the 3D printed interface part.

water<sup>18</sup> and the analysis CE(SDS)-separated monoclonal antibody fragments.<sup>19</sup> Moreover, we were able to overcome some of the aforementioned problems by introducing a two capillary approach.<sup>20</sup>

Here, we describe the development of the nanoCEasy interface based on 3D printed parts. The main benefits of this interface are the easy and fast setup, easy maintenance, and troubleshooting during operation as well as cheap manufacturing costs. We systematically evaluated the capabilities of such an interface to operate at high electroosmotic flow (EOF), demonstrated robustness, and showed exemplary applications.

## EXPERIMENTAL SECTION

**Chemicals and Samples.** *Chemicals, Materials, and Samples.* Isopropyl alcohol (IPA), methanol, acetone (all LC-MS grade), formic acid ( $\geq 98\%$ , FA), acetic acid, and ammonium hydrogen carbonate were obtained from Carl Roth GmbH & Co. KG (Karlsruhe, Germany). Hydrofluoric acid (40% (v/v)), sodium hydroxide, and hydrochloric acid (37%) were purchased from Merck KGaA (Darmstadt, Germany). Iodacetamide (IAA), 1,4-dithiothreitol (DTT), bovine serum albumin (BSA), and trypsin were obtained from Sigma-Aldrich (Steinheim, Germany). The amino acids glutamic acid, phenylalanine, tryptophan, and tyrosine were obtained from Fluka Biochemika (Buchs, Switzerland). All solutions were prepared using ultrapure water (UPW, 18  $M\Omega \cdot cm$  at 25 °C, SG Ultra Clear UV from Siemens Water Technologies, USA). Fused silica capillaries (50  $\mu m$  ID, 365  $\mu m$  OD and 100  $\mu m$  ID, 240  $\mu m$  OD) were purchased from Polymicro Technologies (Phoenix, AZ, USA). Emitters with a 30  $\mu m$  ID tip were obtained from BioMedical Instruments (Zoellnitz, Germany).

**Preparation of Amino Acids and BSA Digest.** Tryptophan, tyrosine, glutamic acid, and phenylalanine were dissolved in 0.2 M FA (1 mg/mL). Trypsin digestion of BSA was performed according to the manufacturer's protocol.<sup>21</sup> Briefly, BSA (1 mg/mL) was dissolved in 8 M urea/50 mM Tris-HCl (pH 8). Five mM DTT was added, and the solution was incubated for 1 h at 37 °C for reduction. Fifteen mM iodacetamide was

added and incubated for another 30 min in the dark at room temperature. The protein was precipitated with acetone and centrifuged at 4800 g for 10 min. The pellet was resolved with 50 mM ammonium hydrogen carbonate (pH 7.8), and trypsin was added in an m/m ratio of 1/20 (trypsin/protein). Digestion was performed overnight at 37 °C. The sample was evaporated to dryness with a vacuum centrifuge and stored dried ( $-18$  °C). For measurements, an aliquot was thawed, and 0.2 M FA was added to obtain the final working concentration.

**Instrumentation.** *Construction and Setup of the nanoCEasy Interface.* A Keyence Agilista 3D printer and Keyence AR-M2 material were used for printing the parts of the nanoCEasy interface by an inkjet system with photopolymerization. After printing, the 3D printed parts were ultrasonicated in 80% IPA and dried at room temperature. The two printed parts (positioning unit and interface unit, see Figure 1a) were placed on a polymer block (polyoxymethylene) at a distance of  $\sim 40$  mm. The mounting of the interface to the MS is based on a nanoESI source design from the University of Washington (<https://proteomicsresource.washington.edu/protocols05/nsisource.php>) and was adapted for CE-MS coupling. Polyether ether ketone (PEEK) tubing 1532L, PEEK tubing sleeve F-232, and fluorinated ethylene propylene (FEP) tubing sleeve F-252 (IDEX HS) were used for connecting the electrode, the separation capillary (OD 365  $\mu m$ ), the SL capillary (OD 240  $\mu m$ ), and a borosilicate electrospray emitter to the interface unit.

**Instrumental Setup.** All CZE experiments were performed on an Agilent Technologies HP 3D CE or a CE 7100 A (Agilent Technologies). FS capillaries (50  $\mu m$  ID) with a length of 65–70 cm were used for separation. Separation capillaries were etched at one end with hydrofluoric acid over a length of 10 mm to reduce the outer diameter ( $< 150$   $\mu m$ ) as reported previously<sup>7,20</sup> (**safety consideration: wear appropriate protective gear and perform handling under a fume hood**). Capillaries were initially conditioned by flushing with methanol (10 min), 1 M sodium hydroxide (15 min), UPW (5 min), and finally BGE (10 min). The CE instrument was

coupled to an amaZon ETD ion trap (Bruker Daltonics, Bremen, Germany) or an Orbitrap Fusion Lumos (Thermo Fisher Scientific, San Jose, CA, USA). In separation mode, the tip of the separation capillary was placed 1.8 mm from the emitter tip. The distance between the emitter and MS orifice was set to 3.0 mm for all applications. The emitter and capillary position were observed by a digital microscope (Dino-Lite, Almere, The Netherlands).

**Methods. CE-MS of Amino Acids and BSA Digest.** Hydrodynamic injection was performed for 12 s at 50 mbar. FA (0.2 M) was used as BGE, and separation was performed at 30 kV. For all experiments, 50% IPA + 0.5% FA was used as SL with a delivery flow of 4–8  $\mu\text{L}/\text{min}$ . The electrospray voltage was set between 1500 and 1600 V in positive ion mode, and dry gas flow was set to 3 L/min with a dry gas temperature of 150  $^{\circ}\text{C}$ . The scan range was set to 50–300  $m/z$  with a target mass of 200  $m/z$  for the amino acids and to 250–1500  $m/z$  with a target mass of 650  $m/z$  for the BSA digest.

**Rhodamine B Flow Experiments.** To evaluate the EOF compatibility of the nanoCEasy interface, rhodamine B infusion experiments with both MS instruments were performed. A solution of 125  $\mu\text{g}/\text{mL}$  rhodamine B in 0.2 M FA was infused to the interface through the separation capillary by application of inlet pressure at the CE or with a syringe pump. For infusion via inlet pressure, flow rates were calculated based on the Hagen–Poiseuille equations.

**Data Analysis.** Peak areas for the extracted ion electropherograms (EIEs) of the amino acids and the BSA digest were calculated with Data Analysis 4.3 (Bruker Daltonics). The robustness of the interface was evaluated by a univariate analysis of variance (ANOVA). Triplicates were acquired for all observed parameter settings resulting in a total number of 9 measurements per parameter. An F-test was performed before the ANOVA analysis to demonstrate homogeneity of variances. The ANOVA analysis was performed with a level of significance of  $\alpha = 0.05$ . Therefore, parameters with a  $p$ -value  $> 0.05$  were considered robust.

## ■ RESULTS AND DISCUSSION

**Setup of the nanoCEasy Interface.** The nanoCEasy interface is designed to improve mounting and handling based on our recently described nanoflow SL interface with the two capillary approach.<sup>20</sup> The two capillary approach provides several benefits compared to the conventional approach of using a single capillary in an electrospray emitter. Both capillaries can be moved axially to either place the separation capillary (separation mode) or the SL capillary (conditioning mode) close to the emitter tip. This concept can be considered as a “switching valve” function, as the position of the separation capillary determines whether its effluent is directed to the emitter tip and is thus sprayed (separation mode) or directed to the waste by the high SL flow (conditioning mode). Consequently, capillary conditioning and high matrix loads can be performed without contaminating the MS. Furthermore, this significantly reduces the risk of emitter clogging, thus improving the long-term operational stability of the interface.

Despite these benefits, there were some limitations regarding the handling of this interface. The use of fittings to fix the emitter, electrode, and capillaries to a cross-piece generally made the setup of the interface laborious and time-consuming. To mount the emitter, it had to be fixed at the interface with a fitting after the capillaries were already inserted. This can result in breaking of the emitter or etched capillary and is a laborious

process. Furthermore, the nontransparent crosspiece did not allow visual inspection of the capillaries during the setup.

To overcome these limitations, we designed interface parts with three substantial characteristics: (i) “plug-and-play” using sleeves (no fittings/screws), (ii) ideal geometries for the insertion of capillaries and emitter, including easy replacement as well as prevention of material abrasion during insertion, and (iii) visual inspection of capillary handling and bubbles or particles. 3D printing was chosen for manufacturing, as it has emerged as a commonly applied prototyping tool in analytical chemistry, providing fast and easy fabrication of customized labware.<sup>22</sup> The interface parts were produced using photopolymer inkjet printing technology. Transparency (see Figure 1b,c) and chemical resistance to organic solvents and acids were considered in the selection of the printing material (Keyence AR-M2).

The design of the interface is shown in Figure 1a and consists of two 3D printed parts, the interface unit, and the positioning unit. The interface unit contains an entrance port for the capillaries, a port for the electrospray/grounding electrode, one for the electrospray emitter, and an additional waste port for draining the excess liquid. Sleeves are inserted in each channel of the interface unit and slightly squeezed to fix their position. The interface unit is designed to provide a continuous channel with an inner diameter of about 780  $\mu\text{m}$ , corresponding to the inner diameter of the ES emitter. This continuous channel prevents the breaking of an etched capillary tip during insertion in the interface and smoothly guides both capillaries in parallel into the emitter without material abrasion. The cavity in the middle of the interface unit reduces high current densities at the electrode, thus minimizing bubble formation. In addition, the excess liquid flow passes the electrode toward the waste channel and takes along potential bubbles and particles to the waste. To exchange an emitter, both capillaries are pulled back to the cavity, and the emitter can be removed. After insertion of a new emitter, the capillaries are repositioned at the emitter tip. The transparency of the material helps in the visual inspection during setup and operation, thus simplifying troubleshooting. The whole exchange process takes less than a minute and requires minimal effort. The second 3D printed part (positioning unit) enables easy insertion and moving of the capillaries. The capillaries can be placed in the middle channel (guide channel) during insertion and subsequently pushed through the entrance sleeve until the capillaries reach their position in the emitter. After that, the capillary is squeezed into one of the outer gaps matching their respective OD. The squeezed capillaries are fixed in position but are manually movable with little effort. This enables easy switching between separation and conditioning mode. The complete interface setup is flexible regarding the manufacturer of mass spectrometers. Overall, the improved nanoCEasy interface design simplifies setup and operation. 3D printing allows easy and cheap production of the interface and positioning unit. At the same time, adaptations to optimize the design or tailor it for more specific applications can easily be implemented. A short video showing the setup of the interface is available in the SI.

**Operation under High-EOF Conditions.** The electroosmotic flow (EOF) is an important aspect to consider in CE. Many CE methods involve or even rely on an EOF. During initial experiments with high-EOF methods, reduced intensities and broad peaks were observed (data not shown). In some

cases, obtaining a stable electrospray was not possible at all under such high-EOF conditions.

Compared to the commonly used coaxial SL interface, where high flows of CE effluent can be efficiently diluted by the high SL flow, accumulation of CE effluent might occur at the tip of the emitter in a nanoflow SL interface if the high EOF is not balanced by sufficient electrospray liquid consumption. In our two capillary approach, a SL capillary delivers an excess of SL that is flowing toward the waste channel. Therefore, the nanoCEasy interface operates without external pressure and active SL flow, and the electrospray liquid consumption is only determined by the SL composition and, in particular, the electrospray voltage.<sup>23–25</sup> Thus, we suspected three different ways to increase the compatibility of high-EOF systems with the nanoCEasy interface: (i) increasing the electrospray voltage to increase the overall electrospray liquid consumption, (ii) increasing the distance between the separation capillary and the emitter tip to enable better mixing between CE effluent and SL, and (iii) adapting the SL composition.

To evaluate the effect of CE effluent accumulation at the emitter tip, a solution of rhodamine B was introduced to the interface via the separation capillary with defined flow rates. Besides observing the signal for rhodamine B in the MS, it was also possible to visually inspect the accumulation of CE effluent at the emitter tip due to the intense color of rhodamine B (Figure S1). Flow rates of the rhodamine B solution were increased during the spray process until an accumulation of the solution was visible at the emitter tip. This concurrently resulted in a breakup of the electrospray process due to the different spray conditions of the 100% aqueous solution. In this way, it was possible to determine maximum tolerable flow rates for a given parameter setting. We evaluated the maximum tolerable flow rate as a function of electrospray voltage and the distance between the separation capillary and emitter tip. Furthermore, the function between the maximum tolerable flow rate and electrospray voltage was evaluated for different mass spectrometers and different SL compositions.

Figure 2a shows the maximum flow rate as a function of the electrospray voltage for two different mass spectrometers. The general relationship is the same for both curves, with different onset voltages. The curve for the Orbitrap MS is shifted to higher values compared to the Bruker ion trap. This is most likely due to different effective electric field strengths at the emitter tip caused by the different source interface geometries. In both cases, second-order polynomial regression showed a good correlation between the maximum tolerable flow rate and electrospray voltage, demonstrating that manipulation of the electrospray voltage is an easy way to adapt the maximum tolerable flow rate of the system. We did not observe any effect when changing the position of the end of the separation capillary relative to the emitter tip (Figure S2). This supports the assumption that the issue in operating under high-EOF conditions is related to an insufficient electrospray liquid consumption rather than insufficient mixing of the CE effluent with the SL. Furthermore, the influence of the SL composition on the relationship between the electrospray voltage and maximum tolerable flow rate was compared (Figure 2b). For the same voltages, an SL containing 80% IPA can handle higher CE flow rates compared to the standard SL containing 50% IPA. We attribute this effect to the decreased surface tension of the mixture resulting in higher electrospray liquid consumption rates. In summary, the electrospray voltage has

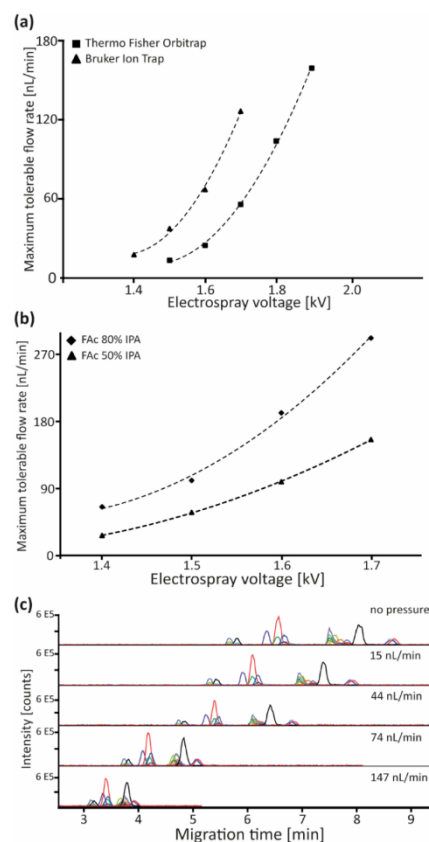


**Figure 2.** Effect of electrospray voltage on the maximum tolerable flow rate and simulated EOF application. (a) Effect of the electrospray voltage on the maximum tolerable flow rate with different MS instruments. (b) Effect of the electrospray voltage on the maximum tolerable flow rate at a high and normal level of organic solvent in the SL. (c) CE-MS of tryptic BSA peptides with simulated EOF at 1700 V electrospray voltage. Applied pressure: 0 mbar, 10 mbar, 30 mbar, 50 mbar, 100 mbar. +30 kV separation voltage.

the highest impact on the maximum tolerable flow rate of the interface.

To evaluate if this parameter can be actively used to operate the interface at high flow rates of the CE, separation of a tryptic BSA digest was performed with additional application of pressure at the CE inlet to mimic an EOF. An electrospray voltage of 1700 V was chosen based on the model in Figure 2a, as the interface should theoretically handle a maximum flow rate of ~150 nL/min with this electrospray voltage. Figure 2c shows the EIEs of selected peptides from the BSA digest with different applied inlet pressures. Flow rates were calculated based on the Hagen–Poiseuille equations. As expected, migration times decrease with increasing applied inlet pressure. We did not observe any impact on the peak shape or width of

the peaks. Furthermore, intensities stayed constant across all applied pressures. Consequently, increasing the electrospray voltage is an easy way to increase EOF compatibility of a nanoflow SL interface without negative impact on separation and sensitivity. An exemplary application of CE-MS using a high-EOF system for the separation of hemoglobin can be found in the [Supporting Information \(SI\)](#).

**Robustness and Applications.** To establish the nanoCEasy interface in routine laboratory work, the analytical robustness of the interface is of utmost importance. The interface must perform equally for different users and should tolerate slight changes in operational parameters.

We defined (i) the electrospray voltage, (ii) the distance between emitter and MS orifice, and (iii) the distance between the end of the separation capillary and the emitter tip as critical parameters that are prone to small changes during the setup and operation of the instrument. Additionally, we evaluated the effect of using three different emitters of the same batch. ANOVA was performed to evaluate the influence of small deviations in these parameters on the signal intensities of a four amino acid mix analyzed by CE-MS. Additionally, data from the analysis of BSA digest applying three different emitters of the same geometry and batch were used as well. Overall, the ANOVA for all parameters and analytes resulted in 24 p-values of which only one was below the critical  $\alpha$ -values of 0.05 (Table S1, SI). This represents <5% of the values and could thus be attributed to a false positive rate of 5% according to  $\alpha$ .

Our data shows that the nanoCEasy interface is robust toward the four evaluated parameters. Small variations in the distances between the emitter and the MS orifice as well as the separation capillary and the emitter tip have no significant influence on the sensitivity. Therefore, a precise adjustment of these parameters is not necessary during setup and changing between conditioning and separation mode. This not only simplifies these processes but should also increase the robustness of the interface toward different users. Emitters of the same geometry and batch are interchangeable without any impact on stability or sensitivity. This enables changing of emitters during coherent sample sequences without any negative effect on data quality.

To characterize the nanoCEasy interface, amino acids and BSA digest were used. These analytes can easily be separated on an untreated FS capillary with high separation efficiency. For the separation of proteins, however, capillary coating is paramount to reduce interactions between the proteins and the capillary wall.<sup>26</sup> Statically adsorbed coatings offer the benefit of easy coating procedures, low reagent consumption, and good batch-to-batch reproducibility. Still, for stable separation conditions, coatings have to be refreshed regularly. Many of these protocols contain nonvolatile, ESI-interfering, or MS-incompatible compounds. In all commercially available CE-MS interfaces, the capillary needs to be removed from the interface during the coating process to avoid MS contamination. By using the two capillary approach, the separation capillary can remain in the interface during the (re)coating procedure since the coating solutions from the separation capillary are effectively flushed to the back-end drain.<sup>20</sup> We successfully applied two different statically adsorbed capillary coatings for the separation of mAb subunits and hemoglobin extracted from clinical DBS samples as shown in the [SI](#).

## CONCLUSIONS

We designed and developed the nanoCEasy interface, a novel nanoflow SL CE-MS interface based on 3D printed parts. The “plug-and-play” approach of this interface allows insertion of capillaries, emitter, and electrode without fittings or screws. This reduces setup and troubleshooting times as well as the risk of breaking any components. In fact, changing the emitter can be performed in less than a minute with minimal effort without the risk of polymer abrasion and particle formation. The concept of using 3D printing allows easy adaption and optimization of the printed parts. The material used for printing is chemically stable, and even after extended use, no blurring, swelling, or abrasion of the material was observed. The transparency of the material not only helps in capillary insertion but also simplifies troubleshooting.

We identified the electrospray voltage as the major parameter to enable operation of the interface at high-EOF conditions. As the set electrospray voltage directly determines the overall flow rate of the electrospray, manipulation is an easy and direct way to counterbalance the high EOF and obtain optimal spray conditions.

The analytical robustness of the nanoCEasy interface was shown, demonstrating that especially the manually set parameters are robust to small deviations. Additionally, the implementation of the two capillary approach makes working with statically adsorbed coatings convenient, and recoating can be performed frequently to prevent sample adsorption and to obtain maximum migration time stability.

To further increase ease-of-use and allow unsupervised operation of the interface, we aspire to automate the movement of the separation capillary between separation and conditioning mode. This would allow running long sequences including flushing, conditioning, and recoating with MS-incompatible solutions in an automated manner.

The nanoCEasy interface is an easy-to-use, flexible, and robust nanoflow sheath liquid CE-MS interface, and we anticipate its use in large-scale studies and by nonexperts in the future.

## ASSOCIATED CONTENT

### Supporting Information

The Supporting Information is available free of charge at <https://pubs.acs.org/doi/10.1021/acs.analchem.1c03213>.

Figure of Rhodamine B infusion experiments, additional experimental results on maximum tolerable flow rate, robustness data, and two exemplary applications (PDF)

Video showing interface setup (MOV)

## AUTHOR INFORMATION

### Corresponding Author

Christian Neusüß – Department of Chemistry, Aalen University, 73430 Aalen, Germany;  
Email: christian.neuseuss@hs-aalen.de

### Authors

Johannes Schlecht – Department of Chemistry, Aalen University, 73430 Aalen, Germany; Department of Pharmaceutical and Medicinal Chemistry, Friedrich Schiller University Jena, 07743 Jena, Germany

Alexander Stolz – Department of Chemistry, Aalen University, 73430 Aalen, Germany; Department of Pharmaceutical and

Medicinal Chemistry, Friedrich Schiller University Jena, 07743 Jena, Germany; [orcid.org/0000-0001-7624-6486](https://orcid.org/0000-0001-7624-6486)  
**Adrian Hofmann** – Department of Chemistry, Aalen University, 73430 Aalen, Germany  
**Lukas Gerstung** – Department of Chemistry, Aalen University, 73430 Aalen, Germany

Complete contact information is available at:  
<https://pubs.acs.org/10.1021/acs.analchem.1c03213>

#### Author Contributions

<sup>§</sup>J.S. and A.S. contributed equally.

#### Notes

The authors declare no competing financial interest.

#### ACKNOWLEDGMENTS

The authors thank the Deutsche Forschungsgemeinschaft (DFG, German Research Foundation—grant 446330632), F. Hoffmann La-Roche, Ltd. and Agilent Technologies for financial support. Thanks to Andreas Heinrich and Christian Eder for support with 3D printing and Jens Meixner and Jana Steflava for technical support and valuable discussions.

#### REFERENCES

- (1) Stolz, A.; Jooß, K.; Höcker, O.; Römer, J.; Schlecht, J.; Neusüß, C. *Electrophoresis* **2019**, *40* (1), 79–112.
- (2) Gomes, F. P.; Yates, J. R. *Mass Spectrom. Rev.* **2019**, *38* (6), 445–460.
- (3) Zhang, W.; Hankemeier, T.; Ramautar, R. *Curr. Opin. Biotechnol.* **2017**, *43*, 1–7.
- (4) Lindenburg, P. W.; Haselberg, R.; Rozing, G.; Ramautar, R. *Chromatographia* **2015**, *78* (5–6), 367–377.
- (5) Krenkova, J.; Kleparnik, K.; Luksch, J.; Foret, F. *Electrophoresis* **2019**, *40* (18–19), 2263–2270.
- (6) Wilm, M.; Mann, M. *Anal. Chem.* **1996**, *68* (1), 1–8.
- (7) Höcker, O.; Montealegre, C.; Neusüß, C. *Anal. Bioanal. Chem.* **2018**, *410* (21), 5265–5275.
- (8) Hsieh, F.; Baronas, E.; Muir, C.; Martin, S. A. *Rapid Commun. Mass Spectrom.* **1999**, *13* (1), 67–72.
- (9) González-Ruiz, V.; Codesido, S.; Far, J.; Rudaz, S.; Schappler, J. *Electrophoresis* **2016**, *37* (7–8), 936–946.
- (10) Choi, S. B.; Zamarbide, M.; Manzini, M. C.; Nemes, P. J. *Am. Soc. Mass Spectrom.* **2017**, *28* (4), 597–607.
- (11) Konášová, R.; Koval, D.; Hošek, J.; Kašíčka, V. *Talanta* **2021**, *228*, 122212.
- (12) Wojcik, R.; Dada, O. O.; Sadílek, M.; Dovichi, N. J. *Rapid Commun. Mass Spectrom.* **2010**, *24* (17), 2554–2560.
- (13) Peuchen, E. H.; Zhu, G.; Sun, L.; Dovichi, N. J. *Anal. Bioanal. Chem.* **2017**, *409* (7), 1789–1795.
- (14) Sun, L.; Zhu, G.; Zhang, Z.; Mou, S.; Dovichi, N. J. *J. Proteome Res.* **2015**, *14* (5), 2312–2321.
- (15) Amenson-Lamar, E. A.; Sun, L.; Zhang, Z.; Bohn, P. W.; Dovichi, N. J. *Talanta* **2019**, *204*, 70–73.
- (16) Gou, M.-J.; Nys, G.; Cobraiville, G.; Demelene, A.; Servais, A.-C.; Fillet, M. J. *Chromatogr. A* **2020**, *1618*, 460873.
- (17) Wu, H.; Tang, K. *Rev. Anal. Chem.* **2020**, *39* (1), 45–55.
- (18) Höcker, O.; Bader, T.; Schmidt, T. C.; Schulz, W.; Neusüß, C. *Anal. Bioanal. Chem.* **2020**, *412*, 4857.
- (19) Römer, J.; Stolz, A.; Kiessig, S.; Moritz, B.; Neusüß, C. *J. Pharm. Biomed. Anal.* **2021**, *201*, 114089.
- (20) Höcker, O.; Knierman, M.; Meixner, J.; Neusüß, C. *Electrophoresis* **2021**, *42* (4), 369–373.
- (21) Promega Corporation. Trypsin Gold, Mass Spectrometry Grade. pp 1–9. <https://www.promega.de/-/media/files/resources/protocols/technical-bulletins/101/trypsin-gold-mass-spectrometry-grade-protocol.pdf>(accessed 2021-10-13).
- (22) Gross, B.; Lockwood, S. Y.; Spence, D. M. *Anal. Chem.* **2017**, *89* (1), 57–70.
- (23) Schmidt, A.; Karas, M.; Dülcks, T. J. *Am. Soc. Mass Spectrom.* **2003**, *14* (5), 492–500.
- (24) Smith, K. L.; Alexander, M. S.; Stark, J. P. W. *Phys. Fluids* **2006**, *18* (9), 092104.
- (25) Ryan, C. N.; Smith, K. L.; Stark, J. P. W. *Appl. Phys. Lett.* **2014**, *104* (8), 084101.
- (26) Huhn, C.; Ramautar, R.; Wuhrer, M.; Somsen, G. W. *Anal. Bioanal. Chem.* **2010**, *396* (1), 297–314.

## 2.2 Manuscript II

### FORM 1

Manuscript No. II

Manuscript title:

**Characterization of Therapeutic mAb Charge Heterogeneity by iCIEF  
Coupled to Mass Spectrometry (iCIEF-MS)**

**Authors:** Johannes Schlecht, Bernd Moritz, Steffen Kiessig, and Christian Neusüß

The candidate is

First author,  Co-first author,  Corresponding author,  Co-author.

**Bibliographic Information:**

Schlecht J, Moritz B, Kiessig S, Neusüß C, 2023 Electrophoresis 44(5-6):540-548.  
<https://doi.org/10.1002/elps.202200170>

**Authors' contributions (in %) to the given categories of the publication**

Author	Conceptual	Data analysis	Experimental	Writing the manuscript	Provision of material
Johannes Schlecht	70%	70%	100%	80%	
Bernd Moritz		5%			x
Steffen Kiessig		5%			x
Christian Neusüß	30%	20%		20%	
Total:	100%	100%	100%	100%	

# Characterization of therapeutic mAb charge heterogeneity by iCIEF coupled to mass spectrometry (iCIEF-MS)

Johannes Schlecht<sup>1,2</sup>  | Bernd Moritz<sup>3</sup>  | Steffen Kiessig<sup>3</sup> | Christian Neusüß<sup>1</sup><sup>1</sup>Department of Chemistry, Aalen University, Aalen, Germany<sup>2</sup>Department of Pharmaceutical and Medicinal Chemistry, Friedrich Schiller University Jena, Jena, Germany<sup>3</sup>F. Hoffmann-La Roche Ltd., Basel, Switzerland**Correspondence**Christian Neusüß, Department of Chemistry, Aalen University, Beethovenstrasse 1, 73430 Aalen, Germany.  
Email: christian.neusuess@hs-aalen.de**Color online:** See article online to view Figures 1–4 in color.**Abstract**

Imaged capillary isoelectric focusing (iCIEF) has emerged as an important technique for therapeutic monoclonal antibody (mAb) charge heterogeneity analysis in the biopharmaceutical context, providing imaged detection and quantitation by UV without a mobilization step. Besides quantitation, the characterization of separated charge variants ideally directly by online electrospray ionization–mass spectrometry (ESI–MS) is crucial to ensure product quality, safety, and efficacy. Straightforward direct iCIEF–MS coupling combining high separation efficiency and quantitative results of iCIEF with the characterization power of MS enables deep characterization of mAb charge variants. A short technical setup and optimized methodical parameters (30 nl/min mobilization rate, 2%–4% ampholyte concentration, 0.5–2 mg/ml sample concentration) allow successful mAb charge variant peak assignment from iCIEF to MS. Despite a loss of separation resolution during the transfer, separated intact mAb charge variants, including deamidation as well as major and minor glycoforms even from low abundant charge variants, could be characterized by online ESI–MS with high precision. The presented setup provides a large potential for mAb charge heterogeneity characterization in biopharmaceutical applications.

**KEYWORDS**

imaged capillary isoelectric focusing, intact antibodies, mass spectrometry

## 1 | INTRODUCTION

Therapeutic monoclonal antibodies (mAbs) have become increasingly important during the past decades and are the major treatment option for various diseases [1]. Due

to their complex nature and manufacturing, mAbs are prone to structural heterogeneity, in particular, charge heterogeneity [2, 3]. Charge heterogeneity of mAbs can also occur through storage-related degradation, leading to a potential negative impact on the binding efficiency and therapeutic effect [4–6]. Imaged capillary isoelectric focusing (iCIEF) is frequently applied for charge heterogeneity determination in the biopharmaceutical context and is considered a reliable and robust routine method in

**Abbreviations:** AD, acrylamide derivative; FC, fluorocarbon; iCIEF, imaged capillary isoelectric focusing; MC, methyl cellulose; WCID, whole-capillary-imaged detection.

This is an open access article under the terms of the [Creative Commons Attribution-NonCommercial-NoDerivs](https://creativecommons.org/licenses/by-nc-nd/4.0/) License, which permits use and distribution in any medium, provided the original work is properly cited, the use is non-commercial and no modifications or adaptations are made.

© 2022 The Authors. *Electrophoresis* published by Wiley-VCH GmbH.



the development and quality control of therapeutic mAbs [7–11]. iCIEF provides whole-capillary-imaged detection (WCID) and quantitation by UV without a mobilization step [12] and has replaced conventional CIEF in many cases due to superior separation without a mobilization step, reduced analysis time (<15 min per sample), less laborious sample preparation, and faster method development time. In addition to the obtained charge variant UV profile, the identification of single charge variants by electrospray ionization–mass spectrometry (ESI–MS) is highly demanded. However, generic IEF methods mostly rely on ESI-interfering compounds such as ampholytes, methylcellulose (MC), or gel-based buffers and therefore limit the accessibility to online mass spectrometric characterization. Nevertheless, there have been several approaches to overcome this issue by direct or 2D approaches [13, 14]. The increasing availability and distribution of ESI–MS interfaces operating in the nanoliter regime during the last years enabled sensitive and direct CIEF–MS of mAbs in intact, middle-down, and top-down approaches but still require further method optimization and additives to work [15–20]. Another limitation of direct CIEF–MS is the lack of online UV data as a reference of the focusing process and the mobilization process. The first combination of online UV data and mass spectrometric characterization of imaged capillary isoelectric-focused samples was reported by Montealegre and Neusüß using a *CEInfinite* iCIEF instrument and a mechanical microliter valve [21]. In this way, heart cuts of isoelectric-focused mAb charge variants were transferred to a second dimension and characterized by flow-injection MS or capillary zone electrophoresis–MS with a coaxial sheath liquid sprayer. More recently, Mack et al. introduced a microchip-based iCIEF–MS platform based on multiple power supplies providing chemical mobilization and ESI spray stability [22]. Both applications enabled a mass information of isoelectric-focused mAbs for the identification of intact mAb charge variants and respective glycoforms.

The preparative iCIEF instrument *CEInfinite* from Advanced Electrophoresis Solutions (AES) allows imaged CIEF with subsequent transfer of focused proteins via pressure-assisted mobilization toward fraction collection or online coupling to MS. Here we present online coupling of a preparative iCIEF instrument to mass spectrometry (iCIEF–MS) via the novel nanoCEasy interface providing separation with imaged detection and subsequent online identification of intact mAb charge variants by high-resolution mass spectrometry. The iCIEF instrument *CEInfinite* was coupled to two different MS instruments via the nanoCEasy interface, a nanoflow sheath liquid CE–MS interface [23]. First, we developed the setup of direct iCIEF–MS coupling with the nanoCEasy CE–MS

interface. Second, parameters, such as sample concentration, ampholyte concentration, and mobilization speed, were investigated regarding compatibility toward online ESI–MS operation. Finally, we applied this method to two therapeutic mAbs.

## 2 | MATERIALS AND METHODS

### 2.1 | Chemicals, materials, and samples

Formic acid ( $\geq 98\%$ ) and isopropanol (LC–MS grade) were purchased from Carl Roth GmbH und Co. KG (Karlruhe, Germany). Phosphoric acid (99.99%) and MC were obtained from Sigma-Aldrich (Steinheim, Germany). Formamide (99.5%) was obtained from Alfa Aesar (Kandel, Germany). Sodium hydroxide was purchased from Merck KGaA (Darmstadt, Germany). Urea ( $\geq 99\%$ ), Pharmalyte 3–10 (36% w/v), and Pharmalyte 8–10.5 (36% w/v) were obtained from GE Healthcare Bio-Sciences AB (Waukesha, WI, USA). WCID cartridges (200  $\mu\text{m}$  id) with proprietary acrylamide derivative (AD) or fluorocarbon (FC) coating, AESlyte HR 6–8, and a fusion mAb were received from Advanced Electrophoresis Solutions Ltd. (AES) (Ontario, Canada). Herceptin (trastuzumab), 25 mg/ml (in formulation) was provided by F. Hoffmann-La Roche AG (Basel, Switzerland). Ultrapure water (UPW) was supplied by an SG Ultra Clear UV system (Siemens Water Technologies, USA). Fused silica capillaries (100  $\mu\text{m}$  id, 240  $\mu\text{m}$  od) were purchased from Polymicro Technologies (Phoenix, AZ, USA). ESI emitters with 30  $\mu\text{m}$  tip id were obtained from BioMedical Instruments (Zöllnitz, Germany).

### 2.2 | Imaged capillary isoelectric focusing

Experiments were performed using a preparative *CEInfinite* system from Advanced Electrophoresis Solutions Ltd. (AES) (Cambridge, ON, Canada) equipped with an autosampler, a syringe pump, and UV detection at 280 nm. The separation cartridge (see Figure 1) consists of a separation channel (200  $\mu\text{m}$  id, 50 mm length), a sample transfer capillary (50  $\mu\text{m}$  id, 200  $\mu\text{m}$  od), connected to the autosampler, and a transfer capillary (50  $\mu\text{m}$  id, 200  $\mu\text{m}$  od, 170–250 mm length) for direct coupling to MS. Volumes of 80 mM  $\text{H}_3\text{PO}_4$  and 100 mM NaOH were prepared daily and used as anolyte and catholyte, respectively. The trastuzumab samples consisted of 0.5–2 mg/ml sample and 2%–4% (v/v) ampholytes (Pharmalyte 3–10 and Pharmalyte 8–10.5, 1:3). The fusion mAb samples consisted of 1 mg/ml fusion mAb, 4% ampholytes (AESlyte HR 6–8), and 20% (v/v) formamide. The iCIEF cartridge was flushed with

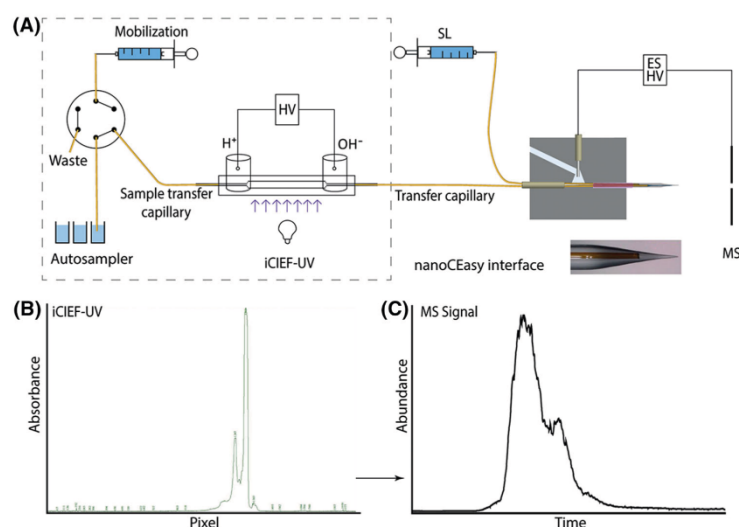


**FIGURE 1** (A) Setup of CEInfinite coupled to mass spectrometry. Schematic view of the CEInfinite with autosampler, syringe pump, and imaged capillary isoelectric focusing (iCIEF) cartridge connected with the nanoCEasy electro-spray ionization–mass spectrometry (ESI–MS) interface; (B) iCIEF–UV profile of trastuzumab (2 mg/ml). Focusing voltage: 1500 V (1 min) and 3000 V (10 min). UV detection at 280 nm; and (C) base peak electropherogram (BPE)  $m/z$  1500–4000 of trastuzumab (2 mg/ml, mobilization speed 30 nl/min) with Orbitrap Fusion Lumos

UPW and conditioning solution (4 M urea, 0.35% MC) before each measurement. Sample solutions were vortexed and centrifuged at 2000 rpm for 2 min prior to injection, 30  $\mu$ l of the sample was loaded, and 17  $\mu$ l was injected for each measurement. After sample injection, a water plug was injected to push out the sample mixture in the sample transfer capillary. In this way, only the separation capillary and the transfer capillary are filled with sample mixture avoiding additional sample peaks during pressurized mobilization. The focusing voltage was 1500 V (1 min) and 3000 V (10 min). To refocus the sample during the mobilization step the voltage (3 kV) was kept on until the focused peaks have left the cartridge. After the focusing step, pressure-assisted mobilization was started at a constant flow rate (30 or 50 nl/min) provided by a syringe pump.

### 2.3 | iCIEF–MS parameters

The CEInfinite was coupled to a micrOTOF-Q (Bruker Daltonics, Bremen, Germany) and an Orbitrap Fusion Lumos (Thermo Fisher Scientific, San Jose, CA, USA) using the nanoCEasy interface [23]. The nanoCEasy interface provides two different modes, a conditioning mode, where the SL capillary is positioned in the front of the ESI

emitter, and a separation mode, where the separation capillary is positioned in the front of the ESI emitter. Any liquid leaving the separation capillary is flushed toward the drain during the conditioning mode and sprayed toward MS during separation mode. The iCIEF transfer capillary was kept in conditioning mode during all washing steps, sample injection, and the focusing process. The iCIEF transfer capillary was moved to the separation mode after the start of the mobilization. For all experiments, 50% isopropanol + 0.5% formic acid was used as sheath liquid. The distance between the emitter and MS orifice was set to 3 mm. Spray voltages were set to 1600 V (quadrupole time of flight [QTOF]) and 1700 V (Orbitrap Fusion Lumos). MS data were acquired in positive mode. The scan range for the Orbitrap MS was  $m/z$  1500–5000 with a resolution of 7500 (fusion mAb) and 15000 (trastuzumab) with 10 microscans, an automatic gain control target of  $4e^5$ , and a maximum injection time of 100 ms. A radio frequency lens was set to 100%, and fragmentation voltage was set to 80 V. Scan range for the QTOF was  $m/z$  1750–5000. Transfer settings were adapted for the high mass range, in particular the collision energy (45 eV) and the collision cell RF (3800  $V_{pp}$ ) for effective declustering. MS data were analyzed with DataAnalysis 4.3 (Bruker Daltonics), Freestyle 1.7 (Thermo Fisher Scientific), and Intact Mass 3.4 (Protein Metrics, Cupertino, CA, USA).

### 3 | RESULTS AND DISCUSSIONS

#### 3.1 | iCIEF-MS setup

Hyphenation of an iCIEF-UV instrument and a mass spectrometer can be realized in several ways. In our view, three different approaches can be considered for direct iCIEF-MS coupling: (i) The iCIEF transfer capillary can be connected directly to a (low-flow) ESI sprayer (ii) inserting a t-piece delivering an organic modifier at any position of the iCIEF transfer capillary between the catholyte vessel and the MS (iii) via a (nanoflow) sheath liquid interface without any additional connection. The first approach lacks general ESI compatibility due to the usual sample composition (water-based, ampholytes, no organic solvents). The low mobilization flow rate of 10–80 nl/min also hampers direct coupling to low-flow ESI sprayers that operate well in the range only down to a few hundred nl/min. The second approach implies additional connections with the risk of dead volume, potential clogging, and therefore changes to the backpressure causing breaks and leakages in the microfluidic parts of the cartridge. In addition, the position of the t-piece (closer to the catholyte vessel or closer to the MS), the connection angle, the organic modifier composition, and flow rate have to be considered carefully to maintain the isoelectric-focused peak profile during the mobilization. The third approach requires no additional connection as the iCIEF transfer capillary is directly placed in a sheath liquid CE-MS interface. In this setup, the transfer capillary length determines the mobilization time because the mobilization speed is limited depending on the separation channel id. Considering the best possible sensitivity and the required transfer capillary length, we decided to utilize approach (iii), that is, a nanoflow sheath liquid interface with an optimized distance setup for iCIEF-MS coupling.

Figure 1A shows the schematic setup of iCIEF-MS coupling using the *CEInfinite* and the nanoCEasy CE-MS interface. The *CEInfinite* instrument consists of an autosampler with a 6-port valve for rinsing and sample injection, a syringe pump for pressurized mobilization, and an imaging detection system (UV). The prefabricated iCIEF cartridges consist of a sample transfer capillary, a separation channel, and a transfer capillary. The sample transfer capillary from the iCIEF cartridge is connected to the 6-port valve of the autosampler, whereas the transfer capillary is positioned in the nanoCEasy interface. The sample was introduced via the 6-port valve, and two electrodes were dipped in the anolyte and catholyte buffer vessel, respectively. Positive high voltage was applied at the anolyte vessel, the electrode in the catholyte vessel served as floating ground. Parts of the nanoCEasy source setup were adapted to keep the mobilization dis-

tance (corresponds to transfer capillary length) as short as possible to obtain minimal transfer times. All shown experiments were carried out with the minimum transfer capillary length of 170 mm. Strong peak broadening or failed experiments could be observed using up to 250 mm transfer capillary length (data not shown). Mobilization was carried out by pressure via the syringe pump, and the mobilization flow rate could be set between 10 and 80 nl/min (for the separation channel id of 200  $\mu\text{m}$ ).

#### 3.2 | iCIEF-MS with Bruker QTOF

Trastuzumab, a humanized mAb, was already introduced more than 20 years ago and is still used in the treatment of breast cancer patients. The well-known and characterized mAb shows basic and acidic variants in a non-stressed state and was selected as an example application with a narrow iCIEF profile for iCIEF-MS analysis. The maintenance of the isoelectric-focused peak profile toward mass spectrometric detection is crucial for successful iCIEF-MS coupling using the *CEInfinite* instrument, in particular during pressurized mobilization. Two effects contribute to peak broadening during pressurized mobilization in a capillary, the parabolic hydrodynamic flow profile (Taylor dispersion), and wall adsorption of analytes to the capillary wall [24]. The latter can be prevented by efficient covalent or dynamic capillary coatings, whereas the dispersion effect of the flow rate can at most be mitigated by a low velocity. The *CEInfinite* was coupled to a Bruker micrOTOF-Q using the nanoCEasy interface with optimized distance setup. The sample concentration (0.5–2 mg/ml), the mobilization flow rate (30–50 nl/min), and the ampholyte concentration (2%–4%) were tested in the iCIEF-MS setup, and effects on the MS peak profile maintenance were investigated, all experiments were performed twice.

Figure 1B shows the iCIEF-UV profile of trastuzumab after focusing and before mobilization (see also Figure S1). Figure 2A–E shows the MS base peak electropherograms (BPEs) of the mobilized sample under different conditions. The BPEs show different absolute intensities and were not normalized for a better comparison of the peak profile maintenance. In general, the UV profile could not be preserved perfectly during transfer, the peak width of the MS signals increased compared to the iCIEF-UV profile. This can be partly explained by the id change from the separation channel (200  $\mu\text{m}$ ) to the transfer capillary (50  $\mu\text{m}$ ), which increases the theoretical peak width by the factor of 16 and by Taylor dispersion due to pressurized mobilization. Figure 2C shows the best outcome for the peak profile maintenance at 0.5 mg/ml, 4% total ampholyte concentration, and 30 nl/min mobilization rate

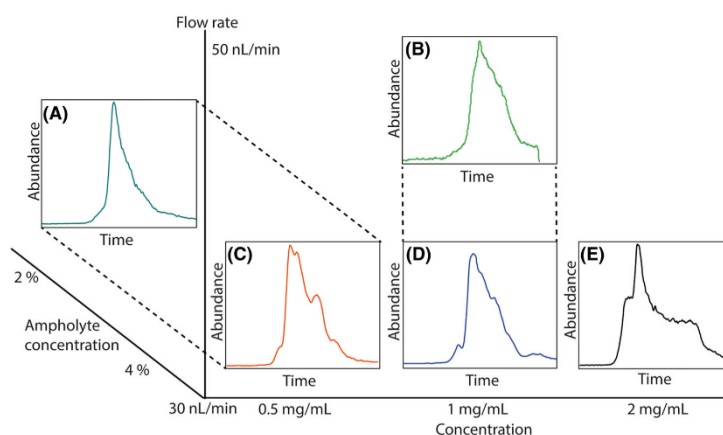


**FIGURE 2** Effect of ampholyte concentration, sample concentration, and mobilization flow rate on the maintenance of the trastuzumab peak profile during transfer toward mass spectrometry (MS): (A) 0.5 mg/ml, 2% ampholytes (0.5% Pharmalyte 3–10, 1.5% Pharmalyte 8–10.5), 30 nl/min; (B) 1 mg/ml, 4% ampholytes (0.5% Pharmalyte 3–10, 1.5% Pharmalyte 8–10.5), 50 nl/min; (C) 0.5 mg/ml, 4% ampholytes (0.5% Pharmalyte 3–10, 1.5% Pharmalyte 8–10.5), 30 nl/min; (D) 1 mg/ml 4% ampholytes (0.5% Pharmalyte 3–10, 1.5% Pharmalyte 8–10.5), 30 nl/min; and (E) 2 mg/ml, 4% ampholytes (0.5% Pharmalyte 3–10, 1.5% Pharmalyte 8–10.5), 30 nl/min

in this experimental setup. The basic, main, and two acidic variants can be assigned despite the double peak in the main variant, which is attributed to electrospray instability. Figure 2A shows the MS BPE with 0.5 mg/ml, 2% total ampholyte concentration, and 30 nl/min mobilization rate. The peak profile maintenance is strongly reduced and distinct variants cannot be observed anymore for the lower ampholyte concentration of 2%. A higher concentration of ampholytes (4%) indicates a preserving effect on the peak profile during pressurized mobilization despite the parabolic flow profile and zone broadening effects. Using a higher carrier ampholyte concentration did not lead to any observable effect on the ESI and the overall mass spectra quality in the selected mass range of  $m/z$  1750–5000. Figure 2D,E shows the concentrations of 1 and 2 mg/ml with 4% ampholytes and 30 nl/min, respectively. The peak profile was less maintained for 1 mg/ml (Figure 2D) compared to 0.5 mg/ml (Figure 2C) and strongly reduced for 2 mg/ml (Figure 2E) showing overloading effects. The mobilization flow rate was investigated as the third parameter. Figure 2B shows the MS BPE with 1 mg/ml, 4% ampholytes, and 50 nl/min. The peak profile maintenance is strongly reduced and distinct variants cannot be observed anymore with a flow rate of 50 nl/min. The velocity (or flow rate) and the transfer capillary length define the total transfer time. A transfer capillary length of 170 mm corresponds to  $\sim$ 330 nl and  $\sim$ 11 min transfer time at a flow rate of 30 nl/min. The total transfer time corresponds simultaneously to the interaction time for potential

analyte adsorption. Albeit high mobilization flow rates provide faster transfer times, increased zone broadening could be observed, most likely due to the parabolic flow profile. A sample concentration of 0.5–1 mg/ml combined with 4% ampholyte and 30 nl/min is therefore suggested as an optimal setup for the Bruker QTOF combining maximum sensitivity and the best possible peak profile preservation.

### 3.3 | iCIEF–MS with Orbitrap

Trastuzumab was characterized using the iCIEF–MS setup with an Orbitrap Fusion Lumos. Figure 3A shows the BPE acquired during pressurized mobilization from the iCIEF syringe pump. Compared with the respective iCIEF–UV analysis (see Figure 1B), a basic variant, the main variant, and two acidic variants can be assigned to the BPE peak profile. The isoelectric focused peaks can be assigned to the MS signals with low overlapping areas. Figure 3B shows the raw mass spectrum ( $m/z$  1500–4000), and Figure 3C shows a zoom of charge state +50. Both spectra indicate only a negligible effect of ESI-interfering substances from the isoelectric focusing process or sample matrix to deconvolution and mass determination. Figure 3E shows the deconvoluted mass spectrum of the main variant. The mass of the main glycoform (GOF/GOF) of the main variant was experimentally determined to 148 058.4 Da with a mass deviation of 8 ppm to the theoretically

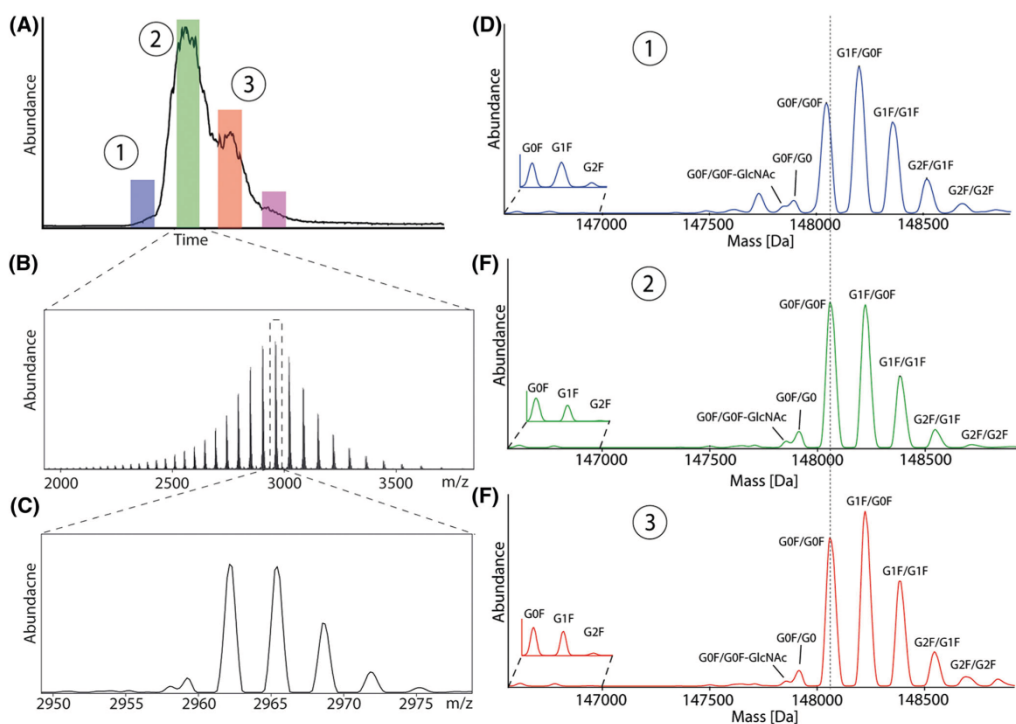


**FIGURE 3** Imaged capillary isoelectric focusing instrument to mass spectrometry (iCIEF-MS) analysis of trastuzumab (2 mg/ml, mobilization speed 30 nl/min) with Orbitrap Fusion Lumos: (A) base peak electropherogram (BPE)  $m/z$  1500–4000; (B) raw spectrum main peak charge state +50; (C) main peak charge state +50 zoomed; (D) deconvoluted spectrum of basic peak (1); (E) deconvoluted spectrum of the main peak (2); and (F) deconvoluted spectrum of acidic peak (3)

calculated mass of 148 057.2 Da [25]. Experimental standard deviations of 13 ppm (basic variant,  $n = 4$ ), 3 ppm (main variant,  $n = 4$ ), 3 ppm (acidic variant #1,  $n = 4$ ), and 4 ppm (acidic variant #2,  $n = 4$ ) could be achieved by averaging the glycoforms G0F/G0F, G0F/G1F, G1F/G1F (or G0F/G2F), G1F/G2F, and G2F/G2F. Figure 3D shows the deconvoluted mass spectrum of the low abundant basic peak, also including the low abundant singly glycosylated species G0F, G1F, and G2F. The mass difference from the main variant to the basic variant was determined to  $-19.4$  Da indicating succinimide formation from Asn ( $-17$  Da) or Asp/isoAsp ( $-18$  Da), both modifications have been previously reported for this mAb [4, 26–28]. The mass difference among main, acidic, and basic variants was determined by averaging the mass difference of the three major glycoforms G0F/G0F, G0F/G1F, and G1F/G1F (or G0F/G2F). Figure 3F shows the deconvoluted mass spectrum of the first acidic variant. Mass differences of  $+1.2$  Da (first acidic variant) and  $+1.8$  Da (second acidic

variant) could be determined indicating a single deamidation or double deamidation, respectively [4, 26–28]. The data show the potential of the presented iCIEF-MS coupling approach and the possible deep characterization of all abundant trastuzumab charge variants including glycoforms.

### 3.4 | iCIEF-MS of a fusion mAb

The second presented application is a 190 kDa fusion antibody. Due to the specific amino acid sequence and the related hydrophobic character, the fusion mAb could not be analyzed with an AD-coated cartridges (no mAb peaks in iCIEF-UV observable, data not shown). Instead, an FC-coated cartridge was applied using formamide as an additive to prevent sample aggregation and precipitation [29]. In addition, formamide is MS-compatible and does not interfere with ESI as the in FC-coated assays usually

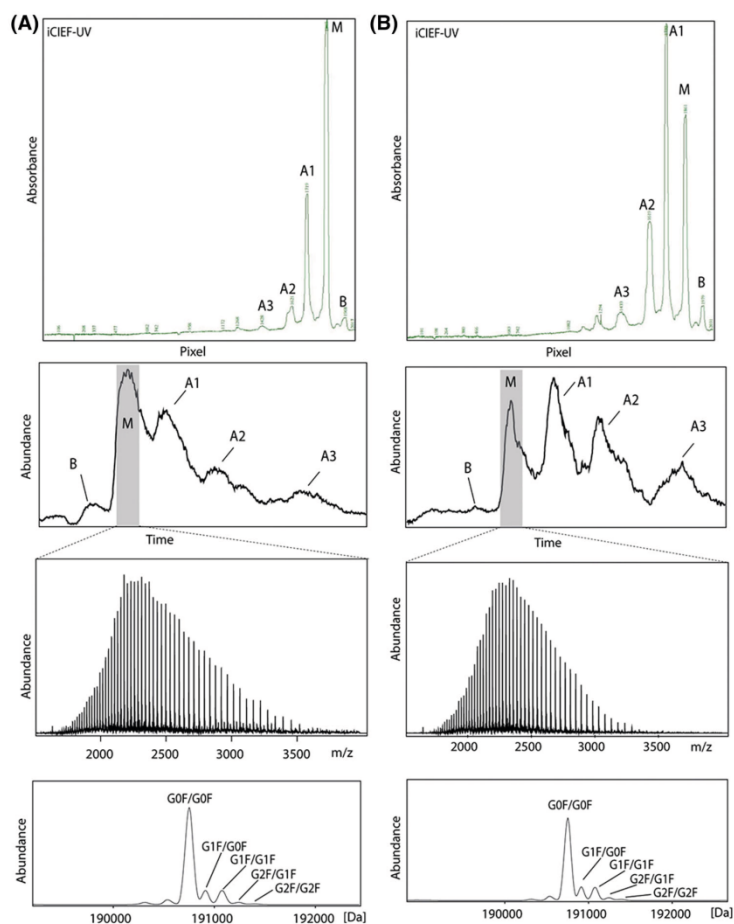


**FIGURE 4** Imaged capillary isoelectric focusing instrument to mass spectrometry (iCIEF-MS) of monoclonal antibody (mAb) 2 (1 mg/ml, 4% AESlyte HR 6–8, 30 nl/min): (A) iCIEF-UV signal (top), MS base peak electropherogram (BPE), raw mass spectrum of the main variant and deconvoluted mass spectrum (bottom) of the main variants of unstressed mAb 2; and (B) iCIEF-UV signal (top), MS BPE, raw mass spectrum of the main variant and deconvoluted mass spectrum (bottom) of the main variant of stressed mAb 2

applied additives MC or urea. Unstressed and stressed sample material was analyzed using the *CEInfinite* coupled to an Orbitrap Fusion Lumos via the nanoCEasy interface. Figure 4 shows the iCIEF-UV signals and the respective MS BPE's after mobilization. The iCIEF-UV peak profiles can be assigned clearly to the MS BPE and show low zone broadening and low peak overlap. The intact mass, represented by the most abundant glycoform GOF/GOF of the main variant, could be determined with an accuracy of 15 ppm (unstressed) and 18 ppm (stressed) with an SD of 2 ppm ( $n = 3$ ) and 3 ppm ( $n = 5$ ), respectively.

Despite the obtained low mass accuracy, the small SD's allow reliable determination of relative mass differences from the main variant to basic and acidic species (referring to GOF/GOF). The basic variant shows a mass difference of  $-19$  Da (unstressed, SD 2 ppm,  $n = 3$ ) to  $-20$  Da (stressed, SD 3 ppm,  $n = 5$ ) to the main variant indicating pyroglutamate formation ( $-18$  Da) that has already been detected on peptide level for this molecule. The acidic variants A1, A2, and A3 show a mass shift up 6 Da (unstressed, SD 6–12 ppm,  $n = 3$ ; stressed, SD 3–10 ppm,  $n = 5$ ), most likely attributed to multiple deamidated species.

#### 4 | CONCLUDING REMARKS

This study emphasizes the direct coupling of an iCIEF instrument to MS via the nanoCEasy interface. The presented setup allows the successful application of iCIEF-MS for mAbs, in particular for the narrow charge variant profile of trastuzumab. Methodical parameters for optimal peak profile maintenance during pressurized mobilization and mass spectrometric detection of imaged capillary isoelectric focused peaks were investigated. Charge variant signals could be assigned from iCIEF to MS with two different MS instruments and two exemplary applications of mAbs could be shown. Mass data of intact mAb charge variants with high spectra quality as well as high precision could be demonstrated and several major and minor glycoforms could be identified. The best possible iCIEF-MS performance can be achieved by an optimal combination of sample amount, ampholyte concentration, and mobilization rate. The sample composition, in particular, the type and concentration of ampholyte and additives, as well as the separation capillary coating, are defined by the respective analyte and have to be optimized individually for successful coupling. The presented parameters should be considered a functional starting point and may require individual optimization depending on the MS instrument used. A high mobilization flow rate (>30 nl/min) and low ampholyte concentration (<2%–3%) contributed to the loss of peak profile preservation during the mobilization step toward mass spectrometric detection. We also want to point out the transfer capillary coating quality as a crucial parameter for successful maintenance of the peak profile during transfer. The overall mass accuracy may be affected by the required ampholyte concentration and could therefore be improved, especially for >150 kDa. The general setup could still be improved in terms of distance (transfer capillary length) by a closer position of the cartridge mount to the instrument housing and shorter ESI emitters. The nanoCEasy interface provides sensitive intact mass data and prevents contamination as well as the potential impact of ampholytes on the performance of the mass spectrometer. A short straightforward setup combined with a sensitive CE-MS interface is suggested for successful direct iCIEF-MS coupling and the thus possible mAb charge variant characterization.

#### ACKNOWLEDGMENTS

The authors thank Isogen Life Science (the Netherlands), especially Martin Donker, Thu Ba Nguyen, and Kees Schijf for the provision and support with the *CEInfinite*. The authors also gratefully acknowledge Tiemin Huang and Victor Li from Advanced Electrophoresis Solutions (Canada) for providing cartridges and technical support

with the *CEInfinite*. The authors thank F. Hoffmann-La Roche, Ltd. for financial support.

Open access funding enabled and organized by Projekt DEAL.

#### CONFLICT OF INTEREST

The authors have declared no conflict of interest.

#### DATA AVAILABILITY STATEMENT

The data that support the findings of this study are available from the corresponding author upon reasonable request.

#### ORCID

Johannes Schlecht  <https://orcid.org/0000-0001-9071-5904>

Bernd Moritz  <https://orcid.org/0000-0001-9116-1878>

#### REFERENCES

- Lu RM, Hwang YC, Liu JJ, Lee CC, Tsai HZ, Li HJ, et al. Development of therapeutic antibodies for the treatment of diseases. *J Biomed Sci.* 2020;27:1.
- Liu H, Ponniah G, Zhang HM, Nowak C, Neill A, Gonzalez-Lopez N, et al. *In vitro* and *in vivo* modifications of recombinant and human IgG antibodies. *mAbs.* 2014;6:1145–54.
- Beck A, Liu H. Macro- and micro-heterogeneity of natural and recombinant IgG antibodies. *Antibodies.* 2019;8:1–22.
- Harris RJ, Kabakoff B, Macchi FD, Shen FJ, Kwong M, Andya JD, et al. Identification of multiple sources of charge heterogeneity in a recombinant antibody. *J Chromatogr.* 2001;752:233–45.
- Dick LW, Qiu D, Mahon D, Adamo M, Cheng KC. C-terminal lysine variants in fully human monoclonal antibodies: investigation of test methods and possible causes. *Biotechnol Bioeng.* 2008;100:1132–43.
- Gervais D. Protein deamidation in biopharmaceutical manufacture: understanding, control and impact. *J Chem Technol Biotechnol.* 2016;91:569–75.
- Salas-Solano O, Kennel B, Park SS, Roby K, Sosic Z, Boumajny B, et al. Robustness of iCIEF methodology for the analysis of monoclonal antibodies: an interlaboratory study. *J Sep Sci.* 2012;35:3124–9.
- Goyon A, Excoffier M, Janin-Bussat MC, Bobaly B, Fekete S, Guillaume D, et al. Determination of isoelectric points and relative charge variants of 23 therapeutic monoclonal antibodies. *J Chromatogr.* 2017;1065–6:119–28.
- Wu G, Yu C, Wang W, Wang L. Interlaboratory method validation of iCIEF methodology for analysis of monoclonal antibodies. *Electrophoresis.* 2018;39:2091–8.
- Farmerie L, Rustandi RR, Loughney JW, Dawod M. Recent advances in isoelectric focusing of proteins and peptides. *J Chromatogr A.* 2021;1651:462274.
- Sosic Z, Houde D, Blum A, Carlage T, Lyubarskaya Y. Application of imaging capillary IEF for characterization and quantitative analysis of recombinant protein charge heterogeneity. *Electrophoresis.* 2008;29:4368–76.

12. Wu J, Pawliszyn J. Universal detection for capillary isoelectric focusing without mobilization using concentration gradient imaging system. *Anal Chem.* 1992;64:2934–41.
13. Hühner J, Lämmerhofer M, Neusüß C. Capillary isoelectric focusing-mass spectrometry: coupling strategies and applications. *Electrophoresis.* 2015;36:2670–86.
14. Hühner J, Jooß K, Neusüß C. Interference-free mass spectrometric detection of capillary isoelectric focused proteins, including charge variants of a model monoclonal antibody. *Electrophoresis.* 2017;38:914–21.
15. Wang L, Bo T, Zhang Z, Wang G, Tong W, Da Yong Chen D. High resolution capillary isoelectric focusing mass spectrometry analysis of peptides, proteins, and monoclonal antibodies with a flow-through microvial interface. *Anal Chem.* 2018;90:9495–503.
16. Dai J, Lamp J, Xia Q, Zhang Y. Capillary isoelectric focusing-mass spectrometry method for the separation and online characterization of intact monoclonal antibody charge variants. *Anal Chem.* 2018;90:2246–54.
17. Dai J, Zhang Y. A middle-up approach with online capillary isoelectric focusing/mass spectrometry for in-depth characterization of cetuximab charge heterogeneity. *Anal Chem.* 2018;90:14527–34.
18. Wang L, Chen DDY. Analysis of four therapeutic monoclonal antibodies by online capillary isoelectric focusing directly coupled to quadrupole time-of-flight mass spectrometry. *Electrophoresis.* 2019;40:2899–907.
19. Xu T, Shen X, Yang Z, Chen D, Lubeckj RA, McCool EN, et al. Automated capillary isoelectric focusing-tandem mass spectrometry for qualitative and quantitative top-down proteomics. *Anal Chem.* 2020;92:15890–8.
20. Xu T, Sun L. A mini review on capillary isoelectric focusing-mass spectrometry for top-down proteomics. *Front Chem.* 2021;9:651757.
21. Montealegre C, Neusüß C. Coupling imaged capillary isoelectric focusing with mass spectrometry using a nanoliter valve. *Electrophoresis.* 2018;39:1151–4.
22. Mack S, Arnold D, Bogdan G, Bousse L, Danan L, Dolnik V, et al. A novel microchip-based imaged CIEF-MS system for comprehensive characterization and identification of biopharmaceutical charge variants. *Electrophoresis.* 2019;40:3084–91.
23. Schlecht J, Stolz A, Hofmann A, Gerstung L, Neusüß C. nanoCEasy: an easy, flexible, and robust nanoflow sheath liquid capillary electrophoresis-mass spectrometry interface based on 3D printed parts. *Anal Chem.* 2021;93:14593–8.
24. Minárik M, Groiss F, Gaß B, Blaas D, Kennidler E. Dispersion effects accompanying pressurized zone mobilisation in capillary isoelectric focusing of proteins. *J Chromatogr A.* 1996;738:123–8.
25. Jooß K, Hühner J, Kiessig S, Moritz B, Neusüß C. Two-dimensional capillary zone electrophoresis-mass spectrometry for the characterization of intact monoclonal antibody charge variants, including deamidation products. *Anal Bioanal Chem.* 2017;409:6057–67.
26. Gahoual R, Burr A, Busnel JM, Kuhn L, Hammann P, Beck A, et al. Rapid and multi-level characterization of trastuzumab using sheathless capillary electrophoresis-tandem mass spectrometry. *mAbs.* 2013;5:479–90.
27. Spanov B, Olaley O, Lingg N, Bentlage AEH, Govorukhina N, Hermans J, et al. Change of charge variant composition of trastuzumab upon stressing at physiological conditions. *J Chromatogr A.* 2021;1655:462506.
28. Diepold K, Bomans K, Wiedmann M, Zimmermann B, Petzold A, Schlothauer T, et al. Simultaneous assessment of Asp isomerization and Asn deamidation in recombinant antibodies by LC-MS following incubation at elevated temperatures. *PLoS One.* 2012;7:e30295.
29. Zhang X, Voronov S, Mussa N, Li Z. A novel reagent significantly improved assay robustness in imaged capillary isoelectric focusing. *Anal Biochem.* 2017;521:1–7.

#### SUPPORTING INFORMATION

Additional supporting information can be found online in the Supporting Information section at the end of this article.

**How to cite this article:** Schlecht J, Moritz B, Kiessig S, Neusüß C. Characterization of therapeutic mAb charge heterogeneity by iCIEF coupled to mass spectrometry (iCIEF-MS). *Electrophoresis.* 2023;44:540–548.  
<https://doi.org/10.1002/elps.202200170>



## 2.3 Manuscript III

### FORM 1

**Manuscript No. III**

**Manuscript title:**

**Two-dimensional capillary electrophoresis-mass spectrometry (CE-CE-MS):  
coupling MS-interfering capillary electromigration methods with mass  
spectrometry**

**Authors:** Johannes Schlecht, Kevin Jooß, and Christian Neusüß

#### **Bibliographic Information:**

Schlecht J, Jooß K, Neusüß C, Analytical and Bioanalytical Chemistry 2018  
410(25):6353–6359. <https://doi.org/10.1007/s00216-018-1157-9>

**The candidate is**

First author,  Co-first author,  Corresponding author,  Co-author.

#### **Authors' contributions (in %) to the given categories of the publication**

<b>Author</b>	<b>Conceptual</b>	<b>Data analysis</b>	<b>Experimental</b>	<b>Writing the manuscript</b>	<b>Provision of material</b>
Johannes Schlecht	30%	-	-	60%	-
Kevin Jooß	30%	-	-	30%	-
Christian Neusüß	40%	-	-	10%	-
<b>Total:</b>	<b>100%</b>	<b>100%</b>	<b>100%</b>	<b>100%</b>	



## Two-dimensional capillary electrophoresis-mass spectrometry (CE-CE-MS): coupling MS-interfering capillary electromigration methods with mass spectrometry

Johannes Schlecht<sup>1,2</sup> · Kevin Jooß<sup>1,3</sup> · Christian Neusüß<sup>1</sup>Received: 16 April 2018 / Revised: 17 May 2018 / Accepted: 23 May 2018 / Published online: 4 June 2018  
© Springer-Verlag GmbH Germany, part of Springer Nature 2018

### Abstract

Electromigration separation techniques often demand certain compounds in the electrolyte to achieve the required selectivity and efficiency. These compounds, including the electrolyte itself, ampholytes, polymeric compounds for sieving, complexing agents, tensides, etc. are often non-volatile. Thus, interference with the electrospray ionization process is a common issue, impeding direct coupling of such electrolyte systems to mass spectrometry. Still, several options exist to obtain mass spectra after separation, including offline fractionation, alternative ionization, dilution, or the change to volatile constituents. In the first part of this article, these methods are discussed. However, all of these options are a compromise of separation performance and sensitivity of mass spectrometric detection. Two-dimensional capillary electrophoresis-mass spectrometry (CE-CE-MS) systems represent a promising alternative to the aforementioned challenges, as they allow the use of existing methods with best separation performance in combination with sensitive mass characterization. In this context, the second part of this article is dedicated to the advantages, limitations, and applications of this approach. Finally, an outlook towards future developments is given.

**Keywords** Capillary electrophoresis · Electrospray ionization · Two-dimensional separation · Interference-free mass spectrometry · Pharmaceutical analysis · 2D interface

### Abbreviations

2D	Two dimensional	CIEF	Capillary isoelectric focusing
AA	Ascorbic acid	CZE	Capillary zone electrophoresis
ACE	Affinity capillary electrophoresis	ESI	Electrospray ionization
APCI	Atmospheric pressure chemical ionization	ICP	Inductive-coupled plasma
APPI	Atmospheric pressure photo ionization	mAb	Monoclonal antibody
ASA	Acetylsalicylic acid	MALDI	Matrix-assisted-laser desorption/ionization
BGE	Background electrolyte	MEKC	Micellar electrokinetic chromatography
CD	Cyclodextrin	MS	Mass spectrometry
CE	Capillary electrophoresis	SDS	Sodium dodecyl sulfate
CSE	Capillary sieving electrophoresis		

### Introduction

Electromigration techniques such as capillary electrophoresis (CE) enable highly selective and efficient separation for a variety of ionic compounds. Since its introduction in the early 1980s, CE has emerged as a powerful analytical routine tool in the fields of environmental analysis [1, 2], forensic analysis [3], food analysis [4], and bioanalytical analysis [5]. Electromigration includes several techniques such as capillary zone electrophoresis (CZE), capillary isoelectric focusing (CIEF), capillary sieving electrophoresis (CSE), micellar

✉ Christian Neusüß  
Christian.Neusuess@hs-aalen.de

<sup>1</sup> Faculty of Chemistry, Aalen University, Beethovenstrasse 1, 73430 Aalen, Germany

<sup>2</sup> Pharmaceutical/Medicinal Chemistry, Institute of Pharmacy, Friedrich-Schiller-University Jena, Philosophenweg 14, 07743 Jena, Germany

<sup>3</sup> Research Unit Analytical BioGeoChemistry, Helmholtz Zentrum München, Ingolstädter Landstr. 1, 85764 Neuherberg, Germany

electrokinetic chromatography (MEKC), and affinity capillary electrophoresis (ACE).

The most common mode of operation is CZE. Separation in CZE occurs according to different electrophoretic mobilities of ions based on their charge-to-size ratio in an electric field. Typical analytes span from small to large molecules, such as proteins including monoclonal antibodies (mAbs) [6]. The selectivity is mainly given by pH (charge of the analyte) and the background electrolyte (BGE). It can be altered by the type of solvent (non-aqueous capillary electrophoresis). Furthermore, additives are often used to modify the mobility, e.g., cyclodextrins can be applied for enantiomeric separation (chiral CZE) or affinity interaction can be studied by adding, e.g., antigens.

By adding a (pseudo)gel, molecules with similar charge-to-size ratio but different size can be separated referred as capillary sieving electrophoresis (CSE). This principle is widely applied for DNA sequencing [7] and protein separation [8] (after complexing with sodium dodecyl sulfate (SDS)). In CIEF, proteins and peptides are separated in a pH gradient formed in a capillary after applying an electric field. The pH gradient is formed utilizing an acidic anolyte, a basic catholyte, and ampholytes in the BGE. In MEKC, analytes are separated by the use of a pseudostationary phase consisting of micelles.

Mass spectrometry is a major technique for the characterization and identification of analytes separated in gas or liquid phase. Electrospray ionization (ESI) is an efficient way to transfer analytes separated in liquid phase into the mass analyzer, especially ionic species as separated in CE. Efficient ESI premises the absence of non-volatile constituents, which often can be achieved in liquid chromatography (LC) without compromising separation. However, most capillary electromigration techniques (as discussed above) require dedicated compounds in the electrolyte for selective separation, compatible with optical detection (UV-Vis absorption, fluorescence) but not with ESI-MS. Nevertheless, possible solutions to obtain online mass spectra from such electromigration techniques exist and are discussed in this paper.

### Strategies for direct coupling of MS-interfering capillary electromigration methods to mass spectrometry

Capillary electrophoresis coupled with mass spectrometry (CE-MS) has become a powerful routine tool for analysis of a broad range of analytes. In recent years, several applications about CE-MS have been published highlighting its diversity and importance, including metabolite and intact protein analysis [9–12]. In these applications, almost entirely volatile BGEs have been used.

The pH is the most important parameter for selectivity in CZE. The availability of volatile BGE systems in CZE, covering almost the entire pH range, enables the direct coupling of these methods to ESI-MS. Most common BGEs for CZE-MS applications are formic acid (HFA) and acetic acid (HAc) for low pH values and their respective ammonium salts for acidic to neutral pH values. Other volatile buffers for higher pH ranges include ammonium carbonate  $(\text{NH}_4)_2\text{CO}_3$  as well as ammonium hydroxide  $(\text{NH}_4\text{OH})$ . The mentioned volatile buffer electrolytes cover the total pH range. However, the type of BGE and possible additives can also influence the selectivity in CE separations, which can limit their applicability to CZE-MS. The separation of anionic active ingredients and their degradation products in effervescent tablets using different BGEs is shown in Fig. 1. In this case, only the highly ESI-interfering 100 mM tricine electrolyte enables the complete separation of all analytes. Both, the use of a lower concentrated tricine and the use of volatile acetate- or formate-based BGE are insufficient in this regard. The low number of different electrolytes suitable for CZE-MS does not only restrict the versatility of the separation itself, but also the possible use of preconcentration techniques such as transient-isotachopheresis.

CE modes such as CIEF (ampholytes, anolyte, catholyte), chiral CZE (cyclodextrins), and MEKC (surfactants) often rely on ESI-interfering electrolyte compounds. For these techniques, the complete exchange of the BGE system, avoiding non-volatile or ESI-interfering compounds is often very difficult preserving the original separation efficiency and selectivity. Nevertheless, e.g., for MEKC, volatile [13, 14] or at least semi-volatile [15] surfactants can be used in certain applications. If this most straightforward approach using volatile electrolytes is not accessible, other options need to be considered.

Another approach is the use of BGEs with low concentrated interfering compounds. Still, a compromise between MS compatible conditions and separation performance of the CE method has to be made as shown for tricine-based separation of anions in Fig. 1. In addition, low electrolyte concentration limits the possible injection volume. The most common strategy for coupling CIEF with ESI-MS is the direct hyphenation using low ampholyte concentrations. Tang et al. [16] described the first direct hyphenation of CIEF with MS using an ampholyte concentration of 0.5% for a compromise between CIEF resolution and ESI-MS detection. Further approaches of direct CIEF-MS are described in detail in a recent review [17]. Another alternative is the use of partial filling techniques, which have been applied especially for the coupling of chiral CZE and MEKC to ESI-MS [18, 19]. In these cases, the EOF and the migration direction/order play a crucial role and need to be optimized during method development.

Most CE-MS applications have been performed using a sheath liquid interface, where a sheath liquid at a flow rate in the low microliter-per-minute range provides the contact

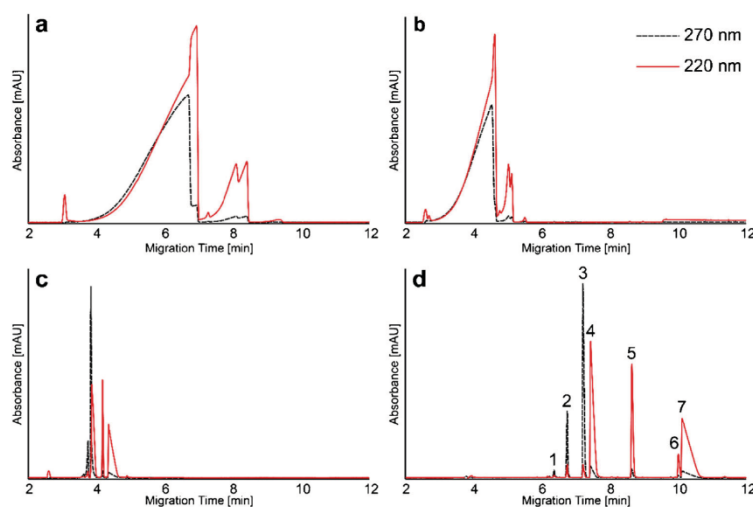


**Fig. 1** Comparison of different BGEs for the separation of ascorbic acid (AA), acetylsalicylic acid (ASA), and related degradation products in degraded effervescent tablets (RH 75%,  $T = 30\text{ }^{\circ}\text{C}$ ,  $t = 72\text{ h}$ ). The CZE-UV separation was performed applying +20 kV in a 50-cm fused silica capillary. Two different wavelengths were used: 220 nm (red, solid) and 270 nm (black, dashed). Four different BGEs are compared: 25 mM

ammonium formate, pH = 6 (a); 25 mM ammonium acetate, pH = 9 (b); 25 mM tricine, pH = 8.8 (c); 100 mM tricine, pH = 8.8 (d). The peaks in the 100 mM tricine BGE were assigned to diacetylated AA (1), monoacetylated AA (2), AA (3), ASA (4), naphatolensulfonic acid as internal standard (5), saccharin (6), and salicylic acid (7)

between the capillary outlet and a surrounding metal needle. In the last years, nanospray interfaces have become more popular, especially since the commercialization of the porous tip and a nanosheath liquid interface. For details of coupling, we refer to recent reviews [20, 21]. NanoESI processes (flow rates  $< 1000\text{ nL/min}$ ) are generally more tolerant to ESI-interfering compounds and offer higher sensitivity. Thus, these interfaces are expected to be more useful for coupling ESI-interfering CE methods with MS. The field of application regarding nanoESI in combination with non-volatile BGEs is relatively new. Nevertheless, the direct hyphenation of CIEF with MS was recently introduced by Dai et al. utilizing a nanosheath liquid interface [22]. Still, there is need for further systematic investigations regarding the degree of compromise considering the concentration of interfering substances, if nanoESI interfaces are used.

A different approach for coupling CE to MS and reduce BGE-related MS interference is the use of alternative ion sources to ESI. Examples are matrix-assisted laser desorption/ionization (MALDI) [23], atmospheric pressure chemical ionization (APCI) [24], atmospheric pressure photo ionization (APPI) [25], and inductive-coupled plasma (ICP) [26]. However, ICP is limited to elemental analysis, especially metals, whereas APCI and APPI are more suited for small, less polar analytes, which are typically not accessible by electromigration separation techniques. The use of MALDI for CE separations is limited to spotted fractions.

Still, in order to maintain the original separation performance in combination with a sensitive mass spectrometric detection, further approaches such as multidimensional separation methods need to be considered.

### CE-CE-MS for coupling MS-interfering capillary electromigration methods to mass spectrometry

Two-dimensional (2D) separation techniques are commonly used to increase peak capacity by combining two separation techniques/modes with different selectivities (e.g., combination of LC and CE methods). Hence, superior separation performance can be achieved compared with the respective individual separation dimensions [27]. Here, we discuss an alternative purpose to allow interference-free mass spectrometric detection of analytes separated in highly ESI-interfering electrolyte systems applied as the 1st dimension [28]. Remaining interfering electrolyte compounds of the 1st dimension are either completely removed from the sample or separated from the analytes of interest in the 2nd dimension prior to MS detection. Considering any CE mode as 1st dimension, there are generally two different approaches classified as offline and online.

Applying offline 2D coupling methods, fractions of a 1st separation dimension are collected and subsequently

transferred to a 2nd separation dimension. This approach is rather simple and often preferred, especially if additional sample preparation steps in between the two separation methods are required (e.g., solvent exchange, derivatization, or digestion). Nevertheless, fraction collection in CE is associated with high dilution of the sample, as typical fractions in CE are in the lower nanoliter range which have to be collected in at least a few microliters of solvent [29]. This challenge can be tackled by performing an additional concentration step prior to injection in the 2nd dimension; however, this makes the entire 2D system more complex and sensitive against disturbances. In general, offline methods are time consuming, labor intensive, and also automation is limited. Thus, in contrast with LC, fraction collection is rarely applied in CE.

In contrast, online coupling of two CE dimensions potentially enables a direct sample transfer with minor dilution. For online coupling a dedicated sample transfer in the nanoliter range from the 1st to a 2nd dimension is required. A variety of 2D concepts have been developed, including dialysis, flow gating interfaces, and microfluidic chips [30, 31]. Still, most of this work has been performed with optical detection and ESI-interfering electrolyte systems in the 2nd dimension. Especially, flow-gating interfaces and interface-free microfluidic chips are challenging to couple to MS, due to the open nature of the system (absence of outlet vial).

Mechanical-valve-based interfaces are frequently used in LC-LC coupling. Regarding the use of such a valve for CE-CE, certain other requirements need to be fulfilled. Due to the high voltages applied in CE, a fully isolated valve is required and thus, metal components in direct contact or near proximity of the electrolyte solutions must be avoided. Furthermore, based on the miniature nature of CE, the transfer of very small volumes (low nanoliter range) from the 1st to the 2nd separation dimension needs to be achieved. In recent years, our group has developed a CE-CE-MS system using a four-port mechanical valve as interface. A scheme of the general CE-CE-MS setup is depicted in Fig. 2. The valve consists of three major parts: the stator, the rotor comprising the sample loop (4–20 nL), and the motor. A mixture of polyether ether ketone and polytetrafluoroethylene was chosen as rotor and stator material to provide sufficient resistivity and tightness of the valve. Due to the material properties and the close distance of the rotor channels, up to  $\pm 15$  kV can be applied in both dimensions in order to avoid potential current breakthroughs [28]. The inlet and outlet capillaries of the 1st and 2nd separation dimension are connected to the four-port valve, respectively. In general, the 1st dimension can be operated in any CE mode (CZE, CIEF, CE(SDS), etc.) and usually UV detection is applied provided by an external detector placed right in front of the valve through the inlet. During the CE separation of the 1st dimension, the mechanical valve is kept in loading position, where the sample loop is connected to the 1st dimension, until the analyte of interest is positioned in the sample

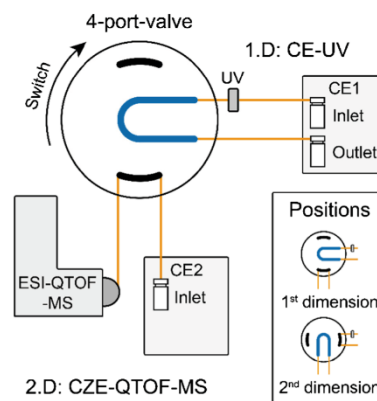


**Fig. 2** General setup of the CE-CE-MS system developed in our group. The inlet and outlet capillary of the 1st dimension CE-UV method (CE1 instrument) are connected to the four-port valve (upper, right side). An external UV detector cell is positioned in front of the valve through the inlet of the 1st dimension. Various CE separation modes can be applied as 1st dimension including CZE, CIEF, and CE(SDS). The inlet and outlet capillaries of the 2nd-dimension CZE-QTOF-MS (CE2 and MS instrument) are connected to the remaining channels of the four-port valve (lower part). During the CE(UV) separation, the mechanical valve is kept in loading position where the sample loop is connected to the 1st dimension. When the desired analyte is located in the sample loop, the valve is switched to inject position transferring the analyte from the 1st to the 2nd dimension. Subsequently, high voltage (10 to 15 kV) is applied for separation. The insert contains the position of the valve for the separation in the 1st dimension and the position of the valve for the separation in the 2nd dimension

loop. The external UV detector and the known distance between detector cell and center of the sample loop is used to determine the correct time to cut desired peaks. Subsequently, the valve is switched to inject position transferring the analyte from the 1st to the 2nd dimension and high voltage ( $\pm 10$  to 15 kV) is applied for separation. Typically, CZE is performed in the 2nd dimension due to the availability of volatile BGEs (e.g., formate or acetate). A major characteristic of this 2D setup is, that both dimension are operated completely independent (e.g., coating and equilibration procedures).

Several applications have been developed utilizing the above-mentioned CE-CE-MS system. In our group, a CZE-UV for the simultaneous determination of ascorbic acid (AA), acetylsalicylic acid (ASA), and their related degradation products in effervescent tablets has been developed. Since the BGE contains 100 mM tricine, direct coupling of this method to ESI-MS was not possible. Thus, this method was the first showcase for a highly ESI-interfering CZE method applied as 1st dimension in the CE-CE-MS setup. In this way, it was possible, for the first time, to identify mono- and diacetylated AA as major degradation products of AA in the presence of ASA [32]. Another example of an MS-incompatible CZE method as 1st dimension was the

characterization of intact monoclonal antibody (mAb) charge variants using a generic  $\epsilon$ -aminocaproic acid (EACA)-based BGE [33]. These electrolyte systems are routinely applied as pharmaceutical application and cannot be coupled directly to MS [6]. The CZE-UV electropherogram of the deglycosylated model mAb Trastuzumab is shown in Fig. 3a. Three peaks, including the main form (1) and two acidic variants (2 + 3), were cut in a heart-cut approach, transferred, and analyzed via CZE-MS in the 2nd dimension. It was possible to separate the co-transferred ESI-interfering EACA in the 2nd separation dimension prior to MS detection, as indicated in Fig. 3b. In this way, interference-free, highly precise mass data (deviation 0.4–0.8 Da) of intact charge variants of Trastuzumab were achieved (Fig. 3c–e). In combination with the electrophoretic separation, the acidic variant peaks 2 and 3 were identified as deamidation products. Another application was the separation and characterization of hemoglobin and its glycosylated form ( $\Delta pI = 0.036$ ) by CIEF-CZE-MS setup [34]. In addition, Trastuzumab was analyzed with the same CIEF-CZE-MS setup, and the results were in accordance with the findings of the CZE-CZE-MS measurements [35]. In this work, the possibility to perform multiple heart-cuts in

the same CIEF analysis was evaluated and confirmed. In addition, the 2D system was extended to imaging (i)CIEF as 1st dimension, which is a powerful technique commonly applied for the analysis of biopharmaceuticals [36]. In this work, the larger injection volume enabled the characterization of a basic variant of Trastuzumab. The observed mass shift could be explained by either succinimide formation (–17 Da) or partial cyclisation of N-terminal glutamic acid (–18 Da). Another interesting field of high ESI interference are CE methods utilizing SDS for mAb impurity analysis. We have developed a CZE method for the characterization of SDS-complexed samples based on the co-injection of positively charged surfactants and methanol as organic solvent to remove SDS from proteins. This method can be applied as 2nd dimension enabling the mass spectrometric characterization of mAb fragments and impurities (manuscript in preparation).

All these examples demonstrate the versatility of this CE-CE-MS approach using a mechanical valve. This is of special interest for the MS coupling of generic and validated methods, utilizing ESI-interfering electrolytes as frequently applied in the pharmaceutical context.

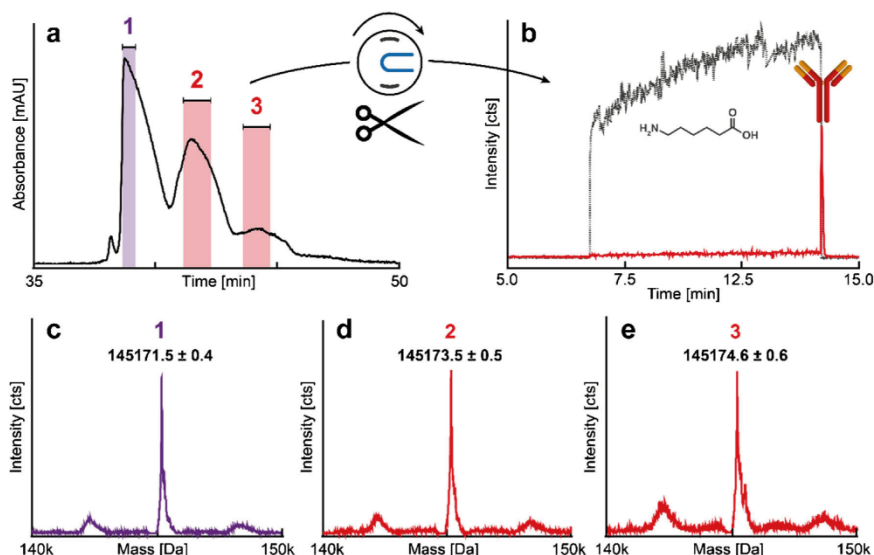


**Fig. 3** CZE-CZE-MS for the characterization of intact monoclonal antibody (mAb) charge variants. 1st-dimension CZE-UV electropherogram of deglycosylated model mAb Trastuzumab (6 mg/mL) (a) at 380 mM EACA, 1.9 mM TETA, and 0.05% HPMC (pH = 5.7) was used as BGE, commonly used as pharmaceutical application [6]. A separation voltage of +10 kV was applied. Analyte peaks (10–20 nL) were transferred in a heart-cut approach from the CZE-UV to the CZE-MS dimension. CZE-MS (2nd dimension) electropherogram of highly ESI-interfering EACA (gray, dashed) and mAb variant (red, solid) (b):

2 M HAc was used as BGE and in-house PVA-coated capillaries were applied. A separation voltage of +10 kV was applied. The co-transferred ESI-interfering EACA was successfully separated from the mAb signal in the 2nd CZE dimension prior to MS detection. Deconvoluted mass spectra of the main form M (peak 1, 10 nL cut) (c) and acidic variant A1 (peak 2, 20 nL cut) (d) and A2 (peak 3, 20 nL cut) (e). The minor mass difference of +2.0 and +3.1 Da is an indication for the presence of deamidation products. For the cut of acidic variant 3, a higher concentrated sample was applied (30 mg/mL). Modified from ref. [33]

## Outlook

Despite the ongoing development of new CE methods, many applications are still not compatible with MS detection due to the nature of the electrolytes used. Thus, there is a need for techniques to enable MS detection of analytes separated in such ESI-interfering BGEs. Nanospray interfacing will certainly make CE-MS more powerful in both, existing and new fields of application. Still, to what extent this will also enable direct coupling of ESI-interfering CE methods with MS remains open.

The introduced CE-CE-MS setup based on a mechanical valve interface is a promising approach to face the above-mentioned challenges, which is substantiated by the presented applications. Despite the already achieved results, there is still room for improvement of this design. So far, the maximum applicable voltage is limited ( $\pm 15$  kV) which influences the total method run time. A complete automation of the mechanical valve-based CE-CE-MS setup is aspired, being supported also by a detection closer to or even in the loop. In addition, interfacing for 2D coupling can be improved potentially by the use of different materials and larger distances of the channels. These characteristics will be tackled in future studies. Such improvements will contribute to expand the application of CE-MS toward classical 2D approaches for the analysis of complex samples. In this context, the combination of chromatographic and electromigration techniques is of major interest. Furthermore, the role of microfluidic chips in one and two-dimensional electromigration techniques will certainly grow in the future.

**Funding information** The authors thank Hoffman-La Roche Ltd. (Basel, Switzerland) for financial support.

## Compliance with ethical standards

**Conflict of interest** The authors declare that they have no conflict of interest.

## References

- Menzinger F, Schmitt-Kopplin P, Freitag D, Kettrup A. Analysis of agrochemicals by capillary electrophoresis. *J Chromatogr A*. 2000;891(1):45–67.
- Fukushi K, Takeda S, Chayama K, Wakida S-I. Application of capillary electrophoresis to the analysis of inorganic ions in environmental samples. *J Chromatogr A*. 1999;834(1–2):349–62.
- Anastos N, Barnett NW, Lewis SW. Capillary electrophoresis for forensic drug analysis: a review. *Talanta*. 2005;67(2):269–79.
- Frazier RA, Papadopoulou A. Recent advances in the application of capillary electrophoresis for food analysis. *Electrophoresis*. 2003;24(22–23):4095–105.
- Kraly J, Fazal MA, Schoenherr RM, Bonn R, Harwood MM, Turner E, et al. Bioanalytical applications of capillary electrophoresis. *Anal Chem*. 2006;78(12):4097–110.
- Moritz B, Schnaible V, Kiessig S, Heyne A, Wild M, Finkler C, et al. Evaluation of capillary zone electrophoresis for charge heterogeneity testing of monoclonal antibodies. *J Chromatogr B Analyt Technol Biomed Life Sci*. 2015;983-984:101–10.
- Mitnik L, Novotny M, Felten C, Buonocore S, Koutny L, Schmalzing D. Recent advances in DNA sequencing by capillary and microdevice electrophoresis. *Electrophoresis*. 2001;22(19):4104–17.
- Zhu Z, Lu JJ, Liu S. Protein separation by capillary gel electrophoresis: a review. *Anal Chim Acta*. 2012;709:21–31.
- Schmitt-Kopplin P, Frommberger M. Capillary electrophoresis-mass spectrometry: 15 years of developments and applications. *Electrophoresis*. 2003;24(22–23):3837–67.
- Desiderio C, Rossetti DV, Iavarone F, Messina I, Castagnola M. Capillary electrophoresis-mass spectrometry: recent trends in clinical proteomics. *J Pharm Biomed Anal*. 2010;53(5):1161–9.
- Klepárník K. Recent advances in combination of capillary electrophoresis with mass spectrometry: methodology and theory. *Electrophoresis*. 2015;36(1):159–78.
- Monton MRN, Terabe S. Recent developments in capillary electrophoresis-mass spectrometry of proteins and peptides. *Anal Sci*. 2005;21(1):5–13.
- Petersson P, Jömtén-Karlsson M, Stålebro M. Direct coupling of micellar electrokinetic chromatography to mass spectrometry using a volatile buffer system based on perfluorooctanoic acid and ammonia. *Electrophoresis*. 2003;24(6):999–1007.
- van Biesen G, Bottaro CS. Ammonium perfluorooctanoate as a volatile surfactant for the analysis of N-methylcarbamates by MEKC-ESI-MS. *Electrophoresis*. 2006;27(22):4456–68.
- Moreno-González D, Haselberg R, Gámiz-Gracia L, García-Campaña AM, de JGJ, Somsen GW. Fully compatible and ultrasensitive micellar electrokinetic chromatography-tandem mass spectrometry using sheathless porous-tip interfacing. *J Chromatogr A*. 2017;1524:283–9.
- Tang Q, Harrata AK, Lee CS. Capillary isoelectric focusing-electrospray mass spectrometry for protein analysis. *Anal Chem*. 1995;67:3515–9.
- Hühner J, Lämmerhofer M, Neusüb C. Capillary isoelectric focusing-mass spectrometry: coupling strategies and applications. *Electrophoresis*. 2015;36(21–22):2670–86.
- Silva M. MEKC: an update focusing on practical aspects. *Electrophoresis*. 2007;28(1–2):174–92.
- Simó C, García-Cañas V, Cifuentes A, CE-MS C. *Electrophoresis*. 2010;31(9):1442–56.
- Týčová A, Ledvína V, Klepárník K. Recent advances in CE-MS coupling: instrumentation, methodology, and applications. *Electrophoresis*. 2017;38(1):115–34.
- Lindenburg PW, Haselberg R, Rozing G, Ramautar R. Developments in interfacing designs for CE-MS: towards enabling tools for proteomics and metabolomics. *Chroma*. 2015;78(5–6):367–77.
- Dai J, Lamp J, Xia Q, Zhang Y. Capillary isoelectric focusing-mass spectrometry method for the separation and online characterization of intact monoclonal antibody charge variants. *Anal Chem*. 2018;90(3):2246–54.
- Stutz H. Advances in the analysis of proteins and peptides by capillary electrophoresis with matrix-assisted laser desorption/ionization and electrospray-mass spectrometry detection. *Electrophoresis*. 2005;26(7–8):1254–90.
- Isoo K, Otsuka K, Terabe S. Application of sweeping to micellar electrokinetic chromatography-atmospheric pressure chemical ionization-mass spectrometric analysis of environmental pollutants. *Electrophoresis*. 2001;22(16):3426–32.
- Mol R, de JGJ, Somsen GW. Atmospheric pressure photoionization for enhanced compatibility in on-line micellar electrokinetic

- chromatography-mass spectrometry. *Anal Chem.* 2005;77(16):5277–82.
26. Chen J, Fu F, Wu S, Wang J, Wang Z. Simultaneous detection of zinc dimethyldithiocarbamate and zinc ethylenebis(dithiocarbamate) in cabbage leaves by capillary electrophoresis with inductively coupled plasma mass spectrometry. *J Sep Sci.* 2017;40(19):3898–904.
  27. Malerod H, Lundanes E, Greibrokk T. Recent advances in on-line multidimensional liquid chromatography. *Anal Methods.* 2010;2(2):110–22.
  28. Kohl FJ, Montealegre C, Neusüß C. On-line two-dimensional capillary electrophoresis with mass spectrometric detection using a fully electric isolated mechanical valve. *Electrophoresis.* 2016;37(7–8):954–8.
  29. Helmja K, Borissova M, Knjazeva T, Jaanus M, Muinasmaa U, Kaljurand M, et al. Fraction collection in capillary electrophoresis for various stand-alone mass spectrometers. *J Chromatogr A.* 2009;1216(17):3666–73.
  30. Kohl FJ, Sánchez-Hernández L, Neusüß C. Capillary electrophoresis in two-dimensional separation systems: techniques and applications. *Electrophoresis.* 2015;36(1):144–58.
  31. Kler PA, Sydes D, Huhn C. Column-coupling strategies for multi-dimensional electrophoretic separation techniques. *Anal Bioanal Chem.* 2015;407(1):119–38.
  32. Neuberger S, Jooß K, Ressel C, Neusüß C. Quantification of ascorbic acid and acetylsalicylic acid in effervescent tablets by CZE-UV and identification of related degradation products by heart-cut CZE-CZE-MS. *Anal Bioanal Chem.* 2016;408(30):8701–12.
  33. Jooß K, Hühner J, Kiessig S, Moritz B, Neusüß C. Two-dimensional capillary zone electrophoresis-mass spectrometry for the characterization of intact monoclonal antibody charge variants, including deamidation products. *Anal Bioanal Chem.* 2017;409(26):6057–67.
  34. Hühner J, Neusüß C. CIEF-CZE-MS applying a mechanical valve. *Anal Bioanal Chem.* 2016;408(15):4055–61.
  35. Hühner J, Jooß K, Neusüß C. Interference-free mass spectrometric detection of capillary isoelectric focused proteins, including charge variants of a model monoclonal antibody. *Electrophoresis.* 2017;38(6):914–21.
  36. Montealegre C, Neusüß C. Coupling imaged capillary isoelectric focusing with mass spectrometry using a nanoliter valve. *Electrophoresis.* 2018; <https://doi.org/10.1002/elps.201800013>



## 2.3 Manuscript IV

### FORM 1

**Manuscript No. IV**

**Manuscript title:**

**Two-Dimensional Capillary Zone Electrophoresis-Mass Spectrometry: Intact mAb Charge Variant Separation Followed by Peptide Level Analysis Using In-Capillary Digestion**

**Authors:** Johannes Schlecht, Kevin Jooß, Bernd Moritz, Steffen Kiessig, and Christian Neusüß.

**Bibliographic Information:**

Schlecht J, Jooß K, Moritz B, Kiessig S, Neusüß C, 2023 Analytical Chemistry 95(8):4059-4066. <https://doi.org/10.1021/acs.analchem.2c04578>

**The candidate is**

First author,  Co-first author,  Corresponding author,  Co-author.

**Authors' contributions (in %) to the given categories of the publication**

Author	Conceptual	Data analysis	Experimental	Writing the manuscript	Provision of material
Johannes Schlecht	30%	60%	90%	80%	
Kevin Jooß	20%	20%	10%	10%	
Bernd Moritz	5%				x
Steffen Kiessig	5%				x
Christian Neusüß	40%	20%		10%	
Total:	100%	100%	100%	100%	

# Two-Dimensional Capillary Zone Electrophoresis-Mass Spectrometry: Intact mAb Charge Variant Separation Followed by Peptide Level Analysis Using In-Capillary Digestion

Johannes Schlecht, Kevin Jooß, Bernd Moritz, Steffen Kiessig, and Christian Neusüß\*

Cite This: *Anal. Chem.* 2023, 95, 4059–4066

Read Online

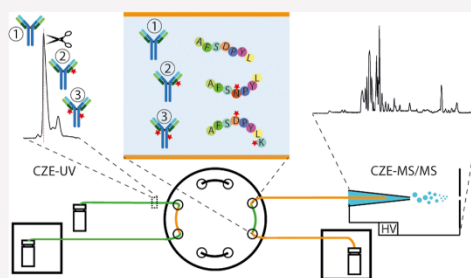
ACCESS |

Metrics & More

Article Recommendations

Supporting Information

**ABSTRACT:** Characterization of charge heterogeneity is an essential pillar for pharmaceutical development and quality control of therapeutic monoclonal antibodies (mAbs). The highly selective and commonly applied capillary zone electrophoresis (CZE) method containing high amounts of  $\epsilon$ -aminocaproic acid (EACA) provides a detailed and robust charge heterogeneity profile of intact mAb variants. Nevertheless, the exact location of protein modifications within these charge profiles remains ambiguous. Electrospray ionization mass spectrometry (ESI-MS) is a promising tool for this purpose; however, EACA is incompatible with electrospray. In this context, we present a two-dimensional CZE-CZE-MS system to combine efficient charge variant separation of intact mAbs with subsequent peptide analysis after in-capillary digestion of selected charge variants. The first dimension is based on a generic CZE(EACA) method in a fused silica capillary. In the second dimension, a neutral-coated capillary is used for in-capillary reduction and digestion with Tris(2-carboxyethyl)phosphine (TCEP) and pepsin, followed by CZE separation and MS/MS-characterization of the resulting peptides. The setup is demonstrated using stressed and nonstressed mAbs where peaks of basic, main, and acidic variants were transferred in a heart-cut fashion, digested, and characterized on the peptide level. Sequence coverages of more than 90% were obtained for heavy chain (HC) and light chain (LC) for four different mAbs, including low-abundance variants (<2% of the main peak). Frequently observed modifications (deamidation, oxidation, etc.) could be detected and localized. This study demonstrates a proof-of-concept for identification and localization of protein modifications from CZE charge heterogeneity profiles and, in this way, is expected to support the development and quality control testing of protein pharmaceuticals.



## 1. INTRODUCTION

Therapeutic monoclonal antibodies (mAbs) have become an indispensable part of modern medicine and associated treatment options. By 2022, more than 100 mAbs were approved by the United States Food and Drug Administration (FDA) and European Medicines Agency (EMA) with cancer and immunological diseases representing the majority of therapeutic applications.<sup>1,2</sup> Global sales of more than 135 billion euros in 2019 are expected to further increase in the coming years, demonstrating the large potential and importance of such biotherapeutics.<sup>3</sup> The production and storage of mAbs are subject to close monitoring as different modifications such as deamidation, C-terminal lysine clipping, oxidation, or pyroglutamate formation can occur.<sup>4,5</sup> These variants, oftentimes affecting charge heterogeneity, can have a potential negative impact on safety or efficacy of the respective drug.<sup>6–8</sup> Therefore, identification of mAb variants is of utmost importance for quality control and release testing of protein pharmaceuticals. Chromatographic<sup>9</sup> and electromigrative<sup>10–12</sup>

separation techniques are frequently utilized for the analysis of therapeutic mAbs in the biopharmaceutical environment. The highly selective capillary zone electrophoresis (CZE) method containing high amounts of  $\epsilon$ -aminocaproic acid (EACA) provides a detailed and robust charge heterogeneity profile of intact variants and is widely applied in the biopharmaceutical industry.<sup>13,14</sup>

Concurrently, mass spectrometry (MS) is one of the most valuable tools for protein characterization today. However, mass spectrometric identification of upfront separated mAb charge variants is challenging, as most of the applicable separation methods such as ion exchange chromatography

Received: October 17, 2022

Accepted: February 8, 2023

Published: February 17, 2023



(IEC), capillary isoelectric focusing (CIEF), and capillary zone electrophoresis (CZE) rely on electrospray (ESI)-interfering compounds either due to their general separation concept or to achieve desired separation performance. One way to overcome this limitation for CE and LC is to employ two- or multidimensional separation systems prior to ESI-MS coupling.<sup>15–19</sup> There are two different approaches to deal with ESI-incompatible substances in two-dimensional systems. Either the second dimension provides an orthogonal separation method resulting in increased separation power or it provides a cleanup method for removing any transferred interfering substances.

Peptide mapping after proteolytic digestion represents a core element for the characterization of mAb modifications which requires several time-consuming steps such as reduction, alkylation, and buffer exchanges. Consequently, it is routinely performed in an off-line fashion. In contrast, digestion methods performed in-capillary provide a shorter overall analysis time and potentially result in fewer artifacts originating from the applied digestion protocol steps. Several examples for multidimensional LC-MS including preceding charge heterogeneity separation followed by on-column reduction and tryptic digestion have been reported, providing high sequence coverages (SC), post translational modification (PTM) localization, and fast analysis times.<sup>20–23</sup> In-capillary digestion has been also developed and reported for capillary electrophoresis (CE) applications using trypsin as proteolytic enzymes by successive injection of plugs containing proteolytic buffer, enzyme, and protein in a sandwich-like manner.<sup>24,25</sup>

More recently, this approach was also applied using IdeS or trypsin digestion for middle-up and bottom-up CE-MS analysis of therapeutic mAbs.<sup>26,27</sup> In-capillary digestion reduces the needed time (minutes instead of hours) and the amount of enzyme (nL instead of  $\mu\text{L}$ ) and increases the digestion efficiency due to the small capillary volume. To date, no CE setup, combining intact and peptide level analysis for mAb charge heterogeneity characterization comparable to multidimensional LC-MS approaches, has been described.

Here, we present a capillary-based two-dimensional CZE-CZE-MS system to combine efficient charge variant separation on the intact mAb level with subsequent fast peptide analysis after in-capillary digestion of selected charge variants. The recently introduced nanoflow sheath liquid interface *nanoCEasy* was used for MS coupling, providing sensitivity and robustness including coating and recoating of the second dimension during ESI operation.<sup>28</sup> A double UV-detector setup was implemented in the first dimension to allow reproducible and precise heart-cuts of charge variants. Four different mAbs were selected, digested, and characterized by CZE-MS/MS in this is proof-of-concept study. To the best of our knowledge, this is the first example of in-capillary reduction and digestion of capillary-based charge heterogeneity separation with subsequent MS detection for peptide mapping and PTM localization.

## 2. EXPERIMENTAL SECTION

**2.1. Chemicals, Materials, and Samples.** Isopropanol (LC-MS grade) and formic acid (FA,  $\geq 98\%$ ) were obtained from Carl Roth GmbH & Co. KG (Karlsruhe, Germany). Hydrofluoric acid (HF, 40% (v/v)), sodium hydroxide (NaOH), hydrochloric acid (HCl, 37%), and acetic acid (HA, 100%) were purchased from Merck KGaA (Darmstadt, Germany). Trypsin, pepsin, hydroxypropyl cellulose (HPC),

triethylenetetramine (TETA), caffeine (99%), and Tris(2-carboxyethyl)phosphine hydrochloride (TCEP) were obtained from Sigma-Aldrich (Steinheim, Germany). Poly(ethylene oxide) (PEO, MW 1,000,000) and  $\epsilon$ -aminocaproic acid (EACA) were obtained from Alfa Aesar (Kandel, Germany). All solutions were prepared using ultrapure water (18 M $\Omega$ -cm at 25 °C, SG Ultra Clear UV from Siemens Water Technologies, USA). Trastuzumab aliquots (25 mg/mL) were provided by F. Hoffmann-La-Roche AG (Basel, Switzerland). NIST mAb (Reference Material 8671) was obtained from the National Institute of Standard and Technology (NIST, Gaithersburg, MD, USA). mAb 3 and mAb 4 were provided by our research collaborators. Fused silica (FS) capillaries (50 and 100  $\mu\text{m}$  inner diameter (ID), 365  $\mu\text{m}$  outer diameter (OD)) were purchased from Polymicro Technologies (Phoenix, AZ, USA). Emitters with 30 and 20  $\mu\text{m}$  tip ID were obtained from BioMedical Instruments (Zoellnitz, Germany). Aliquots of trastuzumab were stressed at 40 °C for 4 weeks in an Eppendorf ThermoMixer in the dark without any mixing. Trastuzumab, NIST mAb, mAb 3, and mAb 4 were diluted prior to injection to a final concentration of 1, 2, or 5 mg/mL using ultrapure water. Pepsin aliquots (4 mg/mL) were prepared with ultrapure water and kept at  $-20$  °C until use. Each day, a digestion mix was freshly prepared containing 3.8  $\mu\text{g}/\mu\text{L}$  pepsin, 0.5 M FA (pH  $\sim 2$ ), and 40 mM TCEP.

**2.2. Instrumentation.** **2.2.1. Instrumental Setup and Two-Dimensional Setup.** The technical setup of the two-dimensional CZE-CZE-MS system is shown in Figure 1. The

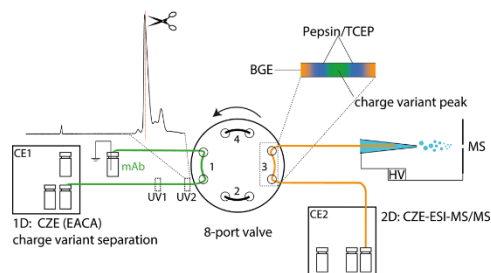


**Figure 1.** Set-up of CZE(EACA)-CZE-MS/MS with in-capillary reduction and digestion. First dimension: 55 (45 + 10) cm FS capillary, UV detection (214 nm) at two positions (32.5 and 40.5 cm). BGE: 380 mM EACA, 2 mM TETA, 0.05% HPC, pH 5.7. Valve: 8-port valve with multiposition actuator (customized C2M-4358). Second dimension: 93 (35 + 48) cm FS capillary connected to an Orbitrap Fusion Lumos via the nanoCEasy interface. BGE: 0.2 M FA. Zoom at loop 3 shows the arrangement of plugs after the cut procedure (mAb peak cut and transferred in between a large plug of pepsin/TCEP solution).

2D-CZE-CZE experiments were performed on two Agilent HP 3D CE instruments (Waldbronn, Germany) equipped with ChemStation software for instrument control. In the first dimension (CZE(EACA)), a capillary (FS, ID 50  $\mu\text{m}$ ) with a total length of 55 cm was used with 45 cm from the CE inlet to the valve and 10 cm from the valve to the external outlet. UV detection was performed at two positions in the first dimension (at 32.5 and 40.5 cm) with two external ECD2600 UV detectors (ECOM spol. s r.o., Prague, Czech Republic) at a wavelength of 214 nm. The capillaries were connected to a customized 8-port valve (C2M-4358, VICI AG International

(Schenkon, Switzerland)) with a multiposition electric micro-actuator and 360  $\mu\text{m}$  fittings. The stator, rotor (24 nL loop volume), and the fittings were manufactured from PEEK material. In the second dimension (CZE-MS), a PEO-coated capillary with a total length of 93 cm was applied with 35 cm from the CE inlet to the valve and 58 cm from the valve to the CE-MS interface. This part of the capillary from the valve to the CE-MS interface was previously etched on one end as described elsewhere.<sup>28</sup> The etched capillary was coupled to an Orbitrap Fusion Lumos (Thermo Fisher Scientific, San Jose, CA, USA) via the nanoCEasy interface.<sup>28</sup> The nanoCEasy interface provides two different modes: a conditioning mode, where the SL capillary is positioned in the front of the ESI emitter, and a separation mode, where the separation capillary is positioned in the front of the ESI emitter. Any liquid leaving the separation capillary during the conditioning mode is flushed to waste and sprayed toward MS during separation mode. The etched capillary of the second dimension was kept in conditioning mode during all rinsing and (re)coating steps, avoiding ESI interference or MS contamination. The etched capillary of the second dimension was positioned in front of the emitter during the separation mode. For all experiments, 50% isopropanol +0.2% FA was used as sheath liquid. Sheath liquid delivery rates were 3–8  $\mu\text{L}/\text{min}$ . In the separation mode, the tip of the separation capillary was placed 1.8 mm from the 30  $\mu\text{m}$  emitter tip and 2 mm from the 20  $\mu\text{m}$  emitter tip. The distance between the emitter and MS orifice was set to 3.0 mm for all measurements.

**2.3. Methods.** **2.3.1. CZE(EACA)-UV (First Dimension).** The BGE was adapted from He et al.<sup>13</sup> and consisted of 380 mM EACA, 2 mM TETA, and 0.05% HPC; the pH was adjusted to 5.7 using HA. For 100 mL of BGE, 125  $\mu\text{L}$  of HA were added. Capillaries were preconditioned prior to each run by rinsing with 0.1 M HCl for 5 min and BGE for 15 min at 3 bar, respectively. Samples were injected hydrodynamically by applying 50 mbar for 16 s (27 nL), the separation voltage was set to 15 kV in normal polarity mode.

**2.3.2. CZE-MS (Second Dimension).** A 93 cm PEO-coated capillary and 0.2 M FA as BGE was used in the second dimension. Briefly, PEO stock solution was prepared by dissolving 100 mg of PEO in 45 mL of water by heating at 95  $^{\circ}\text{C}$ . The PEO coating solution was prepared by adding 0.5 mL of 0.1 M HCl to 4.5 mL of PEO stock solution. Daily (re)coating of the capillary was performed by successive rinsing with 1 M NaOH, water, and 0.1 M HCl for 3 min, respectively; PEO coating solution for 6 min; water for 5 min; and BGE for 5 min applying a pressure of 3 bar for all rinsing steps. A caffeine plug (50 mbar, 10 s) was injected daily in the morning; 50 mbar was applied and detected by MS. The infusion time of the caffeine plug was taken as a reference to determine the infusion time for the 60 nL plug of digestion mix which was placed in the valve loop before the heart-cut procedure. The capillary was preconditioned prior to each run by rinsing with BGE for 5 min.

**2.3.3. Heart-Cut Procedure, In-Capillary Digestion, and Peptide Separation.** The velocity of charge variant peaks during the separation was determined by UV detection at two positions with a fixed distance of 8 cm. The migration time  $t_1$  and the migration time  $t_2$  (determined by UV1 and UV2) allow the calculation of the average velocity between these two positions, and an estimation of the migration time for the peak of interest reaching valve loop 1 ( $t_3$ ) can be performed. During separation in the first dimension, a large plug (60 nL) of

digestion mix (pepsin+TCEP) was positioned in valve loop 3. At  $t_3$ , the separation in the first dimension was stopped and the valve was switched immediately to transfer the peak of interest in the second dimension. The peak of interest from the first dimension was placed between two plugs of roughly 18 nL of digestion mix, and 50 mbar was applied for 60 s to push the digestion mix out of the valve loop. After a digestion time of 10 min, a separation voltage of 15 kV in normal polarity mode was applied. Capillary temperature was not controlled (room temperature,  $\sim 25$   $^{\circ}\text{C}$ ).

**2.3.4. MS Acquisition.** All MS experiments were performed on an Orbitrap Fusion Lumos Tribrid mass spectrometer (Thermo Fisher Scientific, San Jose, CA, USA). The mass spectrometer was operated in positive ionization mode with spray voltage set to 1600 V and temperature of the ion transfer tube set to 300  $^{\circ}\text{C}$ . The instrument was operated in data-dependent acquisition mode with an MS<sup>1</sup> scan range of 350–2,000  $m/z$ , detection in the Orbitrap at a resolution of 120,000, and normalized automatic gain control (AGC) set to 25%. The 5 most intense ions above a threshold ion count of 10,000 were selected for fragmentation at a normalized collision energy of 28% (HCD); dynamic exclusion was set to 60 s. The fragment ion spectra were acquired in the ion trap (rapid mode).<sup>29</sup>

**2.4. Data Analysis.** UV data was acquired using ECOMAC software (version 0.281). MS data was processed with Freestyle 1.7 (Thermo Fisher Scientific), Byonic 3.8 (Protein Metrics), or ProteomeDiscoverer 2.5 (Thermo Fisher Scientific). The digestion specificity was selected to be “non-specific”; the precursor mass tolerance was set to 10 ppm; the fragment tolerance was set to 0.5 Da. Deamidation (+0.984 Da), oxidation (+15.9949 Da), and C-terminal lysine clipping (–128.175 Da) were considered as modifications for the peptide search. Validation of PSMs was done using the Percolator algorithm and 1% FDR. Only peptides with high confidence were considered.

### 3. RESULTS AND DISCUSSION

**3.1. Development of In-Capillary Digestion.** The protocol for in-capillary digestion (for the second dimension) was initially developed in a one-dimensional approach. First, the compatibility of the digestion protocol with the EACA-based BGE was investigated, and therefore, the influence of EACA on trypsin was evaluated in preliminary offline digestion experiments. EACA is not only ESI-incompatible but at the same time, it inhibits serine proteases, including the frequently applied proteolytic enzyme trypsin due to its structural similarity to lysine.<sup>30</sup> In contrast, alternative proteolytic enzymes such as pepsin are not expected to be affected by EACA as aspartate proteases have a different active center containing 2x Asp instead of 2x Ser. Furthermore, pepsin has a pH optimum of  $\sim 2$ ,<sup>31</sup> which fits perfectly with acidic BGEs frequently used in CZE-MS. Consequently, in contrast to other protocols, no complex buffer plug arrangement is required to preserve the pH around the enzymes' optimum. In addition, pepsin provides fast digestion times as well as tolerance toward low temperature and reducing conditions and thus is one of the acidic proteases commonly applied in hydrogen exchange chromatography coupled to mass spectrometry (HDX-MS).<sup>32–34</sup>

Thus, as expected, a low amount of 50 mM EACA added to a trypsin-containing digestion buffer led to strongly reduced proteolytic activity regarding the intensity of selected peptide  $m/z$  ratios (Figure S2a,b). In contrast, pepsin was significantly

less affected by EACA in offline experiments (Figure S2c). For the one-dimensional in-capillary digestion with pepsin, parameters such as plug size (5–30 nL), pepsin concentration (0.4–10 mg/mL), mAb concentration (1–10 mg/mL), TCEP concentration (20–100 mM), plug mixing strategy (alternating voltage, alternating pressure, only forward pressure), digestion time (5–60 min), and digestion temperature (25 or 37 °C) were evaluated and optimized. Figure 2 shows the base peak

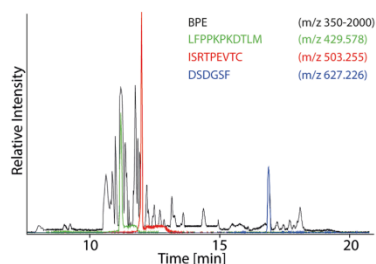


**Figure 2.** BPE of one-dimensional in-capillary reduction and digestion. 1 mg/mL trastuzumab, 3.8 mg/mL pepsin, 40 mM TCEP, 70 cm PEO-coated capillary, BGE 0.2 M FA, 10 min digestion time, 30 kV, 350–2000 *m/z*. Selected EIEs: LFPPKPKDTLM (green trace, 429.578 *m/z*), ISRTPEVTC (red trace, 503.255 *m/z*), DSDGSF (blue trace, 627.226 *m/z*).

electropherogram (BPE) and selected extracted ion electropherograms (EIEs) after in-capillary digestion and reduction of trastuzumab with pepsin providing a total sequence coverage of 100%. Optimized parameters (considering sequence coverage) were found at 18–20 nL plug size, 3.8 mg/mL pepsin, 1 mg/mL mAb, 40 mM TCEP, mixing by pressure (flush 9 s, forward), and 10 min digestion time at room temperature. TCEP was chosen as reducing agent for the acidic conditions and due to its irreversible reduction mechanism. The addition of TCEP increased the sequence coverage from previously ~87% (heavy chain, HC) and ~79% (light chain, LC) to the above-mentioned 100% for both chains. PEO is a neutral hydrophilic coating<sup>35</sup> preventing adsorption of mAb or digestion enzyme to the capillary wall and was applied including frequent regeneration without disassembling via the nanoCEasy interface. A blank run containing only BGE in the first dimension was performed to avoid false-positive peptides coming from pepsin autolysis. Only a single peptide of trastuzumab (HC57, YTRYADSVKGRF) could be detected with low confidence, indicating a high confidence in the previously observed peptides. The potentially false-positive peptide was removed from the list of detected peptides leading to no loss in total sequence coverage as this sequence area was also covered by other peptides. No peptides were found for the other mAbs in blank runs.

**3.2. CE-CE Setup with Double UV Detector for Heart-Cut.** Two-dimensional heart-cut systems require a precise cutting procedure for reproducible transfer of desired analytes from the first into the second dimension. In this context, an accurate determination of the migration time when the analyte reaches the sample loop is necessary. This can be achieved either by assuming a constant migration velocity or by using pressure to position the analyte in the sample loop after a single-point UV detection.<sup>17,18</sup> The first mentioned method works well in viscous BGE systems using electrokinetic

injection but exhibited limited success in nonviscous systems applying hydrodynamic injection. Due to field inhomogeneities after hydrodynamic injection and related stacking effects, the migration velocity of the analyte does not remain constant over the whole capillary length. This issue could be overcome using pressure to position the analyte inside the sample loop after detection and high voltage was turned off. This approach demands a constant internal pressure of the CE system and a constant back pressure of the capillaries and valve connections.<sup>17</sup> In the 2D approach presented here, two UV detectors were implemented for the first dimension bypassing any possible initial field inhomogeneities and related changes in migration velocity after hydrodynamic injection or back pressure-related changes due to potential clogging or dead volume after switching. UV detection at two positions allows precise determination of the migration velocity between these two positions and the expected migration time of the charge variant peak to reach the center of the valve loop for subsequent peak transfer into the second dimension. The relative standard deviation (RSD) of obtained migration times and respective migration velocities using the two-point UV detection approach was less than 1.2% ( $n = 3$ ), which is close to the known achievable repeatability of ~1% for the CZE(EACA) method. In addition, an estimation of the peak volume at the position of detection is possible. Figure 3 shows an electropherogram of trastuzumab and the estimated volume of 24 nL (corresponding to valve loop volume) indicated by blue bars for a basic, the main, and an acidic charge variant. This volume was calculated according to the determined migration velocity of 0.19–0.21 mm/s (depending on the charge variant peak). The blue bars show that the heart-cut volume of 24 nL (valve loop volume) fits well to the obtained peak widths and only low overlap between the peaks can be expected. In the case of more narrow charge variant profiles, it would be possible to exchange the rotor using a smaller rotor loop volume (4–10 nL) to prevent heart-cuts of overlapping peaks.<sup>36</sup>

**3.3. CE-CE-MS/MS with In-Capillary Digestion.** Intact mAb charge variants were separated by CZE in the first dimension; selected peaks were cut and transferred into the second dimension with subsequent in-capillary reduction and digestion as described in Methods. The generated peptides were characterized by CZE-MS/MS, and the obtained data was evaluated regarding SC and PTMs. The total run time was below 2 h per heart-cut, with <60 min (conditioning + separation) for the first dimension and about 60 min (10 min digestion + 50 min separation) for the second dimension. Sequence coverage is an important parameter for peptide mapping and PTM localization. High SCs increase the chance of discovering modifications at relevant sequence areas. A complete list of identified peptides of trastuzumab and the NIST mAb (main peak nonstressed) is included in the Supporting Information (Tables S3 and S4). This list also indicates the heterogeneous cleavage sites related to pepsin which has lower specificity than other more frequently used proteases such as trypsin (see section 3.4). Sequence areas and peptides not covered are probably caused by either pepsin specificity or low ESI efficiency. In this work, SCs of 94%–97% (HC+LC for all investigated mAbs) could be achieved (see Table 1). The SCs listed in Table 1 were calculated for the main peak with a concentration of 1 mg/mL and correspond to ~19–22 ng (based on peak area in UV), depending on the respective mAb (injection volume 27 nL = 27 ng mAb). An

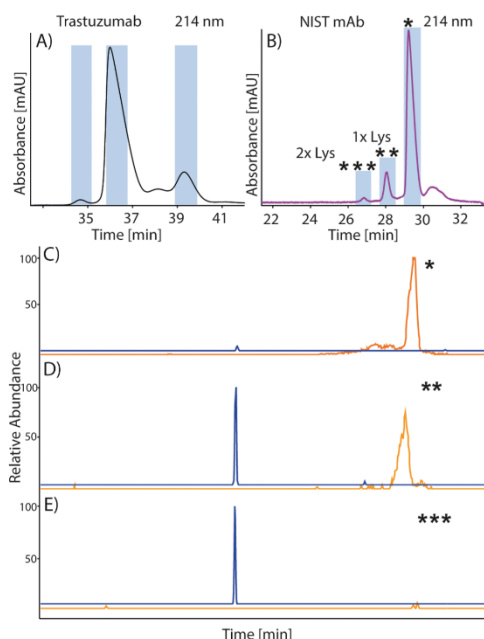


**Figure 3.** CZE-UV of (A) trastuzumab and (B) NIST mAb (1 mg/mL), 55 cm (40.5 cm), 15 kV, 214 nm. BGE: 380 mM EACA, 2 mM TETA, 0.05% HPC, pH 5.7. Blue bars indicate a volume of 24 nL (corresponds to valve loop volume) calculated according to the determined migration velocity between two UV detectors of the respective charge variant peak. (C) EIEs of LSLSPG (orange) and LSLSPGK (blue), basic peak containing 2x Lys (C-terminal). (D) EIEs of LSLSPG (orange) and LSLSPGK (blue), basic peak containing 1x Lys (C-terminal). (E) EIEs of LSLSPG (orange) and LSLSPGK (blue), main peak containing 0x Lys (C-terminal). Migration times and abundance of panels C–E were normalized.

**Table 1.** Main Variant Sequence Coverage after Charge Heterogeneity Separation (CZE) and In-Capillary Digestion with Pepsin

mAb	HC	LC
NIST mAb ( $n = 3$ )	98.8%	96.6%
trastuzumab ( $n = 3$ )	93.3%	94.4%
mAb 3 ( $n = 2$ )	94.5%	93.9%
mAb 4 ( $n = 2$ )	99.3%	88.8%

example of the sensitivity of this method is the lowest abundant basic variant of NIST mAb, corresponding to 2x C-terminal Lys.<sup>37</sup> Combined sequence coverage (HC+LC) of 91.5% could be achieved after transferring approximately 640 pg of this species (1.2% by peak area in UV). In this peak, the peptide LSLSPGK (HC444–450) was detected as the major form (see Figure 3E), whereas in the second, higher-abundant basic peak a mixture in a ratio of ~1:1 between LSLSPGK (HC444–450) and LSLSPG (HC444–449) could be identified (Figure 3D). The main peak of NIST mAb (Figure 3C) contained the peptide LSLSPG (HC444–449) as the major form. These results show the accuracy of the heart-cut

procedure preventing overlapping peaks and the sensitivity of the presented method.

The presented approach enables peptide mapping with high sequence coverage and PTM localization, considering the in-capillary approach, ambient temperature, digestion time, and matrix load. The sensitivity could be shown by transferring and digesting less than 1 ng in the second dimension.

**3.3.1. Trastuzumab Stressed.** Trastuzumab (Herceptin) is a humanized monoclonal antibody (mAb) that has been used in the treatment of breast cancer patients for more than 20 years. Trastuzumab was still under the 5 top-selling biopharmaceuticals in 2017 achieving sales of more than 7 billion per year.<sup>38</sup> Under nonstressed conditions, the well-known and characterized mAb exhibits basic and acidic variants and was selected as an example application for PTM localization by in-capillary digestion. Trastuzumab was thermally stressed at 40 °C for 4 weeks. Panels A and D of Figure 4 show the CZE-UV signal of trastuzumab in a nonstressed and stressed state, respectively. The main peak of a nonstressed sample and an acidic peak of a stressed sample were cut separately and transferred into the second dimension applying in-capillary reduction and digestion as described in Methods. Figure 4B,E shows the BPEs of the cut peaks (indicated by blue bars) after subsequent in-capillary reduction and digestion. Figure 4C,F shows the EIEs of the peptide YKCKVSNKALPAPIE (HC322–336) and the modified peptide YKCKVSDKALPAPIE (HC322–336). This peptide occurred in two different charge states (2 and 3) with a ratio of ~2:1 by abundance and was chosen as an example for the deep insight possible applying the presented approach. Deamidation of HC328 (Asn) upon temperature stress of 40 °C was described by Yang et al.<sup>39</sup> The ion traces of the deamidated peptide did not occur in the main peak of the nonstressed sample but did appear in the acidic peak of the stressed sample (Figure 4D) with a shift in migration time. The migration time shift to longer migration times is expected for deamidated (more acidic) peptides compared to their nondeamidated version. This peptide YKCKVSNKALPAPIE and its deamidated version YKCKVSDKALPAPIE show a rare example of a PTM localization with a peptide pair. MS/MS spectra of the native and modified peptide can be found in the Supporting Information (Figure S5). Many more peptides could only be found in either their modified or nonmodified state, which is most likely attributed to the complex cleavage pattern of pepsin. Still, several hot spots for deamidation could be detected exclusively in the stressed sample as listed in Table S2. Prominent representatives are HC55 (WVAR-IYPTNG)<sup>40,41,8</sup> and several peptides containing the “WESNGQPENNY” motif (HC387, HC392–393).<sup>40,42</sup> These results demonstrate the capabilities of the chosen experimental approach regarding PTM localizations also in hot spots regardless of the enzymes’ specificity.

**3.4. Pepsin Specificity and Reproducibility of the Complete CZE-CZE-MS/MS Approach.** Pepsin is known to cleave preferably after hydrophobic and bulky amino acids.<sup>43</sup> The specificity is influenced by several factors, such as the amino acid at the positions P1 and P1' (P1 is the N-terminal amino acid and P1' the C-terminal amino acid to the cleaved peptide bond), pH, digestion time, the concentration relative to the digested protein, and the globule conformation of proteins in acidic conditions.<sup>44,45</sup> It is also established that pepsin shows lower specificity and reproducibility compared to other frequently used proteases, which is certainly a challenge for the workflow presented here.<sup>44</sup> Initially, the data evaluation

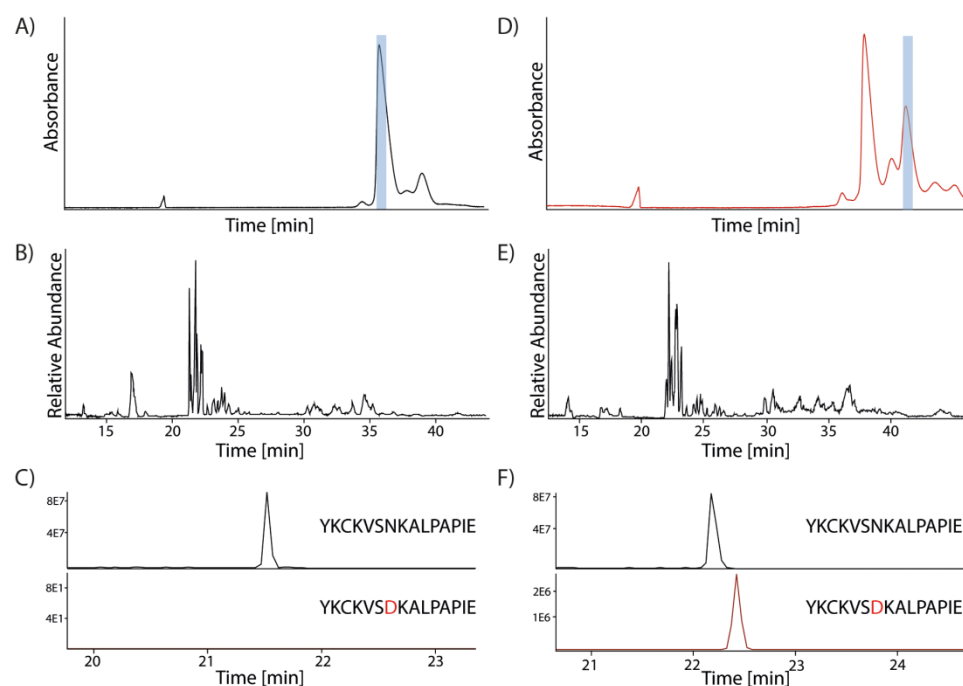


**Figure 4.** Separation of intact charge variants of nonstressed and stressed trastuzumab followed by in-capillary digest and peptide mapping of selected peaks using CZE-CZE-MS. (A) CZE-UV of 1 mg/mL nonstressed trastuzumab. (B) BPE (350–2000  $m/z$ ) of the in-capillary-digested transferred main peak. (C) EIEs of the peptide HC322–336, ion traces of not deamidated and deamidated species. (D) CZE-UV of 1 mg/mL stressed trastuzumab. (E) BPE (350–2000  $m/z$ ) of the in-capillary-digested transferred acidic peak. (F) EIEs of the peptide HC322–336, ion traces of not deamidated and deamidated species.

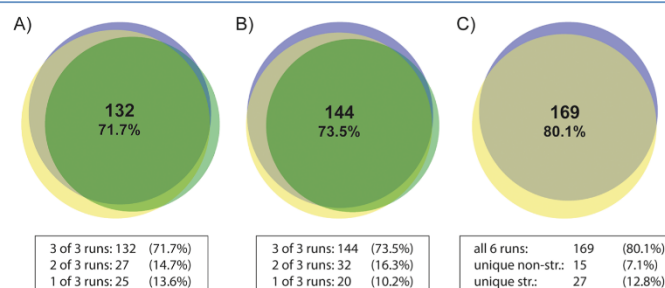


**Figure 5.** VENN diagrams of trastuzumab peptides after in-capillary reduction and digestion (high confidence;  $PSM \geq 2$ ). (A) Nonstressed main peak, three consecutive experiments (B) stressed acidic peak, and three consecutive experiments (C) combined lists of nonstressed (nonstr.) main peak versus combined list of the stressed acidic peak.

included the amino acids F, L, W, Y, A, E, and Q and yielded low sequence coverage as well as numerous unassigned spectra. Changing the search parameters to include any possible cleavage site resulted in high sequence coverages of >90% for all mAbs. The experiments performed here showed up to 16 different amino acids in different ratios as possible cleavage sites for pepsin, showing a low specificity for the chosen experimental parameters. Although pepsin provides many

unique peptides and complex data, it enables high sequence coverages and a high overlap rate for PTM characterization. The reproducibility of pepsin in the presented setup was investigated by generating VENN diagrams (Figure 5) of consecutive measurements (BioVenn).<sup>46</sup> Figure 5A (main peak, nonstressed) and Figure 5B (acidic peak #2, stressed) show a comparison of the peptide lists from three consecutive runs of trastuzumab. From 184 identified peptides (Figure 5A,

nonstressed), 132 peptides (71.7%) were found in all three consecutive experiments and 49 peptides (28.3%) were found either in only one or two of three measurements. The combination of identified peptides in at least two measurements yielded 159 reproducible peptides (86.4%). From 196 identified peptides (Figure 5B, stressed), 144 peptides (73.5%) were found in all three consecutive experiments and 52 peptides (26.5%) were detected either in only one or two of three measurements. The combination of identified peptides in at least two measurements yielded 176 reproducible peptides (89.8%). Though the data landscape of pepsin generated peptides is certainly more complex and varied than, for example, trypsin-based digestion, the numbers shown here indicate the reproducibility of the introduced work flow. Figure 5C shows the comparison of the peptide lists from the nonstressed and stressed digestion experiments. In total, 169 peptides (80.1%) could be identified in both combined lists (nonstressed and stressed) while 15 peptides (7.1%) were found only in the nonstressed samples and 27 peptides (12.8%) were found only in the stressed sample, 7 of them with a modification (Tables S1 and S2). The latter mentioned difference could be explained by either the stressed sample status or a modification-dependent pepsin cleavage site change.

In summary, pepsin was shown to be a fast and efficient digestion enzyme in our experimental setup providing high SCs already with a single-shot experiment. Regardless of the lower specificity and lower reproducibility compared to other proteases, the generated data allows a deep view into modifications on the peptide level.

#### 4. CONCLUSION

We describe here a two-dimensional CZE method for the characterization of charge-based separated mAb variants. Intact mAb charge variants were separated by CZE, and selected variants were transferred in a second dimension by heart cut with subsequent in-capillary digestion and peptide analysis by CZE-MS/MS. Localization of distinct PTMs in nonstressed and stressed material was possible and revealed possible PTM combinations in a single charge variant peak. We have obtained comprehensive results demonstrating the applicability of the chosen method by analyzing four different mAbs and respective charge variants. The presented approach applying in-capillary reduction and digestion after CZE(EACA) separation provided high sequence coverages (>90%) using pepsin even with a low amount of mAb per heart-cut. Acidic conditions during reduction, digestion, and separation reduce the risk of artificial deamidation and preserve succinimide from further reaction. We showed that a second UV detector in the first dimension strongly enhances the reproducibility and stability of the heart-cut procedure in the CZE(EACA) dimension. Pepsin generated many reproducible and overlapping peptides which is in general beneficial for high sequence coverage and PTM localization. Changes to the pH and further optimization to the plug system in the second dimension could enable other suitable enzymes for peptide mapping (Trypsin, Asp-N, Glu-C) or subunit analysis (IdeS, Kgp). The reproducibility of pepsin could be even further improved by ensuring more constant digestion conditions (pH, protein and enzyme ratio, mixing) in the presented two-dimensional approach. Though the transferred amount of material can be estimated based on loop size and UV profile, the quantitative aspect of this setup remains challenging, especially considering the complex cleavage pattern of pepsin

affecting ESI-MS of the generated peptides. The quantitative aspect is further hampered by missing or undetected peptide pairs in their respective modified and nonmodified states. The sequence coverage and the total run time are important aspects of the presented system and are in the same range as current multidimensional LC-MS approaches. Overall, the total time is significantly shorter than in off-line approaches. The total run time could be further improved by applying higher voltages and shorter separation lengths. A multiheart cut method with "peak parking" including automation of the cut procedure and CE-MS interface would also accelerate the analysis significantly. This auspicious proof-of-concept study shows a capillary-based two-dimensional system for the in-depth MS characterization of intact mAb variants up to the PTM level after selective charge-based separation. The presented in-capillary digestion approach provided high sensitivity and high SC even for minor charge variants and can potentially become an important technique in biopharmaceutical development and quality control.

#### ■ ASSOCIATED CONTENT

##### Supporting Information

The Supporting Information is available free of charge at <https://pubs.acs.org/doi/10.1021/acs.analchem.2c04578>.

Additional experimental details and results, including photograph of experimental setup (PDF)

#### ■ AUTHOR INFORMATION

##### Corresponding Author

Christian Neusüß – Department of Chemistry, Aalen University, 73430 Aalen, Germany;  
Email: christian.neusuess@hs-aalen.de

##### Authors

Johannes Schlecht – Department of Chemistry, Aalen University, 73430 Aalen, Germany; Department of Pharmaceutical and Medicinal Chemistry, Friedrich Schiller University Jena, 07743 Jena, Germany; [orcid.org/0000-0001-9071-5904](https://orcid.org/0000-0001-9071-5904)

Kevin Jooß – Departments of Chemistry and Molecular Biosciences, the Chemistry of Life Processes Institute, and the Proteomics Center of Excellence, Northwestern University, Evanston, Illinois 60208, United States; [orcid.org/0000-0003-1669-7837](https://orcid.org/0000-0003-1669-7837)

Bernd Moritz – F. Hoffmann La-Roche Ltd., 4058 Basel, Switzerland

Steffen Kiessig – F. Hoffmann La-Roche Ltd., 4058 Basel, Switzerland

Complete contact information is available at: <https://pubs.acs.org/doi/10.1021/acs.analchem.2c04578>

##### Notes

The authors declare no competing financial interest.

#### ■ ACKNOWLEDGMENTS

The authors thank F. Hoffmann-La Roche, Ltd. for financial support.

#### ■ REFERENCES

- (1) Kaplon, H.; Chenoweth, A.; Crescioli, S.; Reichert, J. M. *mAbs* 2022, 14 (1), 2014296.
- (2) Mullard, A. *Nat. Rev. Drug Discov* 2021, 20 (7), 491–495.



- (3) Lu, R.-M.; Hwang, Y.-C.; Liu, I.-J.; Lee, C.-C.; Tsai, H.-Z.; Li, H.-J.; Wu, H.-C. *J. Biomed Sci.* **2020**, *27* (1), 1.
- (4) Beck, A.; Liu, H. *Antibodies* **2019**, *8* (1), 18.
- (5) Liu, H.; Ponniah, G.; Zhang, H.-M.; Nowak, C.; Neill, A.; Gonzalez-Lopez, N.; Patel, R.; Cheng, G.; Kita, A. Z.; Andrien, B. *MAbs* **2014**, *6* (5), 1145–1154.
- (6) Dick, L. W.; Qiu, D.; Mahon, D.; Adamo, M.; Cheng, K.-C. *Biotechnol. Bioeng.* **2008**, *100* (6), 1132–1143.
- (7) Gervais, D. *J. Chem. Technol. Biotechnol.* **2016**, *91* (3), 569–575.
- (8) Harris, R. J.; Kabakoff, B.; Macchi, F. D.; Shen, F. J.; Kwong, M.; Andya, J. D.; Shire, S. J.; Bjork, N.; Totpal, K.; Chen, A. B. *J. Chromatogr. B* **2001**, *752* (2), 233–245.
- (9) Robotham, A. C.; Kelly, J. F. *Approaches to the Purification, Analysis and Characterization of Antibody-Based Therapeutics* **2020**, *11*, 1–33.
- (10) Dadouch, M.; Ladner, Y.; Perrin, C. *Separations* **2021**, *8* (1), 4.
- (11) Kaur, H.; Beckman, J.; Zhang, Y.; Li, Z. J.; Sziget, M.; Guttman, A. *Trends Anal. Chem.* **2021**, *144*, 116407.
- (12) Kumar, R.; Guttman, A.; Rathore, A. S. *Electrophoresis* **2022**, *43* (1–2), 143–166.
- (13) He, Y.; Isele, C.; Hou, W.; Ruesch, M. *J. Sep. Sci.* **2011**, *34* (5), 548–555.
- (14) Moritz, B.; Schnaible, V.; Kiessig, S.; Heyne, A.; Wild, M.; Finkler, C.; Christians, S.; Mueller, K.; Zhang, L.; Furuya, K.; Hassel, M.; Hamm, M.; Rustandi, R.; He, Y.; Solano, O. S.; Whitmore, C.; Park, S. A.; Hansen, D.; Santos, M.; Lies, M. *J. Chromatogr. B* **2015**, *983–984*, 101–110.
- (15) Camperi, J.; Goyon, A.; Guillarme, D.; Zhang, K.; Stella, C. *Analyst* **2021**, *146* (3), 747–769.
- (16) Hühner, J.; Neusüß, C. *Anal. Bioanal. Chem.* **2016**, *408* (15), 4055–4061.
- (17) Jooß, K.; Hühner, J.; Kiessig, S.; Moritz, B.; Neusüß, C. *Anal. Bioanal. Chem.* **2017**, *409* (26), 6057–6067.
- (18) Römer, J.; Montealegre, C.; Schlecht, J.; Kiessig, S.; Moritz, B.; Neusüß, C. *Anal. Bioanal. Chem.* **2019**, *411*, 7197.
- (19) Schlecht, J.; Jooß, K.; Neusüß, C. *Anal. Bioanal. Chem.* **2018**, *410* (25), 6353–6359.
- (20) Camperi, J.; Grunert, I.; Heinrich, K.; Winter, M.; Özipek, S.; Hoeltherhoff, S.; Weindl, T.; Mayr, K.; Bulau, P.; Meier, M.; Mølhøj, M.; Leiss, M.; Guillarme, D.; Bathke, A.; Stella, C. *Talanta* **2021**, *234*, 122628.
- (21) Gstöttner, C.; Klemm, D.; Habberger, M.; Bathke, A.; Wegele, H.; Bell, C.; Kopf, R. *Anal. Chem.* **2018**, *90* (3), 2119–2125.
- (22) Pot, S.; Gstöttner, C.; Heinrich, K.; Hoeltherhoff, S.; Grunert, I.; Leiss, M.; Bathke, A.; Dominguez-Vega, E. *Anal. Chim. Acta* **2021**, *1184*, 339015.
- (23) Verscheure, L.; Cerdobbel, A.; Sandra, P.; Lynen, F.; Sandra, K. *J. Chromatogr. A* **2021**, *1653*, 462409.
- (24) Ladner, Y.; Mas, S.; Coussot, G.; Bartley, K.; Montels, J.; Morel, J.; Perrin, C. *J. Chromatogr. A* **2017**, *1528*, 83–90.
- (25) Ladner, Y.; Mas, S.; Coussot, G.; Montels, J.; Perrin, C. *Talanta* **2019**, *193*, 146–151.
- (26) Dadouch, M.; Ladner, Y.; Bich, C.; Larroque, M.; Larroque, C.; Morel, J.; Bonnet, P.-A.; Perrin, C. *Analyst* **2020**, *145* (5), 1759–1767.
- (27) Dadouch, M.; Ladner, Y.; Bich, C.; Montels, J.; Morel, J.; Perrin, C. *Electrophoresis* **2021**, *42* (11), 1229–1237.
- (28) Schlecht, J.; Stolz, A.; Hofmann, A.; Gerstung, L.; Neusüß, C. *Anal. Chem.* **2021**, *93* (44), 14593–14598.
- (29) Espadas, G.; Borrás, E.; Chiva, C.; Sabidó, E. *Proteomics* **2017**, *17* (9), 1600416.
- (30) Kupcsik, L.; Alini, M.; Stoddart, M. J. *Tissue Eng. Part A* **2009**, *15* (8), 2309–2313.
- (31) Cornish-Bowden, A. J.; Knowles, J. R. *Biochem. J.* **1969**, *113* (2), 353–362.
- (32) Cravello, L.; Lascoux, D.; Forest, E. *Rapid Commun. Mass Spectrom.* **2003**, *17* (21), 2387–2393.
- (33) Wales, T. E.; Engen, J. R. *Mass Spectrom. Rev.* **2006**, *25* (1), 158–170.
- (34) Zhang, H.-M.; McLoughlin, S. M.; Frausto, S. D.; Tang, H.; Emmett, M. R.; Marshall, A. G. *Anal. Chem.* **2010**, *82* (4), 1450–1454.
- (35) Iki, N.; Yeung, E. S. *Journal of Chromatography A* **1996**, *731* (1–2), 273–282.
- (36) Hühner, J.; Jooß, K.; Neusüß, C. *Electrophoresis* **2017**, *38* (6), 914–921.
- (37) Li, W.; Kerwin, J. L.; Schiel, J.; Formolo, T.; Davis, D.; Mahan, A.; Benchaar, S. A. *ACS Symp. Ser.* **2015**, *1201*, 119–183.
- (38) Walsh, G. *Nat. Biotechnol.* **2018**, *36* (12), 1136–1145.
- (39) Yang, Y.; Zhao, J.; Geng, S.; Hou, C.; Li, X.; Lang, X.; Qiao, C.; Li, Y.; Feng, J.; Lv, M.; Shen, B.; Zhang, B. *J. Pharm. Sci.* **2015**, *104* (6), 1960–1970.
- (40) Diepold, K.; Bomans, K.; Wiedmann, M.; Zimmermann, B.; Petzold, A.; Schlothauer, T.; Mueller, R.; Moritz, B.; Stracke, J. O.; Mølhøj, M.; Reusch, D.; Bulau, P. *PLoS One* **2012**, *7* (1), No. e30295.
- (41) Gahoual, R.; Burr, A.; Busnel, J.-M.; Kuhn, L.; Hammann, P.; Beck, A.; François, Y.-N.; Leize-Wagner, E. *MAbs* **2013**, *5* (3), 479–490.
- (42) Liu, Y. D.; van Enk, J. Z.; Flynn, G. C. *Biologicals* **2009**, *37* (S), 313–322.
- (43) Fruton, J. S. *Adv. Enzymol. Relat. Areas Mol. Biol.* **2006**, *33*, 401–443.
- (44) Ahn, J.; Cao, M.-J.; Yu, Y. Q.; Engen, J. R. *Biochim. Biophys. Acta* **2013**, *1834* (6), 1222–1229.
- (45) Palashoff, M. H. *Determining the specificity of pepsin for proteolytic digestion*. Thesis; Northeastern University, Boston, MA, 2008.
- (46) Hulsen, T.; de Vlieg, J.; Alkema, W. *BMC Genomics* **2008**, *9*, 488.

## 3 Discussion

This thesis deals with different ways of CE-MS coupling using MS-interfering substances. This includes the development of a sensitive and flexible CE-MS interface (manuscript I) and the application of this interface for mass spectrometric characterization of intact and digested charge-based separated mAbs (manuscripts II and IV). Another focus was on the concept of two-dimensional CE-MS coupling (CE-CE-MS) including a novel in-capillary digestion approach (manuscript III).

### 3.1 nanoCEasy CE-MS interface

Sensitivity is a top priority in the development of CE-MS interfaces. In addition, simplified handling and ease of use are also important parameters for CE-MS coupling approaches. The *nanoCEasy* interface closes the gap in terms of usability with the so far existing types of CE-MS interfaces. It was developed to allow easy and flexible operation while providing sufficient sensitivity for many kinds of CE-MS applications. The first and one of the most important parameters during the development was usability. Other so far available commercial interfaces operating in the nanoESI range suffer from the ease of use as they require quite some handling expertise. The introduced plug & play approach using two 3D printed devices and matching sleeves makes any exchanges of emitters capillaries easily accessible. The combination of the previously presented two-capillary approach provides flexibility regarding sample matrix and coatings during ESI operation without removing the separation capillary from the interface. This valve-like approach enabled the operation of CE modes using ESI-interfering substances with a minimum of hands-on-time (exchanging the position of the two capillaries). It enabled also on-line (re)coating of capillaries and modes as CIEF-MS, including exchange of the SL (corresponds catholyte or anolyte, depending on used polarity) for chemical mobilization. The two capillaries were arranged in the “conditioning mode”, where the SL capillary is in front of the emitter and the separation capillary is pulled back (see Figure 6A). Any flow of the separation capillary (for example coating solution) is flushed back to the waste. When the separation starts, the positions are switched (see Figure 6B) and the separation capillary is in front of the

## Discussion

emitter. Incoming separated analytes are then mixed with the SL and ionized during the ESI process. In this way, the analytes of interest in a specific time window can be selected for ESI and MS detection without the risk of contamination or ESI interference.

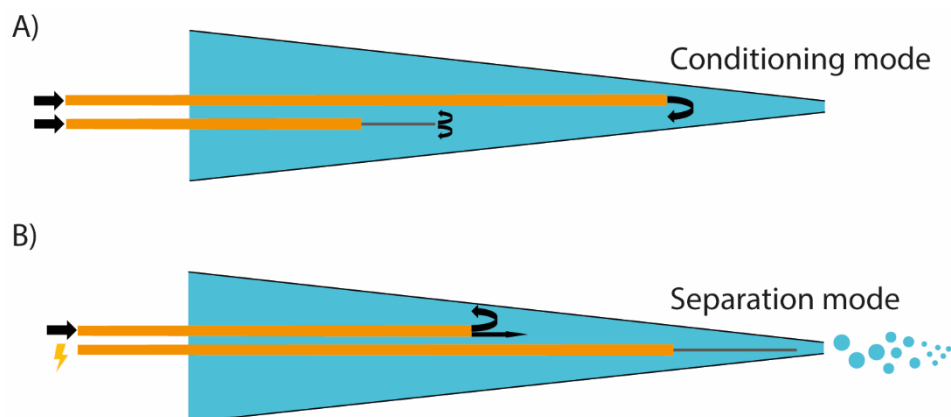


**Figure 6.** Conditioning mode and separation mode in the ESI emitter with the two-capillary approach. **A)** Conditioning mode, SL capillary in front. Any flow of the CE flows to the waste. **B)** Separation mode, CE capillary in front, analytes are ionized and sprayed toward MS.

The robustness of the interface could be shown regarding the distance of the emitter to the MS orifice, the distance of the separation capillary to the emitter tip, and between different emitters. The robustness between different emitter batches and sizes was not included in the discussed study and could be an interesting and important topic for future studies, especially if the demand for emitters would increase due to more users of this type of interface. Another parameter regarding emitters would be the application of coatings to prevent potential sample adsorption to the inner emitter glass wall. The emitters could also be coated hydrophobically on the outside of the tip to stabilize the ES process. Other factors contributing to potentially different emitter performance are the length of the emitter tip and therefore shape and geometry. These parameters change with the tip ID (small tip ID = longer tip length).

The positioning of the separation capillary in the emitter tip was previously shown to be robust within certain limits. The capillary tip can be very close to the emitter tip but should not touch the inner emitter walls to still allow sheath liquid to pass and mix with the CE effluent before the ES process. Therefore, the outer diameter of the separation capillary must be reduced. This was accomplished by an etching process with hydrofluoric acid (HF). This process required the preparation of the capillaries, a workplace suited for the use of HF including safety measures and very cautious handling with HF. As not every university or industrial employer is open about using

## Discussion

HF for obvious safety reasons, other alternatives such as capillary grinding could be considered for the future. This would enable a mechanical capillary treatment to manufacture tapered capillaries in a reproducible manner. In addition, the preparation of pre-coated capillaries would be simplified with a lower risk of damaging any possible capillary coating.

The liquid consumption or ES flow rate using a specific emitter and type of SL can be an important and interesting parameter for method development and troubleshooting. The precise determination of the absolute flow rate / liquid consumption is challenging as it depends on many factors, such as MS instrument, ES voltage, distance, type of SL, resistivity, amount of CE effluent, and mixing of CE effluent and SL. In addition, the emitter tip size and tip surface may have an impact on the ES and the sensitivity.[74] Therefore, an approach using different isotopically labeled standards (C12/C13) in the SL and the CE effluent (BGE) would help to investigate to determine the actual flow rate under specific conditions.

Using 3D printed parts allowed fast development and testing of prototypes for the interface. The 3D printing process and the material were chosen with respect to the high accuracy of the printed parts and the smoothness of the material. The 3D printing process using a layer-by-layer technique applying selective droplets of light-curable resin was chosen as the printing process as it provides high precision and resolution for structures in the  $\mu\text{m}$  range.[75] Two different materials are used in this process, one is a non-light curable material forming a supportive structure with spatially constrained volumes which are filled with the second material, a light-curable resin. The desired structures (channels or cavities) were printed with the second material which can be dissolved at the end of the polymerization process.[76] The accuracy was important as the used PEEK tubing and sleeves should fit in the interface part without any additional fixation. The smoothness of the inner surface was important to avoid material abrasion and breaking of etched capillaries during insertion or position changes. Another important parameter was the stability of the material against chemical solvents and organic acids such as IPA, MeOH, FA, and HAc. Another big advantage of using 3D printed parts is low development and material costs, as well as easy adaptation for different future designs and developments.[77]

Figure 7 shows schemes of the two different parts of the *nanoCEasy* interface, the interface unit (Figure 7A) and the positioning unit (Figure 7B).

## Discussion

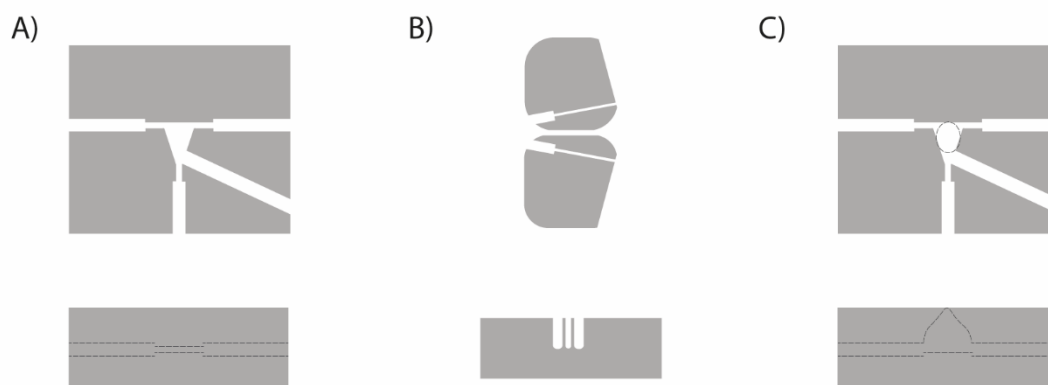


**Figure 7.** Schemes of the interface unit and the positioning unit of the *nanoCEasy* interface. **A)** Interface unit with channels for emitter, electrode, waste, and capillaries (left to right). Lower part: side view. **B)** Positioning unit with three channels. Two for capillary positioning, and the middle channel for insertion of the capillaries into the interface unit. Lower part: side view. **C)** Suggested improvement for the interface unit with a cavity on top of the triangle shape (dashed line).

The channels shown in Figure 7A were designed in a way that PEEK and FEP tubing sleeves fit into them holding by themselves. The capillaries could thus be inserted from the right side through a sleeve and further into an emitter (left channel, held by another sleeve) without touching the inner wall of the interface unit. The electrode was inserted with a third sleeve from the lower side of the scheme, protruding into the middle of the triangle shape. The fourth sleeve serves as a waste channel for the excess sheath liquid. Figure 7B shows the positioning unit with three channels. The two outer channels were designed in a way that the capillaries can be squeezed into the narrower part of the channel without sleeves. The middle channel served as insertion help for the capillaries into the first tubing sleeve. The two capillaries were thus first inserted via the middle channel and then fixed via the outer channels. All channels in both parts were on the same height level to facilitate easier capillary insertion and to avoid the risk of breaking the etched separation capillary at a solid surface.

One potential issue during the operation of the *nanoCEasy* interface was the formation of bubbles from the compression/decompression of SL by the SL syringe pump. These bubbles were occasionally transported to the emitter tip and caused ES interferences or disruptions. A big advantage of the chosen material was the transparency which allowed observation and mitigation of these occurring bubbles. The bubble formation could be prevented by using constant low flow rates of the SL syringe and avoiding high-pressure peaks. Another option for air bubble mitigation could be adapting the design of the interface by adding another channel ranging from the middle channel to

## Discussion

the top surface to catch occurring air bubbles before they enter the front part of the emitter as depicted in Figure 7C. A third option would be to use another type of pump, either a pump originating from HPLC with degassing technology, or any other pump operated by air pressure providing constant pressure. This would also allow longer operation times without refilling the SL syringe. Longer operation times without refilling the SL syringe are crucial for the future automation of the interface and unattended operation.

A first automation setup could be realized after the publication of manuscript I using a step motor with 50 nm increments for the positioning of the separation capillary (AG-LS25 Linear Stage and AG-UC2 Agilis Controller by Newport Corporation, Irvine, CA, USA). Therefore, the separation capillary was fixed on the moving plate of the step motor enabling automated movement between the conditioning mode and the separation mode (Figure 8B). In addition, an Arduino ATmega328 microcontroller (AZdelivery, Deggendorf, Germany) was used to communicate the CE trigger signal (start of the measurement by voltage drop) to a LabView virtual instrument (VI) that controls the step motor (with the separation capillary attached) either to the conditioning position or the separation position (Figure 8A and C). In this way, automated movement of the separation capillary to the separation position or conditioning position triggered by the CE could be shown. This automation setup is expected to be improved and simplified in the future to increase the sample throughput and drastically reduce the hands-on-time of the *nanoCEasy* interface during long experiments and sequences.

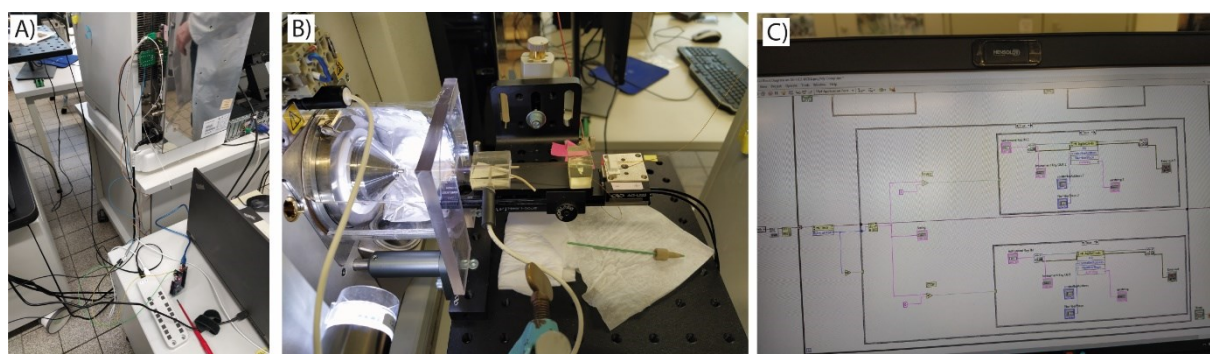


**Figure 8.** Automation of the *nanoCEasy* interface. **A)** Agilent G7100 CE connected to an Arduino microcontroller (connected to a laptop with LabView running). **B)** photograph of the automated *nanoCEasy* interface installed at an Orbitrap Fusion Lumos **C)** Screenshot of the LabView VI that receives the Arduino command triggered by the CE (“start” or “stop”) and then communicates the motor movement to the conditioning or the separation position.

## Discussion

There could still be several improvements to the interface itself which are more focused on product development such as a housing cabinet (more protection from surrounding and dust, high voltage safety) and an easily usable user interface (UI) for the automation. Ultimately, a more streamlined product with the chance of possible commercialization would increase the publicity and availability even more.

The *nanoCEasy* CE-MS interface provides sensitivity and flexibility for CE-MS experiments in biological and biopharma applications, enabling a broad user community. In comparison to other commercially available interfaces, it provides an increased level of ease of use, a valve-like approach for liquid control in the emitter in combination with less risk of emitter clogging, and a fast exchange of SL and emitters. In this way, it is expected to spread more into academic and industrial research CE-MS labs to support the thorough characterization of biopharmaceuticals.

### 3.2 iCIEF-MS coupling

Imaged capillary isoelectric focusing (iCIEF) is currently one of the most important analytical methods for the characterization of charge heterogeneity in protein biopharmaceuticals. The standard detection technique in iCIEF is UV-absorption and does not provide any specific information on the kind of modification besides the pI value and the relative charge difference of occurring charge species. In this work, a preparative iCIEF-UV instrument was coupled to MS using the *nanoCEasy* interface to combine quantitative UV data of charge heterogeneity with MS data to also obtain knowledge about the type of modifications. The *CEInfinite* from AES was operated using standard iCIEF cartridges (AD or FC coated) and ampholytes (Pharmalyte or AESlyte). The *nanoCEasy* interface platform was slightly adapted in terms of the required space in front of the MS instrument to fit the needs of direct iCIEF-MS coupling. Several important parameters such as sample concentration, ampholyte concentration, and mobilization speed were investigated to find suitable parameters for different therapeutic mAbs. Two mAbs were investigated and intact masses from the main, basic, and acidic species could be determined.

Different possibilities for the hyphenation of an iCIEF-UV instrument to MS were tested as described in manuscript II. The first and most straightforward approach was to use a (low flow) ESI sprayer and connect the iCIEF transfer capillary directly to it (see Figure 9A) but this approach did lack general ESI compatibility due to the iCIEF sample composition. The second described approach is depicted in Figure 9B and includes a microfluidic connector (t-piece) at any position of the iCIEF transfer capillary which allows the addition of a “make-up” liquid (organic solvent, water, and a small percentage of acid; composition is comparable to a sheath liquid) at a certain flow rate which transports the peaks towards MS and provides ESI compatibility.



## Discussion

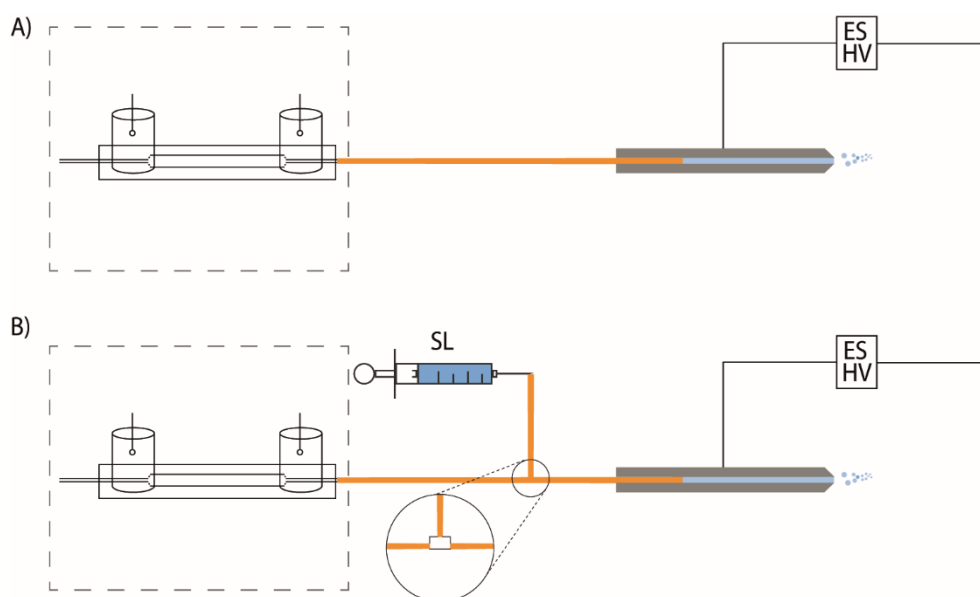


**Figure 9.** Different ways of iCIEF-MS coupling. **A)** iCIEF transfer capillary connected to a conventional (low flow) ESI source. **B)** iCIEF transfer capillary comprises a t-piece with a connected sheath liquid pump.

This approach includes additional connections, potential dead volumes (especially in the t-piece itself), and backpressure with the risk of clogging or leakages. Some prototypes of iCIEF cartridges with a microfluidic t-piece were tested but suffered from the difficulties mentioned above. Nevertheless, there are now also examples available utilizing this approach (Figure 9B) with a microfluidic connector in the transfer capillary. One advantage of this approach is, that it can be connected to any ESI-MS source, independently of the manufacturer and the type of source (nanoESI, low flow ESI, etc.). Several research groups have worked with this approach in the meantime and have shown successful results for iCIEF-MS coupling using a microfluidic connector. [78–80] Although this approach adds additional steps for the development (make-up liquid composition, flow rate, position of the microfluidic connector, and angle of the microfluidic connection) is this the currently preferred approach of the instrument manufacturer AES due to its flexibility regarding the ESI-MS interface.

The third suggested approach utilizing a nanoflow sheath liquid interface was the method of choice in manuscript II as it worked without any additional connections inserting the transfer capillary directly into the ESI emitter of the interface. Figure 10 shows the iCIEF-MS setup of the *CEInfinite* with the *nanoCEasy* interface.

## Discussion

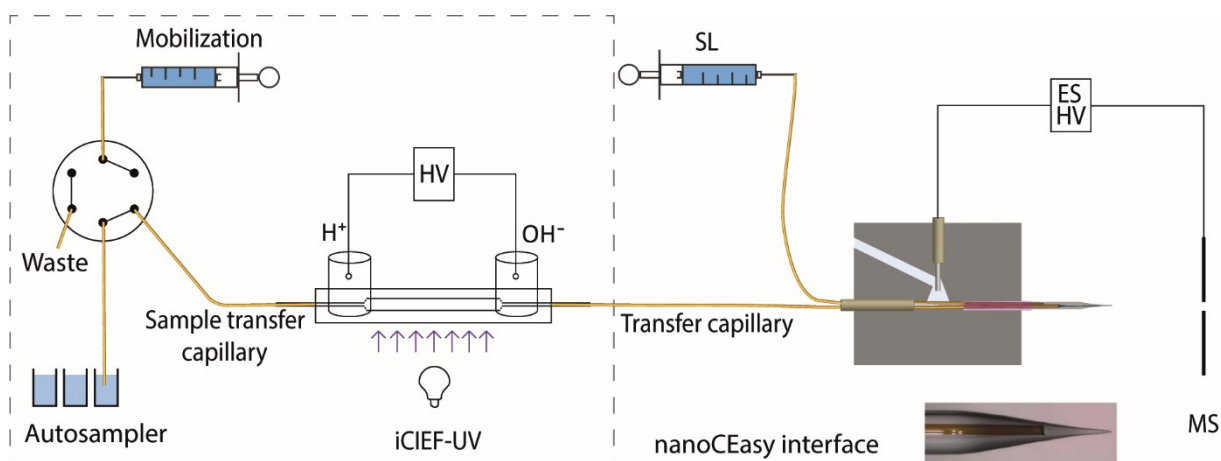


**Figure 10.** Schematic view of the *CEInfinite* including autosampler, syringe pump, and imaged capillary isoelectric focusing (iCIEF) cartridge coupled to mass spectrometry via the *nanoCEasy* interface.

Figure 11 shows the iCIEF-UV of trastuzumab before the mobilization (left) and the MS signal after the mobilization (right). The obtained zones after the isoelectric focusing process could not be maintained and show peak broadening during the mobilization process.

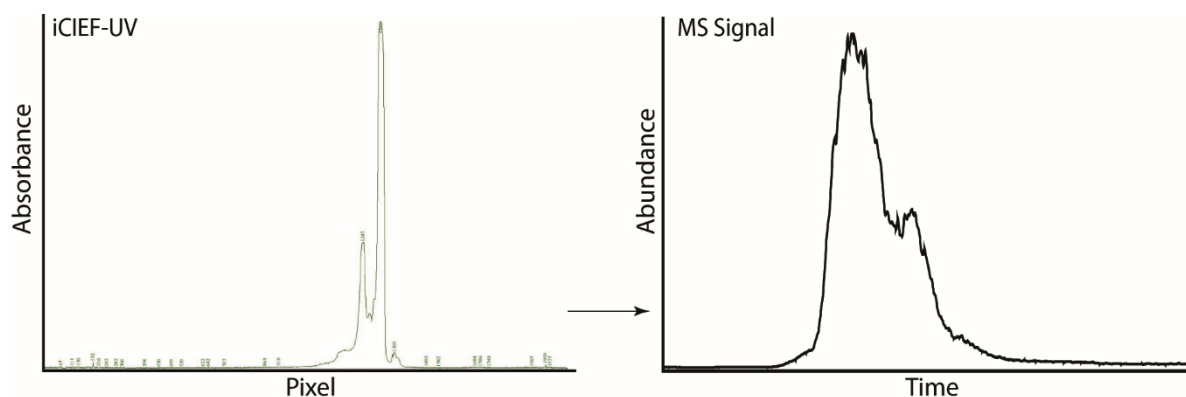


**Figure 11.** Left: iCIEF-UV of trastuzumab after the focusing process has finished. Right: BPE of trastuzumab after pressurized mobilization (30 nL/min). The peak profile is mirrored as the basic peak enters the MS first.

The first possible reason for peak broadening during the mobilization is Taylor dispersion, increasing with longer distances and higher flow rates. Taylor dispersion during the pressure-driven transfer of focused peaks can cause peak broadening and therefore overlapping of previously (in the focusing area) separated species during MS detection. From the experiments, it became clear that increasing the mobilization speed to more than 30 nL/min would deteriorate the gained focused peak resolution drastically and cause a massive overlap of peaks. In addition, there is no refocusing

## Discussion

voltage during the mobilization after the peaks have left the iCIEF cartridge part where the cathodic vessel is connected. Refocusing voltage is a common method in conventional CIEF to maintain the focused peak zones. Another associated reason for peak broadening in the utilized set-up was therefore the transfer capillary length (total distance from the end of the focusing area to the emitter). The standard set-up of the introduced *nanoCEasy* interface was not developed for the shortest possible set-up as the usually used capillary length for CE-MS is in the range of 60-70 cm and the available space is not an issue. Figure 12 shows the adapted parts of the interface which were optimized regarding distances (except the 3D-printed ones) for the iCIEF-MS setup.

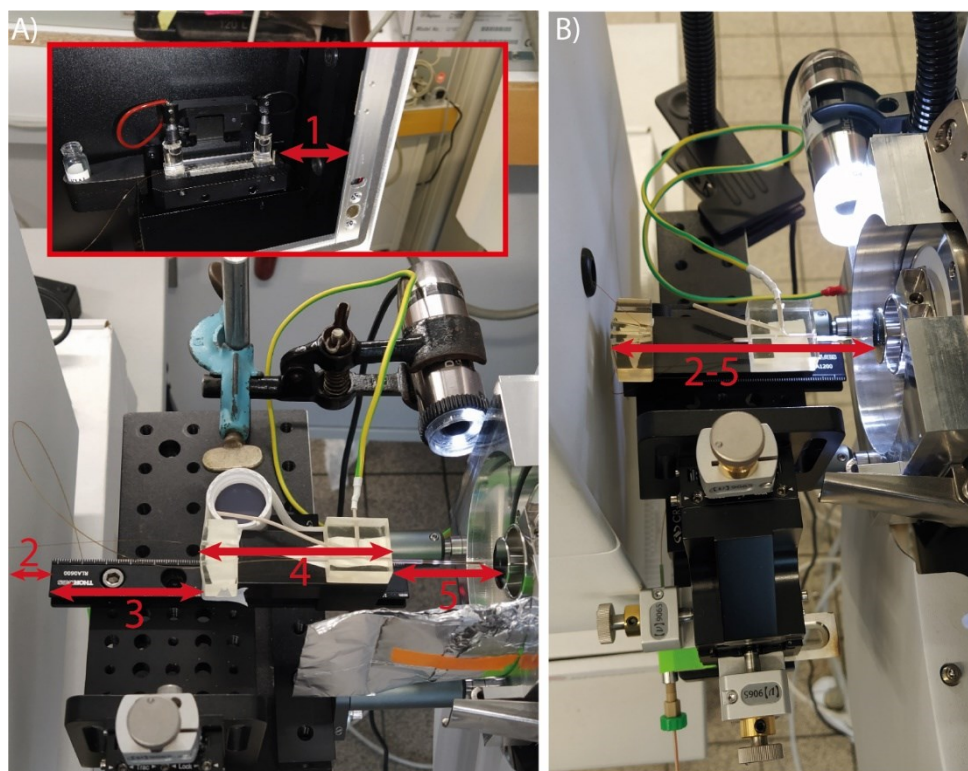


**Figure 12.** iCIEF-MS setup with *nanoCEasy* interface. **A)** Conventional *nanoCEasy* interface setup with the *CEInfinite* instrument. Distance #1 is instrument-limited, distances #2-#5 can be optimized. The total capillary length required is ca. 25 cm. **B)** Distance-optimized *nanoCEasy* setup for the *CEInfinite*. Distance #1 is instrument-limited, distances #2, #3, and #5 (interface parts) were adapted for shorter lengths. The total capillary length required is ca. 15 cm.

Distance #1 could not be changed as it is defined by the instrument manufacturer (AES) and the technical assembly. Distance #1 was the length between the start of the transfer capillary and the housing of the iCIEF instrument (about 5 cm). A shorter distance #1 is suggested for future generations of this instrument to allow a distance-

## Discussion

optimized set-up which will in general also save time due to shorter capillary lengths. The distances (#2, #3, and #5) were related to parts of the interface as the ground plate, optical rail, and the emitter itself. Cutting the emitter was done with a ceramic plate but is not recommended for general usage as the sharp cutting edge can abrade material from the purple emitter sleeve during insertion or form other particles which can cause emitter clogging.

The technical design of the iCIEF cartridge is another possible source of peak broadening. There is a transition of the ID from 200  $\mu\text{m}$  (50 mm focusing channel) to 50  $\mu\text{m}$  (transfer capillary) and at the same point, the electric field from the isoelectric focusing process ends. The change of geometry at this point from 200  $\mu\text{m}$  to 50  $\mu\text{m}$  could cause peak distortion and in addition, the available cathodic  $\text{OH}^-$  from the vessel could affect the net charge of the passing mAb species.

In addition, possible analyte-wall interaction or adsorption could also contribute to peak broadening during the mobilization process. This was mitigated by using coated capillaries (AD and FC), but the results showed that depending on the mAb (hydrophobic/hydrophilic character) specific coatings had to be used or the respective mAb would not be detected anymore. This observation made the requirements and quality of coatings in this application even more important, also for any future use. Depending on the coating of the focusing channel (AD or FC) there were also hybrids used (AD and FC for the transfer capillary; provided by AES). Depending on the type of coating and the quality/stability of the coating, interactions of mAb with the coating can impact the transfer of the focused peaks toward MS detection. The user has no control over the coating itself besides choosing the prefabricated cartridge with the respective coating composition and must test the compatibility of coatings for desired mAb analytes.

Another possible parameter that could contribute to peak broadening is a residual electric field originating from the ESI source. This is only possible when the ESI HV potential is on the source (Figure 13A) as technically designed by several MS instrument manufacturers (Thermo Fisher Scientific, Waters, Sciex) Other manufacturers work with grounded ESI sources (see Figure 13B) and have the ESI potential originating from the MS orifice (Agilent Technologies, Bruker Daltoniks). In the case of HV potential on the source, there is the risk of a residual electric field towards the iCIEF instrument having a floating ground at the cathode and conductive

## Discussion

liquid (ampholytes, mAb, potentially spacers as IDA or Arg) in the transfer capillary during the peak mobilization (Figure 13A). This residual electric field would have the opposite direction as the focusing electric field which could then cause unexpected changes for the focused peak zones during the transfer. There was no indication of such a phenomenon in the conducted experiments, however, this possibility should be considered in future experiments using not-grounded MS sources and high ESI voltages. The type of ampholyte and the concentration of ampholytes should in this case be of high focus during the method development.

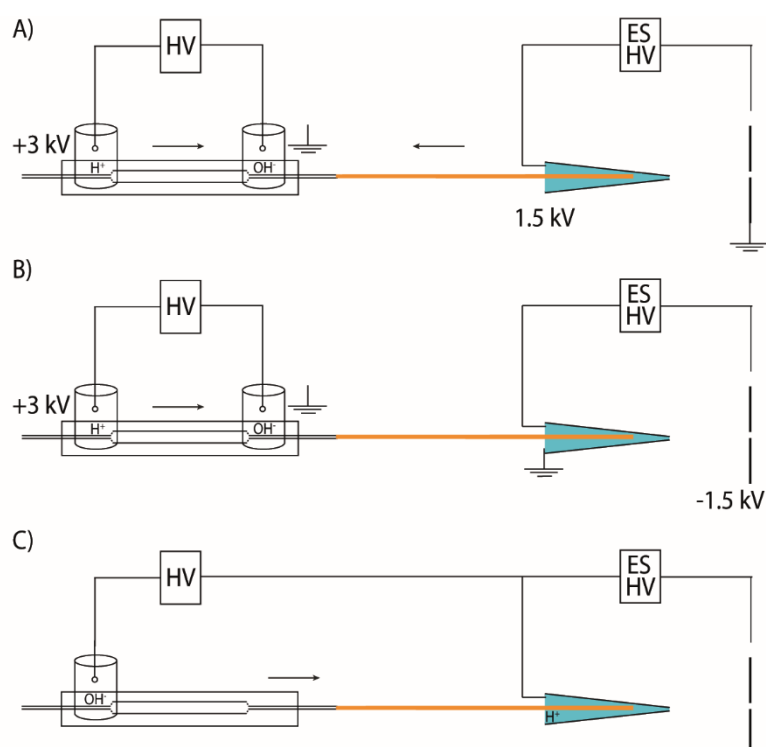


**Figure 13.** Possible iCIEF-MS voltage setups. **A)** iCIEF positive voltage at the anode. Electro spray source with voltage at electro spray needle/emitter. **B)** iCIEF positive voltage at the anode. Electro spray source with grounded electro spray needle/emitter. **C)** One iCIEF cathodic vessel with negative voltage. Exchange of anolyte (SL) is possible to allow chemical mobilization.

There are several possible changes for the iCIEF-UV instrument *CEInfinite* and the cartridge design suggested to improve the hyphenation of this instrument to ESI-MS with the *nanoCEasy* interface. First, the cartridge mounting could be placed closer to the instrument housing to allow shorter transfer capillaries and therefore shorter distance to the MS instrument (see Figure 11 distance #1). The second suggested change is the HV power supply which provides at the moment up to 3 kV at the anode (Figure 13A) or the cathode (this can be controlled by connecting the wire to the

## Discussion

respective electrode). If the power supply could also provide a negative potential (up to -3 kV), the potentially opposed electric fields in certain MS instrument set-ups could not cause any electrophoretic or isotachophoretic peak broadening effects anymore. The biggest change suggestion is to remove the cathodic vessel from the iCIEF cartridge (see Figure 13C). The anodic vessel would stay, with a negative HV applied, and the sheath liquid in the emitter serves as the catholyte. Arg or any other spacer reagent would be needed to block the whole transfer capillary from the interface to the cartridge. This approach would also allow chemical mobilization by changing the SL to an acidic one (fast exchange of SL possible with the *nanoCEasy* interface). This suggested approach requires many changes, combines CIEF and iCIEF concepts, and could be a very promising solution independently of the MS instrument. If the *nanoCEasy* interface would be more widely used in the future, this could be a very promising approach for successful and robust iCIEF-MS coupling.

Different ways exist to hyphenate an iCIEF-UV instrument to MS, however, using the *nanoCEasy* interface in a direct manner (iCIEF-MS) provided deep insight into the charge heterogeneity of intact therapeutic mAbs. The developed setup allowed the mass determination of intact basic, acidic, and main mAb variants including their glycosylation pattern. The isoelectric focused protein species could not be maintained completely during the pressure-assisted mobilization. Nevertheless, the obtained high-quality MS spectra yielded detailed information about low abundant singly glycosylated mAb species and in general mass determination with high accuracy and precision. The utilized *nanoCEasy* interface provided high sensitivity as well as the prevention of contamination of the mass spectrometer with iCIEF matrix components.

### **3.3 Two-dimensional capillary electrophoresis-mass spectrometry**

Certain CE techniques require specific electrolytes to achieve the necessary separation efficiency and selectivity. These substances are often non-volatile and therefore not compatible with ESI-MS. Alternative approaches such as dilution or replacement of these interfering substances often represent a compromise regarding the separation performance and MS detection sensitivity. One way to overcome these difficulties is two-dimensional capillary electrophoresis-mass spectrometry (CE-CE-MS). Two-dimensional separation systems are usually used to increase the peak capacity by the combination of two different separation selectivities. However, two dimensions can also be used to combine an ESI-MS incompatible separation method (first dimension) with an ESI-MS compatible method (second dimension). The two individual dimensions are connected via a nanoliter valve and desired peaks from the first dimension can be transferred in a heart-cut fashion. In addition, the second dimension can have a specific selectivity thereby increasing the separation performance. [81] In liquid chromatography, even more dimensions can be combined in one system by sophisticated technical setups using several individual pumps and columns. In this way, ion exchange chromatography (first dimension), followed by a clean-up step (second dimension) and online tryptic digestion (third dimension), and RPLC as the last MS-compatible fourth dimension could successfully be coupled to MS enabling online mAb charge variant characterization on the peptide level. [82] IEC and CZE are both important methods for the characterization of mAb charge heterogeneity, however, CZE has superior selectivity in some cases and thus, is being used for charge heterogeneity profiling and release testing of therapeutic mAbs. [27] CZE(EACA) of intact mAbs using a two-dimensional CZE-CZE-MS setup could already be shown by our group some time ago.[65] However, the combination of CE-based intact mAb charge variant separation in the first dimension and performing online digestion in a second dimension, coupled to MS, has not been reported so far. Although the in-capillary digestion approach for mAb quality control is already used for a few years, [73, 83] it was never reported in a two-dimensional CE-MS system. A CZE-CZE-MS system was set up to separate mAb charge variants in an EACA-based BGE (first dimension) with subsequent heart-cut of specific peaks, in-capillary denaturation, and digestion, followed by peptide analysis with MS/MS (second dimension).

## Discussion

This setup is shown in Figure 14 and consists of two CE instruments, two external UV detectors, a nanoliter valve, and the previously presented *nanoCEasy* interface.

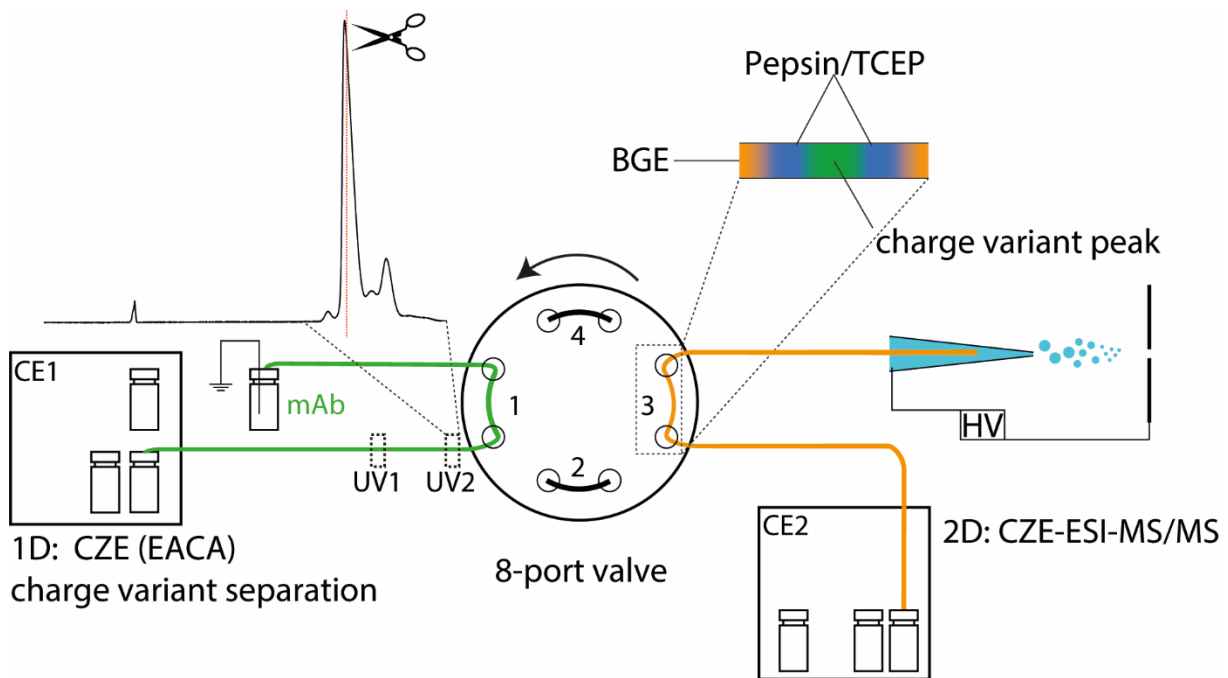


**Figure 14.** Set-up of CZE(EACA)-CZE-MS/MS with in-capillary reduction and digestion. 1D: CZE(EACA) with UV detection at two positions in front of the 8-port valve. 2D: CZE-MS/MS via the *nanoCEasy* interface.

One very important parameter in two-dimensional separation systems is the heart-cut timing during the first dimension. In this method, the sample was diluted with water prior to injection to a concentration of 1 mg/mL. This water-based injection plug provides a beneficial sample stacking effect that is eliminated when BGE is used as the sample matrix. Due to a sample stacking effect, the migration velocity was inhomogeneous during the separation distance from the capillary inlet to the valve. This effect initially caused incorrect heart-cut timings based on the theoretically calculated velocity with a constant voltage and one UV detector in front of the valve as a measuring point. Although this approach has worked well in other separation systems using electrokinetic injection [68], it only worked to a limited extent. One option to mitigate the incorrect timing was to stop the separation voltage when the peak of interest reached the detector window and immediately apply pressure to push the peak of interest into the valve loop with the known distance from the detection window to the valve loop. Although this approach was used in a previous work of our group [65], it relied heavily on a constant backpressure of the capillaries and the valve as well as



## Discussion

constant pressure output from the CE instrument. Another risk from the positioning approach by pressure is peak broadening from the occurring laminar flow profile. Adding a second UV detector in the first dimension with a specific distance to the first detector allowed the precise determination of the migration velocity between the two detection points (32.5 cm and 40.5 cm from the inlet) and at the same time a reliable estimation of the expected migration time from the second detection point to the valve loop while keeping the constant separation voltage. This peak positioning approach by voltage with two UV detectors demonstrated reproducible migration velocities of the CE method in the first dimension and reproducible heart-cut timings. Another benefit of having two UV detectors was the possibility to estimate the peak volumes of the mAb charge variant peaks in the first dimension (see Figure 15).

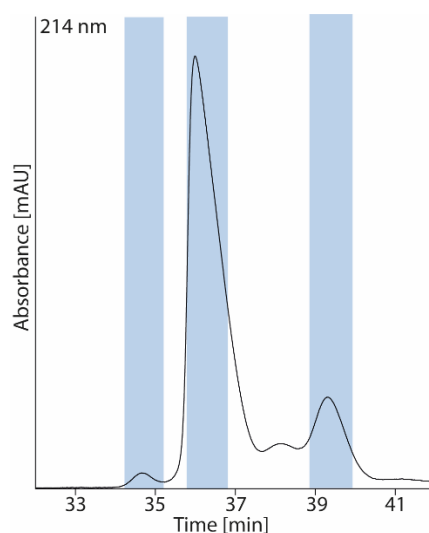


**Figure 15.** Estimated peak volumes (blue bars). Calculated by the respective migration velocity obtained from two detection points with a distance of 8 cm.

The estimated peak volumes were calculated by the migration velocity and the peak width in capillaries with known ID (50  $\mu\text{m}$ ). This enabled further the estimation of the possible peak overlap in the utilized valve rotor with a given volume of 24 nL. The estimated peak volumes were also used to calculate the amount of analyte in peaks that were cut and transferred into the second dimension. The setup using two UV detectors was demonstrated to be very important in the presented two-dimensional CE-MS approach and was applied for the first time in this context. Future two-dimensional CE applications may consider using this approach as well and adapt it to their respective requirements. The CE-CE-MS setup with the two UV detectors and the arrangement of the UV detection cells are shown in Figure 16.

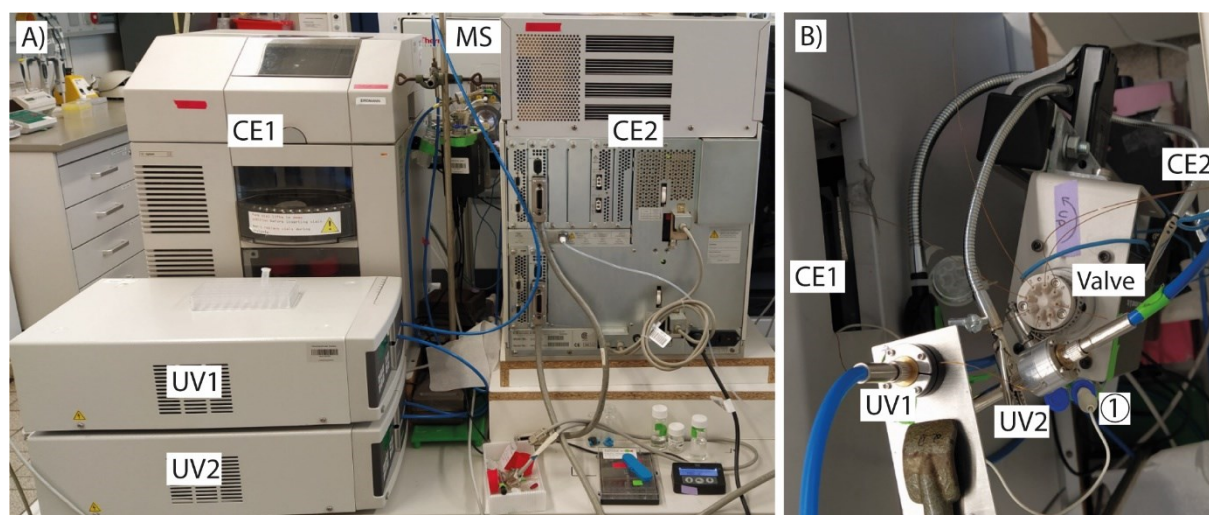


**Figure 16.** CE-CE-MS setup with two UV detectors. **A)** Two CE instruments (left and right), and two UV detectors (in front of CE1). The valve and the UV detection cells are located between the two CE instruments. The MS instrument is in the background. **B)** Arrangement of the UV detection cells in front of the valve. Item labeled with “1” is the external vial with an external electrode from the first dimension. The external electrode is connected to the outlet electrode of CE1 via a wire to close the electric circuit.

The presented in-capillary digestion in the second dimension includes mAb from the first dimension and the digestion enzyme, both in their intact form. To avoid any protein adsorption to the inner capillary wall, the application of a coating reagent was necessary. In general, any neutral coating should work for the in-capillary digestion approach. However, the capillary in the second dimension had to be etched at one side to fit in the emitter. Etching with hydrofluoric acid adds some difficulty for already coated capillaries as there is the risk of damaging certain areas of the capillaries. In addition, the coating must be stable and reproducible. Commercially available coatings would have been an option from a performance point of view but would have increased the costs many times over and included the risk of damaging the coating. Therefore, a renewable static neutral capillary coating was required, adapted from other in-capillary digestion protocols in the literature. This coating proved to work in our setup using mAb and pepsin as a digestion enzyme in one-dimensional preliminary experiments. The coating procedure included 1M NaOH and 0.1M HCl, which are both non-desired ions in the ESI process and the MS interface/entrance. Another step of the coating procedure is the PEO solution itself which was flushed for several minutes through the capillary in the second dimension. Coating reagents can also interfere with the ESI process and tend to stick to surfaces as a part of their properties. The two-capillary

## Discussion

approach was used to control the liquid flow in the emitter and to avoid any contamination of the MS or the emitter tip with ESI-interfering or coating substances.

The preparation for the in-capillary digestion in the second dimension included the injection of a digestion mix consisting of the enzyme pepsin and the reducing reagent TCEP. This digestion mix was injected as a large plug (~60 nL) and positioned via pressure in the valve loop with an overlap of ~18 nL. Initial experiments regarding the plug setup (either one plug only in front or behind the mAb plug or two plugs with one of them on each side) showed a higher digestion efficiency for the two-plug setup. The mixing strategy of the plugs was considered another factor contributing to the digestion efficiency. Electrophoretic mixing is a common option for enzymatic microreactors but lacks generic applicability due to the different possible mobilities of reactants.[84, 85] The TDLFP (transverse diffusion of laminar flow profile) methodology uses pressure to mix reactants and is considered to be a generic method for mixing in capillaries. [85, 86] Using a total of three plugs (digestion mix – mAb – digestion mix) in a sandwich-like manner (see Figure 17) was tested first in a one-dimensional and later also in the two-dimensional setup providing high sequence coverages.



**Figure 17.** Sandwich-like plug setup in the second dimension. The capillary was filled with BGE, then a large plug of pepsin/TCEP mixture was injected and positioned via pressure in the valve loop with some overlap. The mAb peak was transferred from the first dimension in a heart-cut fashion.

The amount of pressure, the duration of the pressure application, and the digestion time have to be considered and optimized for the respective setup and the utilized reagents. Especially the digestion time may vary strongly depending on the enzyme and the surrounding temperature. In the setup presented here, as little as 10 minutes at room temperature was sufficient for pepsin, which, except for the required acidic pH, is quite undemanding as far as environmental conditions are concerned. Pepsin is known to have a lower specificity than other commonly utilized digestion enzymes for peptide mapping such as trypsin or Lys-C).

Still, more than 70% of the identified peptides could be found in two different sets of consecutive experiments (n=3). Independently of the specificity and reproducibility of

## Discussion

pepsin, high sequence coverages and several PTMs could be confirmed. Nevertheless, there were several examples where only one peptide species (non-modified or modified) could be found, but not their respective modified or non-modified version which might be explained by the low specificity of pepsin or PTMs affecting the cleavage pattern of pepsin. In addition to the enzyme specificity, the MS method plays a key role in the detection of peptides. A limitation arises from the MS instrument by using a Top5 method, which chooses for each MS/MS cycle the five highest abundant  $m/z$ . Lower abundant and comigrating peptides were thus excluded with this approach. For future studies, an Orbitrap Tribrid Eclipse or Exploris (TopN capability and therefore higher MS2 frequency) for higher throughput could be an interesting alternative. The MS instrument method limitation could also be one reason for not finding any confirmed peptide pairs with ammonia-loss, dehydration, or N-terminal pyroGlu. Two of these PTMs, ammonia-loss, and dehydration were expected to be found, especially in the acidic peaks as these are common reaction products for deamidated peptides which could be found in several experiments. Succinimide is an intermediate product of the deamidation reaction from Asn. It can be formed either by an ammonia loss of Asn or by dehydration of Asp or isoAsp. Succinimide is very unstable at neutral and basic conditions as it is hydrolyzed rapidly to Asp or isoAsp.[87] In contrast, succinimide hydrolysis is much slower under acidic conditions and accumulates which allows the analysis of this unstable intermediate product.[88] Online digestion after charge-based separation enables also the analysis of the succinimide intermediate, as shown in several examples of multidimensional LC-MS approaches for therapeutic mAbs.[82, 89, 90] Considering this, the presented two-dimensional approach using acidic conditions in combination with online digestion should be capable of succinimide analysis. The previously mentioned multidimensional approach (referred to as 4D-LC-MS) used two separation dimensions (CEX (first), RPLC (fourth)), one dimension for desalting, denaturing, and reduction (second), and a tryptic column for digestion (third). This kind of setup relies heavily on the quality and performance of the tryptic column, as the column age has a large impact on the digestion efficiency and number of miscleaveages.[90] In addition, there are certain challenges in the production of reliable and reproducible tryptic columns, as well as a low number of alternative enzymes available. The presented two-dimensional CE-MS provides flexibility regarding the utilized enzyme and requires only a very low amount

## Discussion

of volume due to the small capillary volumes. Alternatives to pepsin could be trypsin, which would require some plug and BGE optimization to keep the pH for trypsin in the optimal range. Nevertheless, when using an EACA-based BGE, competitive trypsin inhibition would remain. Other interesting enzymes would be IdeS or Kgp for middle-up digestion and subsequent possible top-down MS strategies. For each enzyme, a certain effort will be required to find functional parameters, and the demonstrated proof of concept underlines the flexibility and capabilities of this method.

The introduced two-dimensional CE-MS system is not only limited to the presented CZE(EACA) method and in-capillary digestion. Another possible method could be CIEF in combination with in-capillary digestion in cases where CIEF is needed due to superior resolution than CZE(EACA) for specific mAbs. CIEF-CZE-MS could already be demonstrated earlier by our group including a multi-heart cut approach for proteins. CIEF in combination with in-capillary digestion would possibly allow even deeper insights into the charge species composition of mAbs but would also add challenges for the selected enzyme considering the sample matrix (pH and ampholytes). A more sophisticated approach could be hydrogen-deuterium exchange (HDX) in the first dimension (only low amounts of deuterated BGE necessary in CE) and then perform the denaturation, reduction, and pepsin digestion followed by MS characterization in the second dimension to monitor structural characteristics of therapeutic proteins and mAbs.

One of the most critical parts in the two-dimensional CE-MS system was the valve as the CE-CE interface which had high demands like electrical isolation and defined volumes. The dimension of the stator bore and the rotor loop should ideally fit with the CE capillary dimension of 50  $\mu\text{m}$ . PEEK was chosen as a material for the stator and rotor, and the smallest available bore of 100  $\mu\text{m}$  for the valve stator was selected. Going from larger ID to smaller ID harbor always the risk of clogging, which occasionally was the case during the 2D setup and ultimately required cleaning of the valve stator and rotor with ultrasonication or in some rare cases, with a 50  $\mu\text{m}$  wire. This cleaning procedure had the risk of damaging the stator or rotor surfaces which would then lead to liquid leakages between the rotor and stator and compromise the electrical isolation characteristics. Another possibility for damaging the stator was the formation or introduction of particles that got stuck between the rotor and stator would form scratches due to the switching rotation of the valve. PEEK material provides

## Discussion

chemical stability and electrical isolation capabilities but is a rather soft material. From past experiences with these types of valves in several different two-dimensional CE-MS setups and from the presented work here, the utilized stators and rotors can be considered as a consumable that has to be replaced from time to time to maintain their performance in terms of tightness. Future developments regarding a valve for two-dimensional CE-MS could consider other materials and manufacturing techniques such as glass with laser-supported etching procedures. A specific type of valve dedicated to two-dimensional CE-MS could help to stabilize the performance and robustness of these sophisticated setups.

The presented two-dimensional CE-MS setup using two UV detectors for precise and reproducible heart-cuts combined with the simultaneous in-capillary reduction and digestion methodology has shown promising results for the in-depth characterization of therapeutic mAbs. The in-capillary digestion of four different mAbs provided high sequence coverages of >90% using pepsin as a digestion enzyme. A low abundant basic variant of the NIST mAb (1.2% of the main peak) resulted in a combined sequence coverage of 91.5% using approximately 640 pg of this species for the in-capillary digestion.

The utilized *nanoCEasy* CE-MS interface provided the required sensitivity and flexibility for the analysis of mAb charge species enabling high sequence coverages. This proof of concept for the PTM characterization of charge-based proteins can be considered as an alternative approach to existing multidimensional LC-MS methods providing flexibility regarding the utilized digestion enzyme and the separation mode in the first dimension. Two-dimensional CE-MS setups have shown to be a compelling tool kit for the MS-based characterization of biopharmaceuticals. However, a two-dimensional CE-MS setup requires experienced users and a lot of hands-on time which hampers probably the adoption of this technique in other scientific labs and institutions. For the future, a more automated configuration of the valve and the CE-MS interface would be beneficial to allow further recognition and distribution into scientific and industrial applications.

## 4 Summary

The comprehensive characterization of biotherapeutics plays an essential role in pharmaceutical development and quality control. The characterization of charge heterogeneity is thereby of utmost importance for the efficacy and safety of mAbs. CE as an analytical technique includes separation modes such as CZE and CIEF, which provide high selectivity to charge heterogeneity of proteins and mAbs and are frequently applied in the scientific and biopharmaceutical sectors. However, these separation methods lack ESI-MS compatibility due to the required chemical composition with high amounts of salts or ampholytes which are necessary to achieve high separation performance. The identification of protein charge species and further localization of PTMs by CE-MS methods requires furthermore high sensitivity to detect occurring low abundant species. Therefore, a nanoflow sheath liquid CE-MS interface with a focus on sensitivity, flexibility, and ease of use was developed.

Two different ways were presented to hyphenate ESI-interfering CE methods online to MS using this developed CE-MS interface. The first is a direct way (i.e. iCIEF-MS) with possible compromises regarding separation performance and sensitivity of mass spectrometric detection taken into account. The second way is to use a two-dimensional CE-MS setup with two independent CE dimensions and a nanoliter valve as an interface, where the first dimension contains ESI-interfering substances.

The novel nanoflow sheath liquid interface *nanoCEasy* combines sensitivity, flexibility, and ease of use. It was developed using transparent 3D-printed parts with the concept of “plug&play” to simplify the setup, handling, and troubleshooting. The *nanoCEasy* interface works with two capillaries providing a divert-valve approach for the liquid flow control in the emitter. This ensures maximum flexibility regarding the CE effluent composition toward ESI-MS and prevents emitter clogging. The concept of using 3D-printed parts enabled a short development time and quick iterations for changes and improvements, as well as low costs. The robustness of the interface operation and flexibility regarding different applications such as peptides, small proteins, and mAb subunits including online recoating of the separation capillary could be shown.

## Summary

Increasing the electrospray voltage or adapting the SL composition to higher organic content allowed higher CE effluents without compromising the ESI spray stability or sensitivity. The electrospray voltage was therefore identified as a major parameter to ensure the operation of the interface using CE methods with a high EOF including an application example of hemoglobin species separation. Further, a possible automation concept of the *nanoCEasy* interface was introduced and discussed.

The preparative iCIEF-UV instrument *CEInfinite* was successfully coupled to two different MS instruments utilizing the *nanoCEasy* interface for the characterization of therapeutic mAbs. Parameters such as ampholyte concentration, sample concentration, and mobilization speed were investigated and optimums dependent on the analyte could be found. Depending on the MS instrument, different parameters have shown to be functional and may be optimized individually per analyte. The respective mAbs defined the type of iCIEF cartridge coating and additives necessary for successful analysis. The iCIEF-MS setup using the *nanoCEasy* interface was optimized regarding the transfer capillary length to minimize the distance between the iCIEF instrument and the MS instrument, as short distances showed to be beneficial for good maintenance of the focusing resolution during pressurized mobilization. Intact masses of trastuzumab charge variants could be determined with high spectra quality, accuracy, and precision including low abundant variants. The two-capillary approach of the *nanoCEasy* interface allowed the avoidance of unnecessary MS contamination during flushing phases and separation phases without analytes.

A two-dimensional CE-MS setup was developed for the characterization of mAb charge heterogeneity on the peptide level. The first dimension comprised an MS-incompatible charge-based CZE method for intact mAbs based on EACA with two UV detectors in front of the valve to enable precise and reproducible heart-cuts, an estimation of peak volumes, and potential peak overlap. The second, MS-compatible dimension, was used for an in-capillary approach combining reduction and digestion after the heart-cut of specific peaks, and the subsequent separation and MS/MS detection of the resulting peptides. The capillary of the second dimension was hyphenated to MS using the *nanoCEasy* interface which allowed online coating and recoating to prevent sample adsorption. In this way, distinct PTMs of unstressed and



## Summary

stressed mAbs could be localized including several combinations of charge-related PTMs in one peak. Pepsin as a digestion enzyme provided reproducible peptides up to a certain degree. This proof-of-concept study demonstrated a large potential for the in-depth characterization of mAbs using CE-based methods.

## 5 Zusammenfassung

Die umfassende Charakterisierung von Biotherapeutika spielt eine wesentliche Rolle bei deren pharmazeutischen Entwicklung und Qualitätskontrolle. Die Charakterisierung der Ladungsheterogenität ist dabei von größter Bedeutung für die Wirksamkeit und Sicherheit von monoklonalen Antikörpern. Die Kapillarelektrophorese als analytische Technik umfasst Trennverfahren wie CZE und CIEF, die eine hohe Selektivität für die Ladungsheterogenität von Proteinen und mAbs bieten und häufig im wissenschaftlichen und biopharmazeutischen Bereich eingesetzt werden. Diese Trennmethode sind jedoch aufgrund der erforderlichen chemischen Zusammensetzung nicht kompatibel mit Elektrosprayionisation-Massenspektrometrie, da hohe Mengen an Salzen oder Ampholyten für eine hohe Trennleistung erforderlich sind. Die Identifizierung von Proteinladungsspezies und die weitere Lokalisierung von posttranslationalen Modifikationen durch CE-MS Methoden erfordert darüber hinaus eine hohe Empfindlichkeit, um vorkommende, wenig häufige Spezies zu erkennen. Daher wurde eine CE-MS Ionenquelle mit einem Schleierflüssigkeitsfluss im Nanoliterbereich mit Schwerpunkt auf Empfindlichkeit, Flexibilität und Benutzerfreundlichkeit entwickelt.

Es wurden zwei verschiedene Möglichkeiten vorgestellt, Elektrospray-interferierende Kapillarelektrophoresemethoden mit Hilfe der entwickelten CE-MS Schnittstelle online auf Massenspektrometrie zu übertragen. Die erste Möglichkeit ist ein direkter Weg (d.h. iCIEF-MS), bei dem mögliche Kompromisse in Bezug auf die Trennleistung und die Empfindlichkeit des massenspektrometrischen Nachweises in Betracht gezogen werden müssen. Der zweite Weg ist die Verwendung eines zweidimensionalen CE-MS Aufbaus mit zwei unabhängigen Kapillarelektrophorese Dimensionen und einem Nanoliter-Ventil als Schnittstelle, wobei die erste Dimension Elektrospray-interferierende Substanzen enthält.

Die neuartige CE-MS Ionenquelle mit einem Schleierflüssigkeitsfluss im Nanoliterbereich *nanoCEasy* vereint Empfindlichkeit, Flexibilität und Benutzerfreundlichkeit. Sie wurde unter Verwendung transparenter 3D-gedruckter

## Zusammenfassung

Teile mit dem Konzept "Plug & Play" entwickelt, um die Einrichtung, Handhabung und Fehlerbehebung zu vereinfachen. Die *nanoCEasy* Ionenquelle arbeitet mit zwei Kapillaren, die eine Art Umleitungsventil für die Steuerung des Flüssigkeitsflusses im Emitter bieten. Dies gewährleistet maximale Flexibilität hinsichtlich der Zusammensetzung des Flüssigkeitsflusses von der Kapillarelektrophorese für Elektrosprayionisation-Massenspektrometrie und verhindert gleichzeitig mögliches Verstopfen des Emitters. Das Konzept der Verwendung von 3D-gedruckten Teilen ermöglichte eine kurze Entwicklungszeit für Änderungen und Verbesserungen sowie niedrige Kosten. Die Robustheit der Ionenquelle und die Flexibilität in Bezug auf verschiedene Anwendungen wie Peptide, kleine Proteine und Antikörper-Untereinheiten, einschließlich der Neubeschichtung von Trennkapillaren im laufenden Betrieb konnten gezeigt werden. Die Erhöhung der Elektrospray-Spannung oder die Anpassung der Schleierflüssigkeit-Zusammensetzung an einen höheren organischen Gehalt ermöglichte einen höheren Volumenstrom aus der Kapillarelektrophorese ohne Beeinträchtigung der Elektrospray-Stabilität oder der Empfindlichkeit. Die Elektrospray-Spannung wurde daher als ein wichtiger Parameter identifiziert, um den Betrieb der Ionenquelle bei Kapillarelektrophorese-Methoden mit einem hohen elektroosmotischen Fluss zu gewährleisten, einschließlich eines Anwendungsbeispiels mit der Trennung von Hämoglobinvarianten. Darüber hinaus wurde ein mögliches Automatisierungskonzept für die *nanoCEasy*-Ionenquelle vorgestellt und diskutiert.

Das präparative iCIEF-UV Instrument *CEInfinite* wurde erfolgreich an zwei verschiedene Massenspektrometer gekoppelt, die die *nanoCEasy* Ionenquelle für die Charakterisierung von therapeutischen monoklonalen Antikörpern nutzen. Parameter wie die Ampholyt-Konzentration, die Probenkonzentration und die Mobilisierungsgeschwindigkeit wurden untersucht und Optimierungen in Abhängigkeit vom Analyten konnten gefunden werden. Je nach Massenspektrometer haben sich verschiedene Parameter als funktionell erwiesen und können für jeden Analyten individuell optimiert werden. Die jeweiligen Antikörper definierten die Art der inneren Kapillar-Beschichtung in den iCIEF-Kartuschen und die für eine erfolgreiche Analyse erforderlichen Additive. Der iCIEF-MS Aufbau unter Verwendung der *nanoCEasy* Ionenquelle wurde hinsichtlich der Länge der Transferkapillare optimiert, um den

## Zusammenfassung

Abstand zwischen dem iCIEF Instrument und dem Massenspektrometer zu minimieren, da sich kurze Abstände als vorteilhaft für eine gute Aufrechterhaltung der Fokussierungsauflösung während der Druckmobilisierung erwiesen. Die intakten Massen von Trastuzumab-Ladungsvarianten konnten mit hoher Spektrenqualität, Genauigkeit und Präzision bestimmt werden, einschließlich der Varianten mit geringer Häufigkeit. Der Zweikapillaransatz der *nanoCEasy* Ionenquelle ermöglichte es, unnötige Kontaminationen des Massenspektrometers während der Spülphasen und während der Trennphasen ohne Analyten zu vermeiden.

Für die Charakterisierung der Ladungsheterogenität von monoklonalen Antikörpern auf Peptidebene wurde ein zweidimensionaler CE-MS Aufbau entwickelt. Die erste Dimension umfasste eine MS-inkompatible ladungsbasierte CZE-Methode für intakte monoklonale Antikörper auf der Grundlage von  $\epsilon$ -Aminocapronsäure mit zwei UV-Detektoren vor dem Ventil, um präzise und reproduzierbare Heart-cuts, eine Schätzung der Peakvolumina und eine potenzielle Peaküberlappung zu ermöglichen. Die zweite, massenspektrometrisch kompatible Dimension wurde für einen In-Kapillar-Ansatz verwendet, der Reduktion und Verdauung nach dem Heart-cut spezifischer Peaks und die anschließende Trennung und MS/MS-Detektion der resultierenden Peptide kombiniert. Die Kapillare der zweiten Dimension wurde mit Hilfe der *nanoCEasy* Ionenquelle, die eine Online-Beschichtung und -Wiederbeschichtung zur Verhinderung der Probenadsorption ermöglichte, mit dem Massenspektrometer verbunden. Auf diese Weise konnten unterschiedliche posttranslationale Modifikationen von ungestressten und gestressten monoklonalen Antikörpern lokalisiert werden, einschließlich mehrerer Kombinationen von ladungsbezogenen posttranslationalen Modifikationen in einem Peak. Pepsin als Verdauungsenzym lieferte bis zu einem gewissen Grad reproduzierbare Peptide. Diese „Proof-of-Concept“ Studie zeigte ein großes Potenzial für die umfassende Charakterisierung von monoklonalen Antikörpern mit Kapillarelektrophorese-basierten Methoden.

## 6 References

1. Dimitrov DS. Therapeutic proteins. *Methods Mol Biol.* 2012;899:1–26.
2. Goeddel DV., Kleid DG., Bolivar F, Heyneker HL., Yansura DG., Crea R, et al. Expression in *Escherichia coli* of chemically synthesized genes for human insulin. *Proc Natl Acad Sci U S A.* 1979;76:106–10.
3. Köhler G, Milstein C. Continuous cultures of fused cells secreting antibody of predefined specificity. *Nature.* 1975;256:495–7.
4. Todd PA., Brogden RN. Muromonab CD3. A review of its pharmacology and therapeutic potential. *Drugs.* 1989;37:871–99.
5. Mullard A. FDA approves 100th monoclonal antibody product. *Nat Rev Drug Discov.* 2021;20:491–5.
6. Kaplon H, Chenoweth A, Crescioli S, Reichert JM. Antibodies to watch in 2022. *MAbs.* 2022;14:2014296.
7. Zheng K, Bantog C, Bayer R. The impact of glycosylation on monoclonal antibody conformation and stability. *MAbs.* 2011;3:568–76.
8. Jefferis R. Recombinant antibody therapeutics: the impact of glycosylation on mechanisms of action. *Trends Pharmacol Sci.* 2009;30:356–62.
9. Mariño K, Bones J, Kattla JJ., Rudd PM. A systematic approach to protein glycosylation analysis: a path through the maze. *Nat Chem Biol.* 2010;6:713–23.
10. Liu HF., Ma J, Winter C, Bayer R. Recovery and purification process development for monoclonal antibody production. *MAbs.* 2010;2:480–99.
11. International Conference on Harmonization. Q 6 B Specifications: Test Procedures and Acceptance Criteria for Biotechnological/Biological Products.
12. Harris RJ., Kabakoff B, Macchi FD., Shen FJ., Kwong M, Andya JD., et al. Identification of multiple sources of charge heterogeneity in a recombinant antibody. *J Chromatogr B Analyt Technol Biomed Life Sci.* 2001;752:233–45.
13. Liu H, Ponniah G, Zhang H-M, Nowak C, Neill A, Gonzalez-Lopez N, et al. In vitro and in vivo modifications of recombinant and human IgG antibodies. *MAbs.* 2014;6:1145–54.
14. Beck A, Liu H. Macro- and Micro-Heterogeneity of Natural and Recombinant IgG Antibodies. *Antibodies.* 2019;8.
15. Robotham AC., Kelly JF. LC-MS characterization of antibody-based therapeutics.

## References

- In: Matte A, editor. LC-MS characterization of antibody-based therapeutics. Amsterdam, Netherlands: Elsevier; 2020. p. 1–33.
16. Fekete S, Veuthey J-L, Guillaume D. New trends in reversed-phase liquid chromatographic separations of therapeutic peptides and proteins: theory and applications. *J Pharm Biomed Anal.* 2012;69:9–27.
  17. Hong P, Koza S, Bouvier ES.P. Size-Exclusion Chromatography for the Analysis of Protein Biotherapeutics and their Aggregates. *J Liq Chromatogr Relat Technol.* 2012;35:2923–50.
  18. Fekete S, Veuthey J-L, Beck A, Guillaume D. Hydrophobic interaction chromatography for the characterization of monoclonal antibodies and related products. *J Pharm Biomed Anal.* 2016;130:3–18.
  19. D'Atri V, Guillaume D. Characterization of Glycosylated Proteins at Subunit Level by HILIC/MS. In: Delobel A, editor. *Characterization of Glycosylated Proteins at Subunit Level by HILIC/MS.* New York, NY: Springer US; 2021. p. 85–95.
  20. Fekete S, Beck A, Veuthey J-L, Guillaume D. Ion-exchange chromatography for the characterization of biopharmaceuticals. *J Pharm Biomed Anal.* 2015;113:43–55.
  21. Dadouch M, Ladner Y, Perrin C. Analysis of Monoclonal Antibodies by Capillary Electrophoresis: Sample Preparation, Separation, and Detection. *Separations.* 2021;8:4.
  22. Kaur H, Beckman J, Zhang Y, Li ZJ., Szigeti M, Guttman A. Capillary electrophoresis and the biopharmaceutical industry: Therapeutic protein analysis and characterization. *Trends Anal. Chem.* 2021;144:116407.
  23. Kumar R, Guttman A, Rathore AS. Applications of capillary electrophoresis for biopharmaceutical product characterization. *Electrophoresis.* 2022;43:143–66.
  24. Lechner A, Giorgetti J, Gahoual R, Beck A, Leize-Wagner E, François Y-N. Insights from capillary electrophoresis approaches for characterization of monoclonal antibodies and antibody drug conjugates in the period 2016–2018. *Journal of Chromatography B.* 2019.
  25. Spanov B, Govorukhina N, van de Merbel NC., Bischoff R. Analytical tools for the characterization of deamidation in monoclonal antibodies. *Journal of Chromatography Open.* 2022;2:100025.
  26. Štěpánová S, Kašička V. Applications of capillary electromigration methods for

## References

- separation and analysis of proteins (2017–mid 2021) – A review. *Analytica Chimica Acta*. 2022;10:339447.
27. Moritz B, Schnaible V, Kiessig S, Heyne A, Wild M, Finkler C, et al. Evaluation of capillary zone electrophoresis for charge heterogeneity testing of monoclonal antibodies. *Journal of Chromatography B*. 2015;983-984:101–10.
  28. Wu G, Yu C, Wang W, Wang L. Interlaboratory method validation of icIEF methodology for analysis of monoclonal antibodies. *Electrophoresis*. 2018;39:2091–8.
  29. Salas-Solano O, Babu K, Park SS., Zhang X, Zhang L, Sosic Z, et al. Intercompany Study to Evaluate the Robustness of Capillary Isoelectric Focusing Technology for the Analysis of Monoclonal Antibodies. *Chromatographia*. 2011;73:1137–44.
  30. Hunt G, Nashabeh W. Capillary Electrophoresis Sodium Dodecyl Sulfate Nongel Sieving Analysis of a Therapeutic Recombinant Monoclonal Antibody: A Biotechnology Perspective. *Anal. Chem*. 1999;71:2390–7.
  31. Salas-Solano O, Tomlinson B, Du S, Parker M, Strahan A, Ma S. Optimization and validation of a quantitative capillary electrophoresis sodium dodecyl sulfate method for quality control and stability monitoring of monoclonal antibodies. *Anal Chem*. 2006;78:6583–94.
  32. Geiger T, Clarke S. Deamidation, isomerization, and racemization at asparaginyl and aspartyl residues in peptides. Succinimide-linked reactions that contribute to protein degradation. *Journal of Biological Chemistry*. 1987;262:785–94.
  33. Stephenson RC., Clarke S. Succinimide Formation from Aspartyl and Asparaginyl Peptides as a Model for the Spontaneous Degradation of Proteins. *Journal of Biological Chemistry*. 1989;264:6164–70.
  34. Yang H, Zubarev RA. Mass spectrometric analysis of asparagine deamidation and aspartate isomerization in polypeptides. *Electrophoresis*. 2010;31:1764–72.
  35. Pace AL., Wong RL., Zhang YT., Kao Y-H, Wang YJ. Asparagine deamidation dependence on buffer type, pH, and temperature. *J Pharm Sci*. 2013;102:1712–23.
  36. Laurer H., Rozing G. High performance capillary electrophoresis. Agilent Technologies; 2014.
  37. Jorgenson JW., Lukacs KD. Free-zone electrophoresis in glass capillaries. *Clin Chem*. 1981;27:1551–3.

## References

38. Ragab MA.A., El-Kimary El. Recent Advances and Applications of Microfluidic Capillary Electrophoresis: A Comprehensive Review (2017-Mid 2019). *Crit Rev Anal Chem.* 2021;51:709–41.
39. Hjertén S, Zhu M. Adaptation of the equipment for high-performance electrophoresis to isoelectric focusing. *Journal of Chromatography A.* 1985;346:265–70.
40. Sebastiano R, Simó C, Mendieta ME., Antonioli P, Citterio A, Cifuentes A, et al. Mass distribution and focusing properties of carrier ampholytes for isoelectric focusing: I. Novel and unexpected results. *Electrophoresis.* 2006;27:3919–34.
41. Theresa Kristl, Hanno Stutz, Christian Wenz, Gerard Rozing. *Principles and Applications of Capillary Isoelectric Focusing*; 2014.
42. Wu J, Pawliszyn J. Capillary isoelectric focusing with a universal concentration gradient imaging system using a charge-coupled photodiode array. *Anal. Chem.* 1992;64:2934–41.
43. Wu J, Pawliszyn J. Dual Detection for Capillary Isoelectric Focusing with Refractive Index Gradient and Absorption Imaging Detectors. *Anal. Chem.* 1994;66:867–73.
44. Kahle J, Wätzig H. Determination of protein charge variants with (imaged) capillary isoelectric focusing and capillary zone electrophoresis. *Electrophoresis.* 2018;39:2492–511.
45. Goyon A, Excoffier M, Janin-Bussat M-C, Bobaly B, Fekete S, Guillarme D, et al. Determination of isoelectric points and relative charge variants of 23 therapeutic monoclonal antibodies. *J Chromatogr B Analyt Technol Biomed Life Sci.* 2017;1065-1066:119–28.
46. <https://ceinfinite.com/product/shop-cartridges/>.
47. He Y, Isele C, Hou W, Ruesch M. Rapid analysis of charge variants of monoclonal antibodies with capillary zone electrophoresis in dynamically coated fused-silica capillary. *J. Sep. Sci.* 2011;34:548–55.
48. Michels DA., Ip AY., Dillon TM., Brorson K, Lute S, Chavez B, et al. Separation Methods and Orthogonal Techniques. In: Schiel JE, Davis DL, Borisov OV, editors. *Separation Methods and Orthogonal Techniques.* Washington, DC: American Chemical Society; 2015. p. 237–284.
49. Xu Y, Wang D, Mason B, Rossomando T, Li N, Liu D, et al. Structure,



## References

- heterogeneity and developability assessment of therapeutic antibodies. *MAbs*. 2019;11:239–64.
50. Stolz A, Jooß K, Höcker O, Römer J, Schlecht J, Neusüß C. Recent advances in capillary electrophoresis-mass spectrometry: Instrumentation, methodology and applications. *Electrophoresis*. 2019;40:79–112.
  51. Hühner J, Lämmerhofer M, Neusüß C. Capillary isoelectric focusing-mass spectrometry: Coupling strategies and applications. *Electrophoresis*. 2015;36:2670–86.
  52. Lindenburg PW., Haselberg R, Rozing G, Ramautar R. Developments in Interfacing Designs for CE–MS: Towards Enabling Tools for Proteomics and Metabolomics. *Chromatographia*. 2015;78:367–77.
  53. Mokaddem M, Gareil P, Belgaied J-E, Varenne A. A new insight into suction and dilution effects in capillary electrophoresis coupled to mass spectrometry via an electrospray ionization interface. Part I-Suction effect. *Electrophoresis*. 2008;29:1957–64.
  54. Mokaddem M, Gareil P, Belgaied J-E, Varenne A. New insight into suction and dilution effects in CE coupled to MS via an ESI interface. II--dilution effect. *Electrophoresis*. 2009;30:1692–7.
  55. Matthias Wilm and Matthias Mann, Wilm M, Mann M. Analytical Properties of the Nanoelectrospray Ion Source // Analytical properties of the nanoelectrospray ion source. *Anal. Chem*. 1996;68:1–8.
  56. Moini M. Simplifying CE-MS operation. 2. Interfacing low-flow separation techniques to mass spectrometry using a porous tip. *Anal Chem*. 2007;79:4241–6.
  57. Wojcik R, Dada OO., Sadilek M, Dovichi NJ. Simplified capillary electrophoresis nanospray sheath-flow interface for high efficiency and sensitive peptide analysis. *Rapid Commun. Mass Spectrom*. 2010;24:2554–60.
  58. Maxwell EJ., Zhong X, Zhang H, van Zeijl N, Chen DD.Y. Decoupling CE and ESI for a more robust interface with MS. *Electrophoresis*. 2010;31:1130–7.
  59. Höcker O, Montealegre C, Neusüß C. Characterization of a nanoflow sheath liquid interface and comparison to a sheath liquid and a sheathless porous-tip interface for CE-ESI-MS in positive and negative ionization. *Anal. Bioanal. Chem*. 2018;410:5265–75.

## References

60. Gou M-J, Nys G, Cobraiville G, Demelenne A, Servais A-C, Fillet M. Hyphenation of capillary zone electrophoresis with mass spectrometry for proteomic analysis: Optimization and comparison of two coupling interfaces. *J. Chromatogr. A.* 2020;1618:460873.
61. Wu H, Tang K. Highly Sensitive and Robust Capillary Electrophoresis-Electrospray Ionization-Mass Spectrometry: Interfaces, Preconcentration Techniques and Applications. *Rev. Anal. Chem.* 2020;39:45–55.
62. Höcker O, Knierman M, Meixner J, Neusüß C. Two capillary approach for a multifunctional nanoflow sheath liquid interface for capillary electrophoresis-mass spectrometry. *Electrophoresis.* 2020.
63. Kohl FJ., Montealegre C, Neusüß C. On-line two-dimensional capillary electrophoresis with mass spectrometric detection using a fully electric isolated mechanical valve. *Electrophoresis.* 2016;37:954–8.
64. Neuberger S, Jooß K, Ressel C, Neusüß C. Quantification of ascorbic acid and acetylsalicylic acid in effervescent tablets by CZE-UV and identification of related degradation products by heart-cut CZE-CZE-MS. *Anal Bioanal Chem.* 2016;408:8701–12.
65. Jooß K, Hühner J, Kiessig S, Moritz B, Neusüß C. Two-dimensional capillary zone electrophoresis-mass spectrometry for the characterization of intact monoclonal antibody charge variants, including deamidation products. *Anal Bioanal Chem.* 2017;409:6057–67.
66. Hühner J, Neusüß C. CIEF-CZE-MS applying a mechanical valve. *Anal Bioanal Chem.* 2016;408:4055–61.
67. Hühner J, Jooß K, Neusüß C. Interference-free mass spectrometric detection of capillary isoelectric focused proteins, including charge variants of a model monoclonal antibody. *Electrophoresis.* 2017;38:914–21.
68. Römer J, Montealegre C, Schlecht J, Kiessig S, Moritz B, Neusüß C. Online mass spectrometry of CE (SDS)-separated proteins by two-dimensional capillary electrophoresis. *Anal Bioanal Chem.* 2019;411:7197–206.
69. Römer J, Kiessig S, Moritz B, Neusüß C. Improved CE(SDS)-CZE-MS method utilizing an 8-port nanoliter valve. *Electrophoresis.* 2020.
70. Römer J, Stolz A, Kiessig S, Moritz B, Neusüß C. Online top-down mass spectrometric identification of CE(SDS)-separated antibody fragments by two-

## References

- dimensional capillary electrophoresis. *J Pharm Biomed Anal.* 2021;201:114089.
71. Dick LW., Mahon D, Qiu D, Cheng K-C. Peptide mapping of therapeutic monoclonal antibodies: improvements for increased speed and fewer artifacts. *J Chromatogr B Analyt Technol Biomed Life Sci.* 2009;877:230–6.
  72. Wang D, Nowak C, Mason B, Katiyar A, Liu H. Analytical artifacts in characterization of recombinant monoclonal antibody therapeutics. *J Pharm Biomed Anal.* 2020;183:113131.
  73. Dadouch M, Ladner Y, Bich C, Montels J, Morel J, Perrin C. Fast in-line bottom-up analysis of monoclonal antibodies: Toward an electrophoretic fingerprinting approach. *Electrophoresis.* 2021;42:1229–37.
  74. Konermann L, Ahadi E, Rodriguez AD., Vahidi S. Unraveling the mechanism of electrospray ionization. *Anal Chem.* 2013;85:2–9.
  75. Grajewski M, Hermann M, Oleschuk RD., Verpoorte E, Salentijn G. Leveraging 3D printing to enhance mass spectrometry: A review. *Analytica Chimica Acta.* 2021;88:338332.
  76. Waldbaur A, Rapp H, Länge K, Rapp BE. Let there be chip—towards rapid prototyping of microfluidic devices: one-step manufacturing processes. *Anal. Methods.* 2011;3:2681.
  77. Gross B, Lockwood SY., Spence DM. Recent Advances in Analytical Chemistry by 3D Printing. *Anal. Chem.* 2017;89:57–70.
  78. Zhang X, Kwok T, Zhou M, Du M, Li V, Bo T, et al. Imaged capillary isoelectric focusing (icIEF) tandem high resolution mass spectrometry for charged heterogeneity of protein drugs in biopharmaceutical discovery. *J Pharm Biomed Anal.* 2023;224:115178.
  79. Zhang X, Chen T, Li V, Bo T, Du M, Huang T. Cutting-edge mass spectrometry strategy based on imaged capillary isoelectric focusing (icIEF) technology for characterizing charge heterogeneity of monoclonal antibody. *Anal Biochem.* 2023;660:114961.
  80. Wu G, Yu C, Wang W, Du J, Fu Z, Xu G, et al. Mass Spectrometry-Based Charge Heterogeneity Characterization of Therapeutic mAbs with Imaged Capillary Isoelectric Focusing and Ion-Exchange Chromatography as Separation Techniques. *Anal Chem.* 2023.
  81. Alvarez M, Tremintin G, Wang J, Eng M, Kao Y-H, Jeong J, et al. On-line

## References

- characterization of monoclonal antibody variants by liquid chromatography-mass spectrometry operating in a two-dimensional format. *Anal Biochem.* 2011;419:17–25.
82. Gstöttner C, Klemm D, Habegger M, Bathke A, Wegele H, Bell C, et al. Fast and Automated Characterization of Antibody Variants with 4D HPLC/MS. *Anal Chem.* 2018;90:2119–25.
83. Ladner Y, Mas S, Coussot G, Bartley K, Montels J, Morel J, et al. Integrated microreactor for enzymatic reaction automation: An easy step toward the quality control of monoclonal antibodies. *J. Chromatogr. A.* 2017;1528:83–90.
84. Cheng M, Chen Z. Recent advances in screening of enzymes inhibitors based on capillary electrophoresis. *J Pharm Anal.* 2018;8:226–33.
85. Farcaş E, Pochet L, Fillet M. Transverse diffusion of laminar flow profiles as a generic capillary electrophoresis method for in-line nanoreactor mixing: Application to the investigation of antithrombotic activity. *Talanta.* 2018;188:516–21.
86. Krylova SM., Okhonin V, Krylov SN. Transverse diffusion of laminar flow profiles—a generic method for mixing reactants in capillary microreactor. *J. Sep. Sci.* 2009;32:742–56.
87. Patel K, Borchardt RT. Chemical Pathways of Peptide Degradation. II. Kinetics of Deamidation of an Asparaginylyl Residue in a Model Hexapeptide // Chemical pathways of peptide degradation. II. Kinetics of deamidation of an asparaginylyl residue in a model hexapeptide. *Pharm Res.* 1990;7:703–11.
88. Xie M, Vander Velde D, Morton M, Borchardt RT., Schowen RL. pH-Induced Change in the Rate-Determining Step for the Hydrolysis of the Asp/Asn-Derived Cyclic-Imide Intermediate in Protein Degradation. *J. Am. Chem. Soc.* 1996;118:8955–6.
89. Camperi J, Grunert I, Heinrich K, Winter M, Özipek S, Hoelterhoff S, et al. Inter-laboratory study to evaluate the performance of automated online characterization of antibody charge variants by multi-dimensional LC-MS/MS. *Talanta.* 2021;234:122628.
90. Verscheure L, Cerdobbel A, Sandra P, Lynen F, Sandra K. Monoclonal antibody charge variant characterization by fully automated four-dimensional liquid chromatography-mass spectrometry. *J. Chromatogr. A.* 2021;1653:462409.

## **7 Ehrenwörtliche Erklärung**

Hiermit erkläre ich, dass mir die Promotionsordnung der Fakultät für Biowissenschaften der Friedrich-Schiller-Universität Jena bekannt ist, ich die Dissertation selbst angefertigt habe und alle von mir benutzten Hilfsmittel, persönlichen Mitteilungen und Quellen in meiner Arbeit angegeben sind.

Ich versichere, dass ich keine Hilfe eines Promotionsberaters in Anspruch genommen habe und dass Dritte weder unmittelbar noch mittelbar geldwerte Leistungen von mir für Arbeiten erhalten haben, die im Zusammenhang mit dem Inhalt der vorgelegten Dissertation stehen.

Die vorliegende Dissertation wurde von mir bei keiner bisherigen Prüfungsarbeit für eine staatliche oder andere wissenschaftliche Prüfung eingereicht. Weiterhin versichere ich, dass ich die gleiche, eine in wesentlichen Teilen ähnliche oder eine andere Abhandlung nicht bei einer anderen Universität als Dissertation eingereicht habe.

Karlsruhe, den 22.04.2023

Johannes Schlecht

## 9 Supplementary information

### 9.1 Supplementary information manuscript I

#### Supporting Information

##### **nanoCEasy: an easy, flexible and robust nanoflow sheath liquid CE-MS interface based on 3D-printed parts**

Johannes Schlecht<sup>1,2</sup>, Alexander Stolz<sup>1,2</sup>, Adrian Hofmann<sup>1</sup>, Lukas Gerstung<sup>1</sup> and Christian Neusüß<sup>1\*</sup>

<sup>1</sup> *Department of Chemistry, Aalen University, Beethovenstrasse 1, 73430 Aalen, Germany*

<sup>2</sup> *Department of Pharmaceutical and Medicinal Chemistry, Friedrich Schiller University Jena, 07743, Jena, Germany*

#### Figure S1

Rhodamine B infusion experiments. Injection of 125  $\mu\text{g/mL}$  Rhodamine B with 100 nL/min via the separation capillary at a distance of 1.0 mm to the emitter tip and electrospray voltage of 1500 V. Pictures edited with high pass filter, desaturation of green and yellow for better visualisation; A: start; B: after 8 seconds; C: after 16 seconds; D: after 24 seconds.

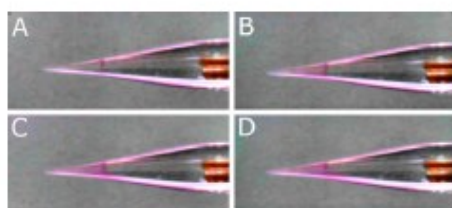
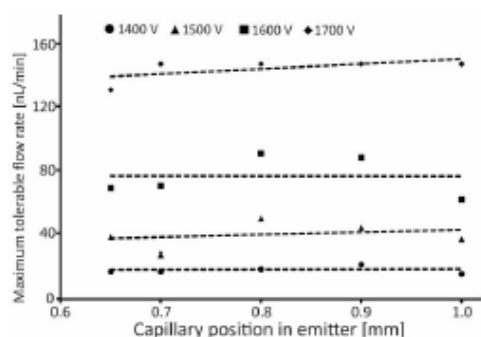


**Figure S2**

Effect of the capillary position in the emitter on the maximum tolerable flowrate at different electro spray voltages.



### Evaluation of Robustness

**Table S1**

Result of ANOVA for the four considered parameters. Given are the p-values for the respective parameter and analyte. Asterisks represent whether amino acids or peptides were used.

<i>m/z</i>		Electrospray Voltage*	Emitter Distance*	Capillary Distance*	Emitter No.**
Amino Acid*	Peptide**				
205.0	585.8	0.91	0.25	0.67	0.02
148.0	653.4	0.70	0.35	0.41	0.11
166.0	395.2	0.43	0.32	0.40	0.07
182.0	547.3	0.56	0.32	0.54	0.48
n.a.	461.7	n.a.	n.a.	n.a.	0.13
n.a.	582.3	n.a.	n.a.	n.a.	0.13

## Supplementary Information

**Figure S3**

95% confidence intervals (averaged over all analytes) of triplicate runs for different parameter settings, to evaluate the robustness of the nanoCEasy interface. For each parameter, values were increased and decreased from the default value in a plausible range for routine application. For evaluation, triplicates with a mixture of four amino acids (a-c) and 6 peptides of a BSA digest (d) were analysed. Peak areas for each analyte were normalised to the average peak area of the respective analyte within the parameter set. For each parameter setting and analyte, the 95% confidence intervals were calculated. For each box, confidence intervals for all analytes were averaged. The grey box represents the mean over all three parameter settings. (a) electrospray voltage, (b) distance between emitter tip and MS orifice, (c) distance of separation capillary and emitter tip, and (d) different emitters of the same size and batch.

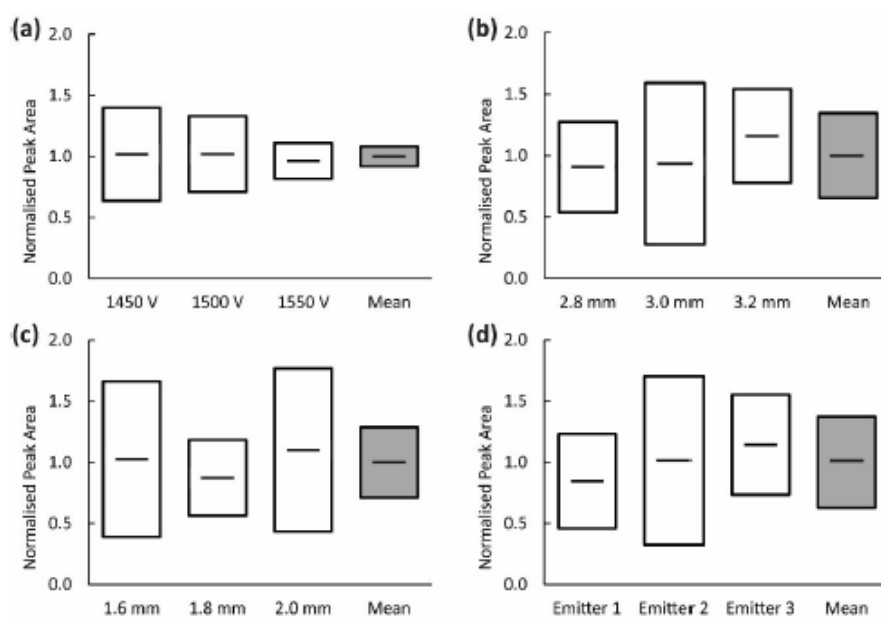
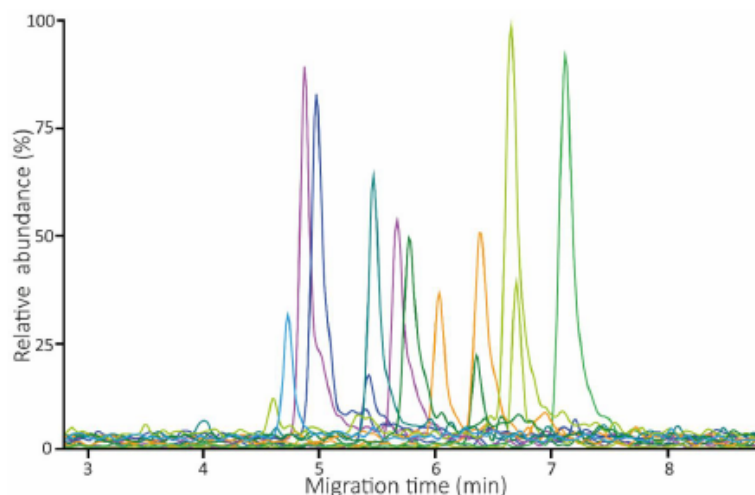


**Figure S4**

CE-MS of BSA digest on a 65 cm FS capillary coupled to the ion trap MS. BGE: 0.2 M FAc, 30  $\mu$ m tip ID emitter. Shown are the EIEs of the 13 most abundant peptides. +30 kV separation voltage.





### Example 1: Trastuzumab Subunit Analysis

#### Preparation of Trastuzumab Subunit Samples

Trastuzumab was digested following an adapted FabRICATOR® instruction protocol (Genovis). Trastuzumab (25 mg/mL) was diluted to a final concentration of 1.5 mg/mL in 40 mM MOPS buffer (pH= 7.3). Prior to incubation at 37 °C for 30 min, 2.2 µL of FabRICATOR enzyme solution was added to 100 µL of mAb solution. Reduction was performed by adding 20 mM DTT to the digested sample and incubating at 57 °C for 20 min. The digested and reduced subunits were stored at -20 °C until use.

#### PEO Coating Procedure

PEO stock solution was prepared by dissolving 100 mg of PEO in 45 mL of water by heating at 95 °C. The PEO coating solution was prepared by adding 0.5 mL of 0.1 M HCl to 4.5 mL of PEO stock solution<sup>1</sup>. Prior to each run, recoating of the capillary was performed by successive rinsing with 1 M NaOH, water and 0.1 M HCl for 3 min, respectively, PEO coating solution for 6 min and BGE for 5 min applying a pressure of 2 bar for all rinsing steps.

#### CE-MS of Antibody Subunits

For the analysis of trastuzumab subunits, the CE system was coupled to the QTOF MS. Separation was performed in a PEO coated capillary with 0.2 M FA as BGE. The sample was introduced by hydrodynamic injection at 50 mbar for 12 s. Separation voltage was set to +20 kV and electrospray voltage was set to 1600 V in positive ion mode. Drying gas flow and temperature were set to 3 L/min and 170 °C, respectively. The scan range was set to 700-3000 *m/z*.

#### Results

To evaluate the applicability of the interface to mAb subunit analysis, trastuzumab was digested with IdeS and reduced to obtain fragments in the size of about 25 kDa (Fc/2, including glycovariants, Fd, and LC). Separation was performed in a neutral (PEO) coated capillary, reducing adsorption of mAb subunits to the inner surface of the capillary. The method repeatability regarding the interface, the coating, and the MS performance was evaluated by five consecutive runs (including recoating of the capillary after every run). Figure S5 shows the extracted ion electropherograms of the most intense species. The observed and calculated masses of the observed fragments are listed in Table S2. Separation was performed in less than

## Supplementary Information

11 min (RSD < 3 % on migration time (n=5)). The major glycoforms observed were G0F, G1F and G2F. Additionally, G0 and G0F-GlcNAc were identified. Low abundant Fc/2 without glycosylation and the Fab fragment could also be detected. RSD of the observed masses (n=5) was in the range of 0.3 ppm to 7.8 ppm (mean = 1.9 ppm). The deviations of the calculated to experimental masses were between -0.5 Da and 0.7 Da. Two additional Fd and underlying LC species observed at higher migration times with a mass shift of +2 Da and a shifted charge envelope towards lower  $m/z$  could be explained by incomplete reduction of one of the two disulfide bridges. These results demonstrate that the nanoCEasy interface combined with the two-capillary approach allows easy (re)coating of capillaries with MS-incompatible reagents without disassembling of the interface. Furthermore, the analytical stability and reproducibility of the interface were clearly shown.

**Table S2**

Result summary of observed and calculated trastuzumab subunit masses.

Species	Glycoform	Exp. Mass [Da] <sup>a</sup>	RSD [ppm] <sup>b</sup>	Calc. Mass [Da] <sup>c</sup>	Deviation [Da]
Fc/2 (S-S) <sub>2</sub>	-	23786.5	1.1	23786.7	-0.2
Fc/2 (S-S) <sub>2</sub>	G0F-GlcNAc	25028.8	7.8	25028.9	-0.2
Fc/2 (S-S) <sub>2</sub>	G0	25086.7	1.4	25086.0	0.7
Fc/2 (S-S) <sub>2</sub>	G0F	25232.0	0.6	25232.1	-0.1
Fc/2 (S-S) <sub>2</sub>	G1F	25394.1	0.6	25394.3	-0.3
Fc/2 (S-S) <sub>2</sub>	G2F	25556.0	1.7	25556.4	-0.4
LC (S-S) <sub>2</sub>	-	23439.0	0.3	23438.9	0.1
Fd (S-S) <sub>2</sub>	-	25379.5	1.0	25379.4	0.1
Fab (S-S) <sub>2</sub>	-	48816.6	4.6	48816.3	0.3
Fd (S-S)	-	25381.0	1.0	25381.4	-0.4
LC (S-S)	-	23440.5	1.0	23441.0	-0.5

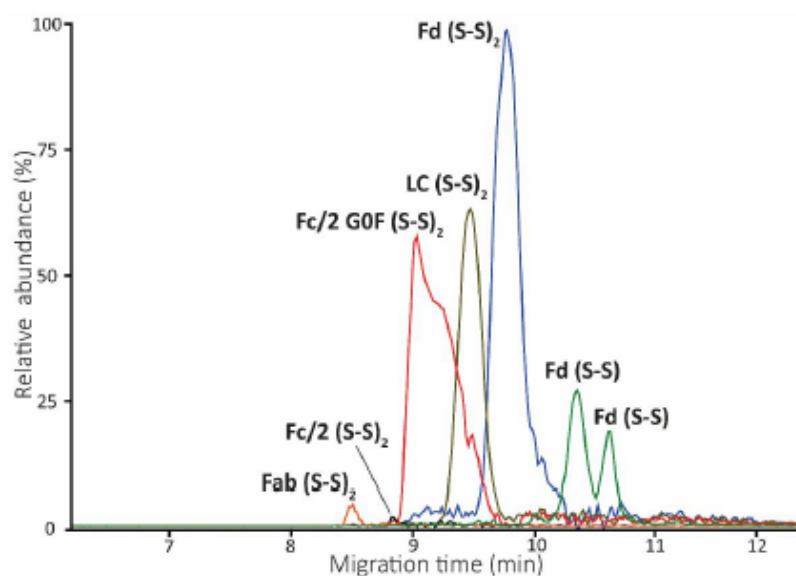
<sup>a</sup> Mean (n=5)

<sup>b</sup> RSD of Exp. Mass (n=5)

<sup>c</sup> Average mass M

**Figure S5**

CE-MS of IdeS digested and reduced trastuzumab subunits on a 65 cm PEO coated capillary coupled to a Bruker QTOF. BGE: 0.2 M FAc, 30  $\mu$ m tip ID emitter. Shown are the EIEs generated by addition of the three most abundant charge states for each species. +20 kV separation voltage.



### Example 2: Hemoglobin Analysis from Dried Bloodspots

#### Preparation of Hemoglobin Samples

Clinical dried blood spot (DBS) samples were leftovers from a previous project and were prepared as described elsewhere<sup>2</sup>. Briefly, DBS samples were prepared by punching out a 3 mm disk on a Whatman cutting mat. Hb was extracted with 100  $\mu$ L deionized water for 30 min under thorough shaking. The resulting solution was centrifuged and subsequently used for analysis.

#### SMIL Coating Procedure

Successive multiple ionic polymer layer (SMIL) coating was prepared according to Stolz et al<sup>2</sup>. Briefly, capillaries were initially flushed for 20 min with 1 M sodium hydroxide, 5 min with water and 10 min with 20 mM HEPES buffer (all flush steps with 2 bar external pressure). Then, the capillary was alternately flushed for 7 min with 3 mg/mL DEAEDq and PMA solutions with a 3 min 20 mM HEPES flush between polycation and polyanion solution. After attachment of the last layer, the capillary was flushed with BGE for 10 min.

#### CE-MS of Hemoglobin

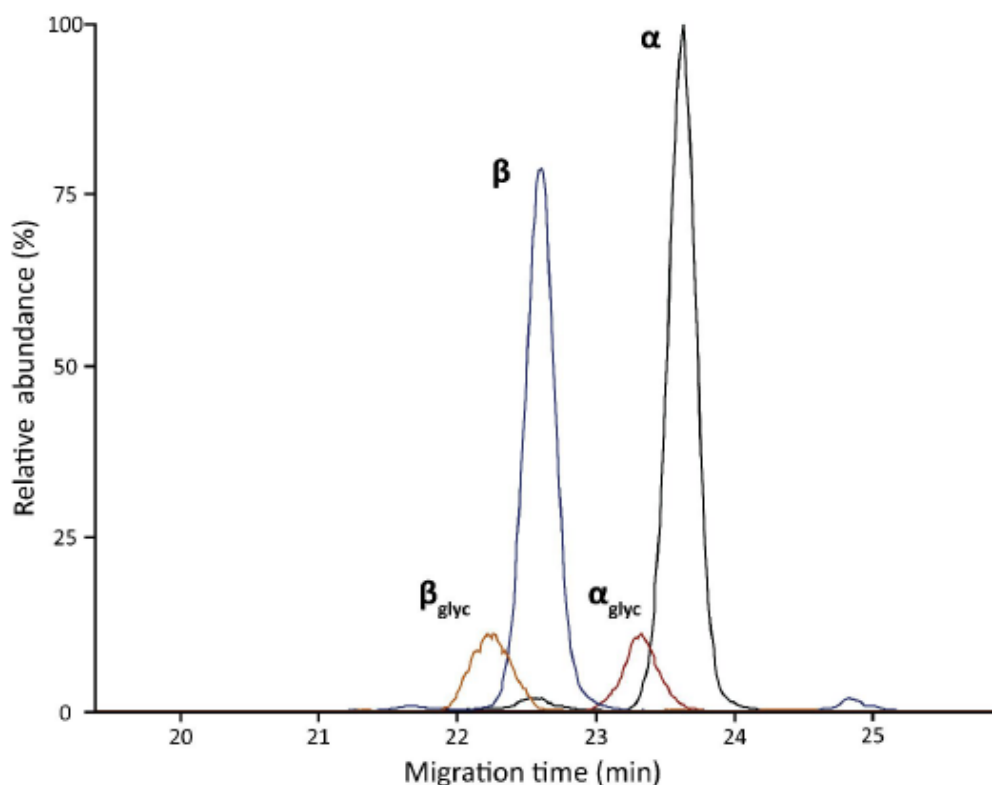
For the analysis of hemoglobin, the CE system was coupled to the Orbitrap MS. Hydrodynamic injection was performed for 8 s at 50 mbar. Separation was performed in 5-layer DEAEDq-PMA coated capillaries at -30 kV with 2 M acetic acid as BGE. Electrospray voltage was set to 1900 V in positive ion mode, the scan range was set to 650-2000  $m/z$  with a resolution of 7500. The active gain control (AGC) target was set to  $1e^6$  with 7 microscans.

#### Results

Besides neutral coatings, ionic coatings are also applied for the separation of intact proteins. In so-called successive multiple ionic polymeric layers (SMIL) coatings, polycations and polyanions are successively attached to the capillary wall. For protein analysis, 5-layer SMIL coatings with a polycationic layer as the last layer are frequently used<sup>3</sup>. Due to the positive charge of the capillary wall and the acidic BGEs used, interactions of the positively charged proteins with the capillary wall are minimised. Furthermore, the coating results in a reversal of EOF, potentially offering high separation power for closely related protein species<sup>4</sup>. Recently, our group developed a CE-MS platform for the separation and characterisation of hemoglobin variants from clinical samples by using such SMIL-coated capillaries<sup>2</sup>. In this study, a coaxial SL interface operating under normal flow conditions ( $> 1\mu\text{L}/\text{min}$ ) was used<sup>5</sup>. To demonstrate the applicability of the nanoCEasy interface to high-EOF systems, hemoglobin extracted from DBS samples were analysed on a 5-layer DEAEDq-PMA coated capillary. With the new interface set-up and optimised parameters for the electrospray voltage (1900 V), stable operation was possible despite the high EOF ( $-4.4 \cdot 10^{-8} \text{ m}^2\text{V}^{-1}\text{s}^{-1}$ ,  $\sim 230 \text{ nL}/\text{min}$ ). As previously reported, separation of the  $\alpha$ - and  $\beta$ -Hb chain, as well as the respective glycosylated variants, was possible. Compared to the SL interface previously used for this application, separation power was comparable. However, application of the nanoCEasy interface resulted, on average, in 6-11 fold increased peak areas (data not shown).

**Figure S6**

CE-MS of hemoglobin chains extracted from clinical DBS samples on a 70 cm DEAE<sub>DQ</sub>-PMA coated capillary coupled to an Orbitrap MS. BGE: 0.2 M FAc, 30  $\mu$ m tip ID emitter. Shown are the EIEs generated by addition of the three most abundant charge states for each chain. -30 kV separation voltage.



## References

- (1) Dadouch, M.; Ladner, Y.; Bich, C.; Larroque, M.; Larroque, C.; Morel, J.; Bonnet, P.-A.; Perrin, C. An in-line enzymatic microreactor for the middle-up analysis of monoclonal antibodies by capillary electrophoresis. *Analyst* **2020**, *145* (5), 1759–1767.
- (2) Stolz, A.; Hedeland, Y.; Salzer, L.; Römer, J.; Heiene, R.; Leclercq, L.; Cottet, H.; Bergquist, J.; Neusüß, C. Capillary Zone Electrophoresis-Top-Down Tandem Mass Spectrometry for In-Depth Characterization of Hemoglobin Proteoforms in Clinical and Veterinary Samples. *Anal. Chem.* **2020**, *92* (15), 10531–10539.
- (3) Nehmé, R.; Perrin, C.; Cottet, H.; Blanchin, M.-D.; Fabre, H. Influence of polyelectrolyte capillary coating conditions on protein analysis in CE. *Electrophoresis* **2009**, *30* (11), 1888–1898.
- (4) Leclercq, L.; Morvan, M.; Koch, J.; Neusüß, C.; Cottet, H. Modulation of the electroosmotic mobility using polyelectrolyte multilayer coatings for protein analysis by capillary electrophoresis. *Anal. Chim. Acta* **2019**, *1057*, 152–161.
- (5) González-Ruiz, V.; Codesido, S.; Far, J.; Rudaz, S.; Schappler, J. Evaluation of a new low sheath-flow interface for CE-MS. *Electrophoresis* **2016**, *37* (7-8), 936–946.

## 9.2 Supplementary information manuscript II

### Supporting Information

**Figure S1**

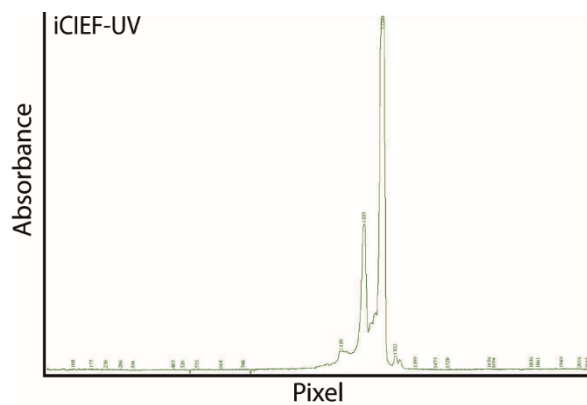


**Figure S1.** iCIEF-UV profile of trastuzumab (1 mg/mL). Focusing voltage: 1500 V (1 min), 3000 V (10 min). UV detection at 280 nm.

## 9.3 Supplementary Information manuscript IV

### Supporting Information

for

# **Two-Dimensional Capillary Zone Electrophoresis-Mass Spectrometry: Intact mAb Charge Variant Separation Followed by Peptide Level Analysis Using In-Capillary Digestion**

Johannes Schlecht<sup>1,2</sup>, Kevin Jooß<sup>3</sup>, Bernd Moritz<sup>4</sup>, Steffen Kiessig<sup>4</sup>, and Christian Neusüß<sup>1\*</sup>

<sup>1</sup>Department of Chemistry, Aalen University, Beethovenstrasse 1, 73430 Aalen, Germany

<sup>2</sup>Department of Pharmaceutical and Medicinal Chemistry, Friedrich Schiller University Jena, 07743, Jena, Germany

<sup>3</sup>Departments of Chemistry and Molecular Biosciences, the Chemistry of Life Processes Institute, and the Proteomics Center of Excellence, Northwestern University, Evanston, IL 60208, USA

<sup>4</sup>F. Hoffmann La-Roche Ltd., Grenzacherstraße 124, 4058 Basel, Switzerland

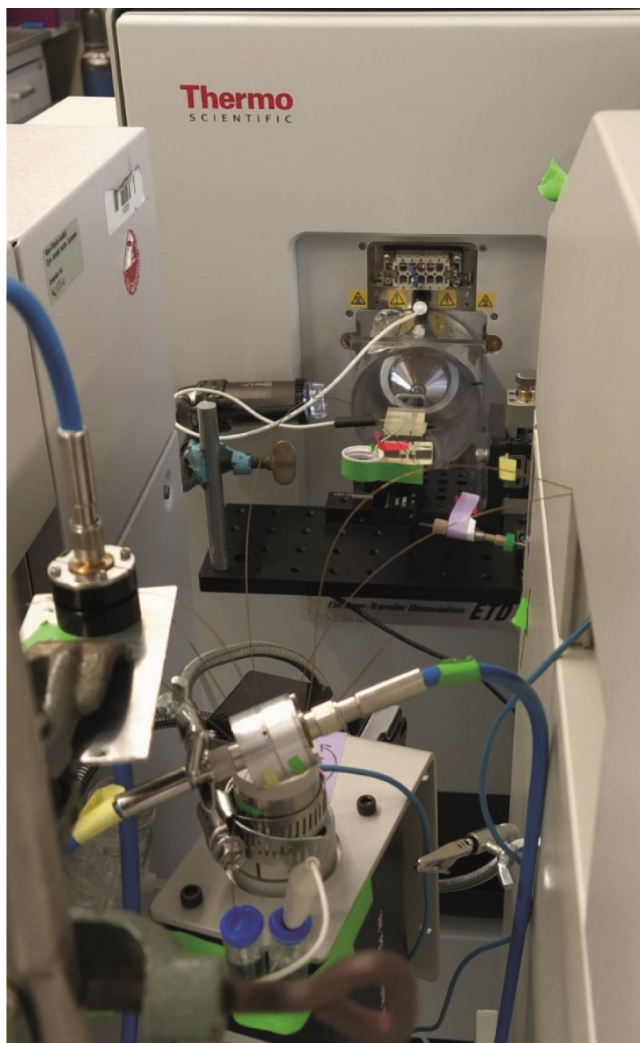


**Figure S1.** Photograph of the 2D-CZE-CZE-MS set-up. Left side: CZE-UV-UV (first dimension) connected to the valve. Bottom foreground: valve and external vials/electrode. Right side: CZE-MS/MS (second dimension) connected to the valve. Background: second dimension coupled to an Orbitrap Fusion Lumos via the *nanoCEasy* interface.

## Supplementary Information

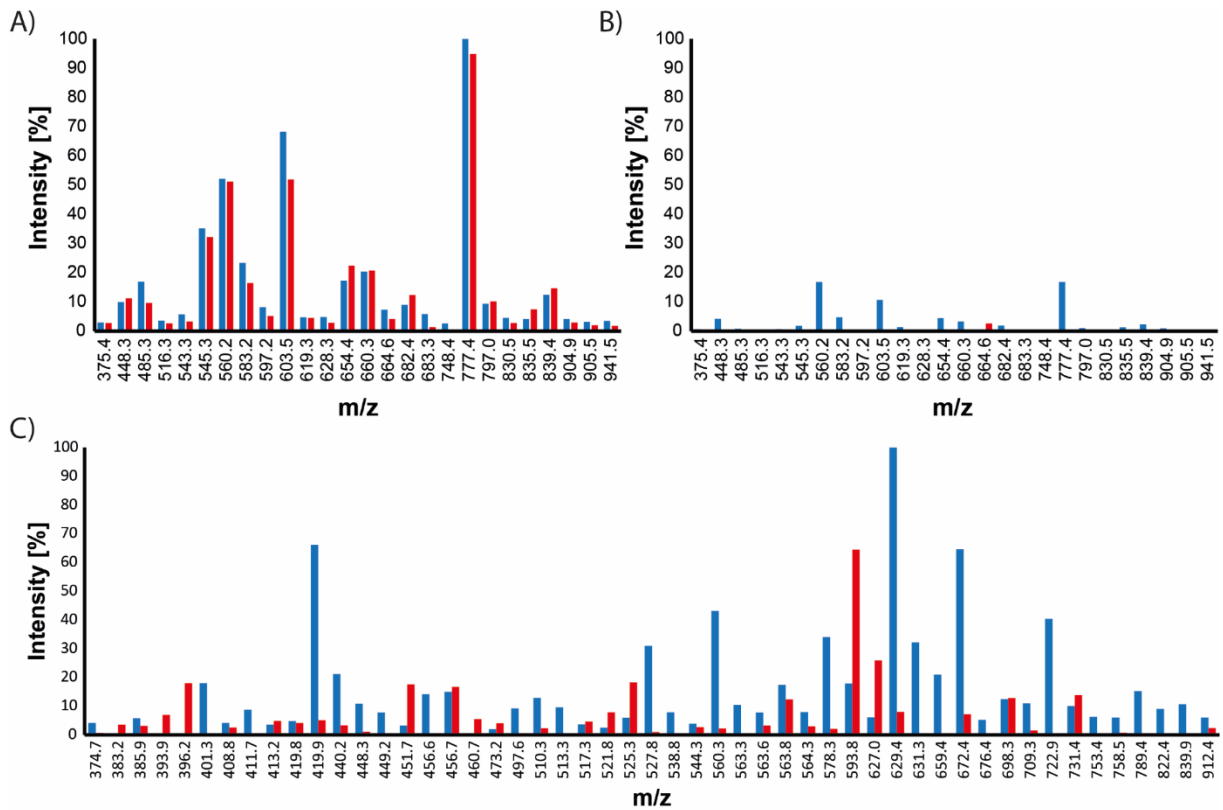


**Figure S2.** Compatibility of trypsin and pepsin with EACA. Blue: 0 mM EACA; Red: 50 mM EACA. **A)** 24 h offline digestion of trastuzumab with trypsin. **B)** 1 h offline digestion of trastuzumab with trypsin. **C)** 1 h offline digestion of trastuzumab with pepsin.



## Supplementary Information

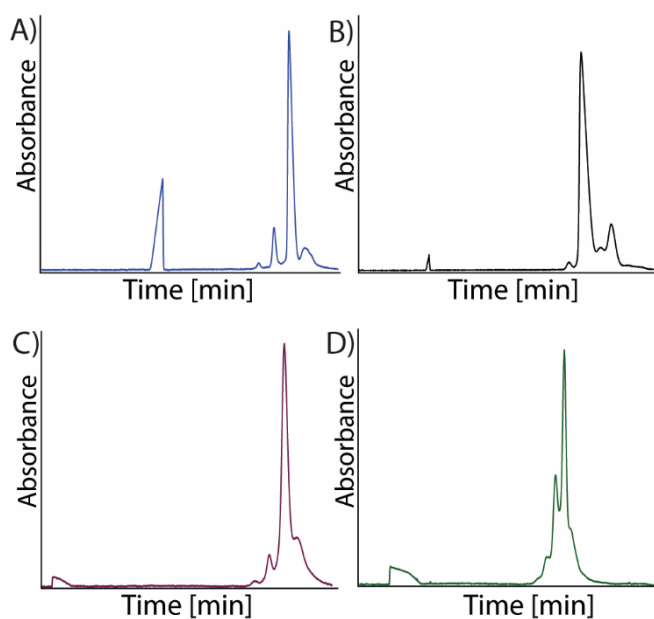


**Figure S3.** CZE(EACA)-UV data of NIST mAb (A), Trastuzumab (B), mAb 3 (C) and mAb 4 (D). 55 (45 +10) cm capillary, 214 nm. BGE: 380 mM EACA, 2 mM TETA, 0.05% HPC, pH 5.7. Injection: 50 mbar for 16 s.

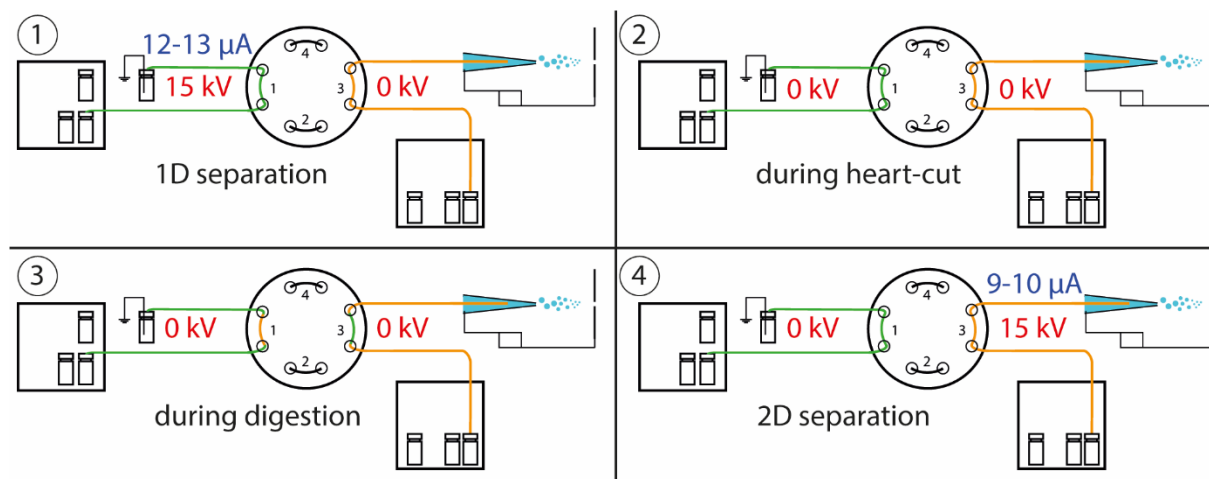
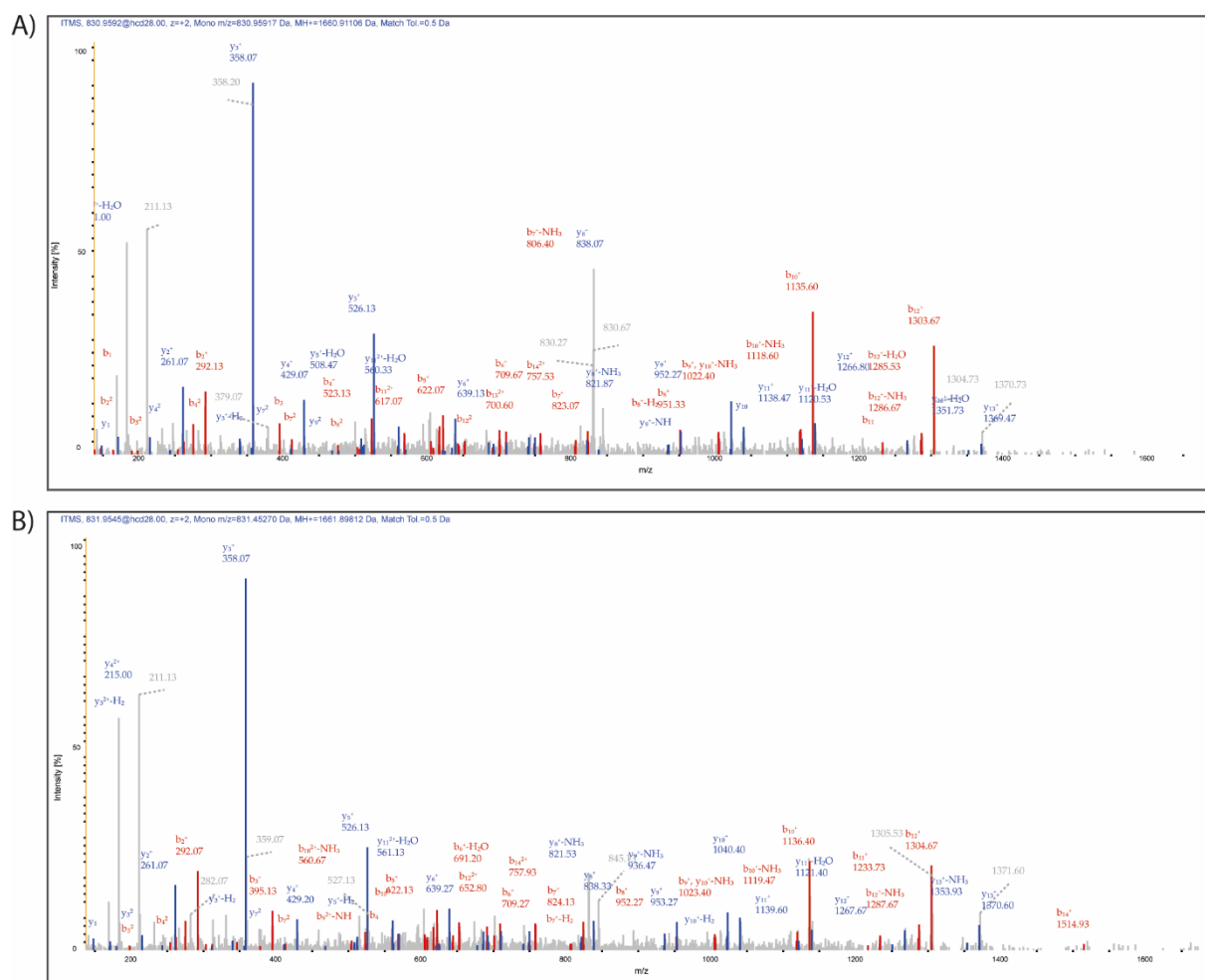


**Figure S4.** Voltage setup and currents during the experiments.

# Supplementary Information



## Supplementary Information

**Table S1** List of identified unique peptides associated with Trastuzumab (main peak) in non-stressed material.

Position	Peptide	Chain	Modification
12-27	SASVGDRVITICRASQ	LC	
55-62	YSGVPSRF	LC	
86-115	YYCQQHYTTPPTFGQGTKVEIKRTVAAPSV	LC	
105-116	EIKRTVAAPSVF	LC	
116-177	VTVSSASTKGPSVFPLAPSSKSTSGGTAALGCLVKDYFPEPVTVSWNSGALTSKVHFFPAVL	HC	
149-175	VKDYFPEPVTVSWNSGALTSKVHFFPA	HC	
149-176	VKDYFPEPVTVSWNSGALTSKVHFFPAV	HC	
183-236	YSLSSVVTVPSSSLGTQTYICNVNHKPSNTKVDKKEPKSCDKTHTCPPCPAPE	HC	
183-237	YSLSSVVTVPSSSLGTQTYICNVNHKPSNTKVDKKEPKSCDKTHTCPPCPAPEL	HC	
267-280	VDVSHEDPEVKFNW	HC	
310-336	TVLHQDWLNGKEYKCKVSNKALPAPIE	HC	Deamidation [N318]
366-375	FSCSVMHEAL	HC	
366-383	FSCSVMHEALHNHHTQKS	HC	
366-389	FSCSVMHEALHNHHTQKSLSLSPG	HC	
367-383	SCSVMHEALHNHHTQKS	HC	

**Table S2** List of identified unique peptides associated with Trastuzumab (acidic peak #2) in stressed material.

Position	Peptide	Chain	Modification
54-85	LYSGVPSRFSGSRSGDFTLTISSLQPEDFAT	LC	
144-153	AKVQWKVDNA	LC	
167-175	DSKDSTYSL	LC	
179-192	LTLKADYEKHKVY	LC	
179-195	LTLKADYEKHKVYACE	LC	
182-195	SKADYEKHKVYACE	LC	
28-46	NIKDTYIHWVRQAPGKGLE	HC	
28-47	NIKDTYIHWVRQAPGKLEW	HC	
34-46	IHWVRQAPGKGLE	HC	
47-56	WVARIYPTNG	HC	Deamidation [N55]
61-68	ADSVKGRF	HC	
116-143	VTVSSASTKGPSVFPLAPSSKSTSGGTA	HC	
118-144	VSSASTKGPSVFPLAPSSKSTSGGTAA	HC	
118-145	VSSASTKGPSVFPLAPSSKSTSGGTAAL	HC	
122-145	STKGPSVFPLAPSSKSTSGGTAAL	HC	
201-236	YICNVNHKPSNTKVDKKEPKSCDKTHTCPPCPAPE	HC	
281-296	YVDGVEVHNAKTKPRE	HC	
310-336	TVLHQDWLNGKEYKCKVSNKALPAPIE	HC	
322-336	YKCKVSNKALPAPIE	HC	Deamidation [N328]
337-368	KTISKAKGQPREPQVYTLPPSREEMTKNQVSL	HC	Deamidation [N364]
380-401	IAVEWESNGQPENNYKTTTPVL	HC	Deamidation [N387]
380-401	IAVEWESNGQPENNYKTTTPVL	HC	
380-407	IAVEWESNGQPENNYKTTTPVLSDGGSF	HC	Deamidation [N387]
380-407	IAVEWESNGQPENNYKTTTPVLSDGGSF	HC	Deamidation [N392]
380-407	IAVEWESNGQPENNYKTTTPVLSDGGSF	HC	
384-401	WESNGQPENNYKTTTPVL	HC	Deamidation [N393]
427-449	SCSVMHEALHNHHTQKSLSLSPG	HC	

## Supplementary Information

**Table S3** List of identified peptides associated with Trastuzumab (main peak) in non-stressed material (sequence from <https://genome.jp/entry/D03257>).

Position	Peptide	Chain	Modification
5-11	TQSPSSL	LC	
12-22	SASVGDRVIT	LC	
12-23	SASVGDRVITC	LC	
12-27	SASVGDRVITCRASQ	LC	
36-46	YQKPGKAPKL	LC	
47-53	LIYSASF	LC	
54-70	LYSGVPSRFSGSRSGTD	LC	
54-84	LYSGVPSRFSGSRSGDFTLTISLQPEDFA	LC	
55-62	YSGVPSRF	LC	
86-112	YYCQQHYTTPPTFGQGTKVEIKRTVAA	LC	
86-115	YYCQQHYTTPPTFGQGTKVEIKRTVAAPSV	LC	
105-116	EIKRTVAAPSVF	LC	
116-122	FIFPPSD	LC	
117-124	FIFPPSDE	LC	
117-126	FIFPPSDEQL	LC	
118-123	IFPPSD	LC	
118-124	IFPPSDE	LC	
118-126	IFPPSDEQL	LC	
120-126	PPSDEQL	LC	
124-132	QLKSGTASV	LC	
126-132	KSGTASV	LC	
133-143	VCLLNFFYPRE	LC	
136-143	LNNFFYPRE	LC	
136-148	LNNFFYPREAKVQW	LC	
140-161	YPREAKVQWKVDNALQSGNSQE	LC	
144-161	AKVQWKVDNALQSGNSQE	LC	
144-154	AKVQWKVDNAL	LC	
149-161	KVDNALQSGNSQE	LC	
162-172	SVTEQDSKDST	LC	
162-173	SVTEQDSKDSTY	LC	
162-175	SVTEQDSKDSTYSL	LC	
162-178	SVTEQDSKDSTYLSST	LC	
173-179	YLSSTL	LC	
180-192	TLSKADYKHKVY	LC	
180-195	TLSKADYKHKVYACE	LC	
182-192	SKADYKHKVY	LC	
196-206	VTHQGLSSPVT	LC	
196-208	VTHQGLSSPVTKS	LC	
196-214	VTHQGLSSPVTKSFNRGEC	LC	
4-11	LVESGGGL	HC	
4-17	LVESGGGLVQPGGS	HC	
4-18	LVESGGGLVQPGGSL	HC	
5-17	VESGGGLVQPGGS	HC	
5-18	VESGGGLVQPGGSL	HC	
10-17	LVQPGGSL	HC	
18-27	LRLSCAASGF	HC	
19-27	RLSCAASGF	HC	
27-36	FNIKDTYIHW	HC	
28-36	NIKDTYIHW	HC	
37-46	VRQAPGKGLE	HC	
37-47	VRQAPGKGLEW	HC	
37-48	VRQAPGKGLEWV	HC	
47-56	WVARIYPTNG	HC	
48-56	VARIYPTNG	HC	
50-56	RIYPTNG	HC	
57-64	YTRYADSV	HC	

## Supplementary Information

60-68	YADSVKGRF	HC	
69-80	TISADTSKNTAY	HC	
72-80	ADTSKNTAY	HC	
84-93	NSLRAEDTAV	HC	
84-91	NSLRAEDT	HC	
94-104	YYCSRWGGDGF	HC	
95-104	YCSRWGGDGF	HC	
96-104	CSRWGGDGF	HC	
105-115	YAMDYWGQGT	HC	
108-115	DYWGQGT	HC	
109-115	YWGQGT	HC	
116-128	VTVSSASTKGPSV	HC	
116-129	VTVSSASTKGPSVF	HC	
116-135	VTVSSASTKGPSVFPLAPSS	HC	
116-144	VTVSSASTKGPSVFPLAPSSKSTSGGTAA	HC	
116-145	VTVSSASTKGPSVFPLAPSSKSTSGGTAAAL	HC	
116-147	VTVSSASTKGPSVFPLAPSSKSTSGGTAAALGC	HC	
116-148	VTVSSASTKGPSVFPLAPSSKSTSGGTAAALGCL	HC	
116-177	VTVSSASTKGPSVFPLAPSSKSTSGGTAAALGCLVKDYFPEPVTVSWNSGALTSVHTFPAVL	HC	
118-129	VSSASTKGPSVF	HC	
122-129	STKGPSVF	HC	
129-145	FPLAPSSKSTSGGTAAAL	HC	
130-135	PLAPSS	HC	
130-145	PLAPSSKSTSGGTAAAL	HC	
130-144	PLAPSSKSTSGGTAA	HC	
130-147	PLAPSSKSTSGGTAAALGC	HC	
130-148	PLAPSSKSTSGGTAAALGCL	HC	
148-158	LVKDYFPEPVT	HC	
149-158	VKDYFPEPVT	HC	
149-160	VKDYFPEPVTVS	HC	
149-175	VKDYFPEPVTVSWNSGALTSVHTFPA	HC	
149-176	VKDYFPEPVTVSWNSGALTSVHTFPAV	HC	
149-177	VKDYFPEPVTVSWNSGALTSVHTFPAVL	HC	
152-158	YFPEPVT	HC	
159-166	VSWNSGAL	HC	
159-173	VSWNSGALTSVHTF	HC	
159-177	VSWNSGALTSVHTFPAVL	HC	
162-173	NSGALTSVHTF	HC	
162-177	NSGALTSVHTFPAVL	HC	
165-177	ALTSVHTFPAVL	HC	
166-177	LTSGVHTFPAVL	HC	
167-173	TSGVHTF	HC	
167-177	TSGVHTFPAVL	HC	
183-188	YSLSSV	HC	
183-236	YSLSSVTVPSSSLGTQTYICNVNHKPSNTKVDKKVEPKSCDKTHTCPPCPAPE	HC	
183-237	YSLSSVTVPSSSLGTQTYICNVNHKPSNTKVDKKVEPKSCDKTHTCPPCPAPEL	HC	
188-195	VTVPSSSL	HC	
188-196	VTVPSSSL	HC	
188-200	VTVPSSSLGTQ	HC	
201-212	YICNVNHKPSNT	HC	
201-237	YICNVNHKPSNTKVDKKVEPKSCDKTHTCPPCPAPEL	HC	
225-237	KTHTCPPCPAPEL	HC	
238-243	LGGPSV	HC	
238-244	LGGPSVF	HC	
244-254	FLFPPKPKDTL	HC	
244-255	FLFPPKPKDTLM	HC	
244-255	FLFPPKPKDTLM	HC	Oxidation [M255]
245-254	LFPPKPKDTL	HC	
245-255	LFPPKPKDTLM	HC	
245-255	LFPPKPKDTLM	HC	Oxidation [M255]
246-255	FPPKPKDTLM	HC	

## Supplementary Information

247-254	PPKPKDTL	HC	
247-255	PPKPKDTLM	HC	
255-263	MISRTPEVT	HC	
255-264	MISRTPEVTC	HC	
256-263	ISRTPEVT	HC	
256-264	ISRTPEVTC	HC	
256-265	ISRTPEVTCV	HC	
256-268	ISRTPEVTCVVVD	HC	
265-277	VVDVSHEDPEVKF	HC	
265-278	VVDVSHEDPEVKF	HC	
265-280	VVDVSHEDPEVKFNW	HC	
266-276	VVDVSHEDPEV	HC	
266-280	VVDVSHEDPEVKFNW	HC	
267-280	VDVSHEDPEVKFNW	HC	
268-278	DVSHEDPEVKF	HC	
268-280	DVSHEDPEVKFNW	HC	
269-276	VSHEDEPEV	HC	
269-278	VSHEDEPEVKF	HC	
269-280	VSHEDEPEVKFNW	HC	
285-296	VEVHNAKTKPRE	HC	
310-316	TVLHQDW	HC	
310-317	TVLHQDWL	HC	
310-321	TVLHQDWLNGKE	HC	
310-336	TVLHQDWLNGKEYKCKVSNKALPAPIE	HC	
310-336	TVLHQDWLNGKEYKCKVSNKALPAPIE	HC	Deamidation [N328]
312-321	LHQDWLNGKE	HC	
313-321	HQDWLNGKE	HC	
315-321	DWLNGKE	HC	
322-336	YKCKVSNKALPAPIE	HC	
325-336	KALPAPIE	HC	
329-336	KVSNKALPAPIE	HC	
337-351	KTISKAKGQPREPQV	HC	
337-359	KTISKAKGQPREPQVYTLPPSRE	HC	
366-375	FSCVMHEAL	HC	
366-383	FSCVMHEALHNHYTQKS	HC	
366-389	FSCVMHEALHNHYTQKSLSLSPG	HC	
367-383	SCVMHEALHNHYTQKS	HC	
369-379	TCLVKGFYPSD	HC	
372-381	VKGFYPSDIA	HC	
382-393	VEWESNGQPENN	HC	
384-393	WESNGQPENN	HC	
384-394	WESNGQPENNY	HC	
384-401	WESNGQPENNYKTTTPVL	HC	
394-401	YKTTTPVL	HC	
395-401	KTTTPVL	HC	
402-407	DSDGSF	HC	
414-425	TVDKSRWQQGNV	HC	
414-426	TVDKSRWQQGNVF	HC	
426-433	FSCVMHE	HC	
426-435	FSCVMHEAL	HC	
426-443	FSCVMHEALHNHYTQKS	HC	
426-449	FSCVMHEALHNHYTQKSLSLSPG	HC	
427-433	SCVMHE	HC	
427-443	SCVMHEALHNHYTQKS	HC	
431-438	HEALHNHY	HC	
431-442	HEALHNHYTQKS	HC	
431-443	HEALHNHYTQKSL	HC	
431-448	HEALHNHYTQKSLSLSPG	HC	
434-443	ALHNHYTQKS	HC	
434-449	ALHNHYTQKSLSLSPG	HC	

## Supplementary Information

436-443	HNHYTQKS	HC
440-449	TQKSLSLSPG	HC
444-449	LSLSPG	HC

**Table S4** List of identified peptides associated with NIST mAb (main peak) in non-stressed material (sequence from NIST Report of Investigation, Reference Material 8671).

Position	Peptide	Chain	Modification
3-13	QMTQSPSTLSA	LC	
6-11	QSPSTL	LC	
8-13	PSTLSA	LC	
12-23	SASVGDRVITIC	LC	
25-39	ASSRVGYMHWYQQKP	LC	
38-53	KPGKAPKLLIYDTSKL	LC	
39-51	PGKAPKLLIYDTS	LC	
45-51	LLIYDTS	LC	
46-53	LIYDTSKL	LC	
49-70	DTSKLAGVPSRFSGSGSSTEF	LC	
54-61	ASGVPSRF	LC	
54-69	ASGVPSRFSGSGSGTE	LC	
62-79	SGSGSGTEFTLTISSLQP	LC	
84-120	TYYCFQGSQYPTFGGGTKVEIKRTVAAPSVFIFPPS	LC	
89-100	QSGYPTFGGG	LC	
115-121	FIFPPSD	LC	
115-124	FIFPPSDEQL	LC	
116-121	IFPPSD	LC	
116-124	IFPPSDEQL	LC	
123-131	QLKSGTASV	LC	
125-131	KSGTASV	LC	
135-142	LNNFYPRE	LC	
139-147	YPREAKVQW	LC	
143-152	AKVQWKVDNA	LC	
143-153	AKVQWKVDNAL	LC	
143-160	AKVQWKVDNALQSGNSQE	LC	
148-153	KVDNAL	LC	
148-162	KVDNALQSGNSQESV	LC	
161-174	SVTEQDSKDYSL	LC	
172-178	YLSSTL	LC	
177-187	TLTSLKADYEK	LC	
178-194	LTLKADYEKHKVYACE	LC	
179-191	TLKADYEKHKVY	LC	
181-191	SKADYEKHKVY	LC	
195-205	VTHQGLSSPVT	LC	
195-213	VTHQGLSSPVTKSFNRGEC	LC	
5-17	RESGPALVKPTQT	HC	
5-19	RESGPALVKPTQTLT	HC	
16-29	QTLTLTCTFSGFSL	HC	
27-34	FSLSTAGM	HC	
28-34	SLSTAGM	HC	
28-35	SLSTAGMS	HC	
35-46	SVGWIRQPPGKA	HC	
35-48	SVGWIRQPPGKALE	HC	
36-46	VGWIRQPPGKA	HC	
36-48	VGWIRQPPGKALE	HC	
51-65	ADIWDDKHKHYNPSL	HC	
53-65	IWWDDKHKHYNPSL	HC	
66-82	KDRLTISKDTSKNQVVL	HC	
70-82	TISKDTSKNQVVL	HC	
83-94	KVTNMDPADTAT	HC	
93-104	ATYYCARDMIFN	HC	

## Supplementary Information

106-128	YFDVWGQGTTVTVSSASTKGPSV	HC	
116-129	VTVSSASTKGPSVF	HC	
116-145	VTVSSASTKGPSVFPLAPSSKSTSGGTAAL	HC	
118-129	VSSASTKGPSVF	HC	
118-144	VSSASTKGPSVFPLAPSSKSTSGGTAA	HC	
118-145	VSSASTKGPSVFPLAPSSKSTSGGTAAL	HC	
118-147	VSSASTKGPSVFPLAPSSKSTSGGTAALGC	HC	
130-144	PLAPSSKSTSGGTAA	HC	
130-145	PLAPSSKSTSGGTAAL	HC	
130-147	PLAPSSKSTSGGTAALGC	HC	
130-148	PLAPSSKSTSGGTAALGCL	HC	
135-142	LNNFYPRE	HC	
135-147	LNNFYPREAKVQW	HC	
148-158	LVKDYFPEPVT	HC	
149-158	VKDYFPEPVT	HC	
159-166	VSWNSGAL	HC	
159-173	VSWNSGALTSGVHTF	HC	
159-177	VSWNSGALTSGVHTFPAVL	HC	
159-182	VSWNSGALTSGVHTFPAVLQSSGL	HC	
162-177	NSGALTSGVHTFPAVL	HC	
165-177	ALTSGVHTFPAVL	HC	
166-177	LTSGVHTFPAVL	HC	
167-177	TSGVHTFPAVL	HC	
178-182	QSSGL	HC	
183-200	YSLSSVTVPSSSLGTQT	HC	
188-196	VTVPSSSL	HC	
188-200	VTVPSSSLGTQT	HC	
189-196	TVPSSSL	HC	
190-196	TVPSSSL	HC	
201-212	YICNVNHKPSNT	HC	
192-200	PSSSLGTQT	HC	
192-206	PSSSLGTQTYICNVN	HC	
225-237	KTHTCPPCPAPEL	HC	
238-243	LGGPSV	HC	
238-244	LGGPSVF	HC	
244-254	FLFPPKPKDNL	HC	
244-255	FLFPPKPKDNL	HC	1xOxidation [M12]
244-255	FLFPPKPKDNL	HC	
245-254	LFPPKPKDNL	HC	
245-255	LFPPKPKDNL	HC	1xOxidation [M11]
245-255	LFPPKPKDNL	HC	
247-254	PPKPKDNL	HC	
247-255	PPKPKDNL	HC	
255-263	MISRTPEVT	HC	
255-264	MISRTPEVTC	HC	
256-265	FPPKPKDNL	HC	
256-263	ISRTPEVT	HC	
256-264	ISRTPEVTC	HC	
256-265	ISRTPEVTCV	HC	
264-268	CVVVD	HC	
265-278	VVDVSHEDPEVKF	HC	
265-280	VVDVSHEDPEVKFNW	HC	
266-276	VVDVSHEDPEV	HC	
266-278	VVDVSHEDPEVKF	HC	
266-280	VVDVSHEDPEVKFNW	HC	
267-280	VDVSHEDPEVKFNW	HC	
268-278	DVSHEDPEVKF	HC	
268-280	DVSHEDPEVKFNW	HC	
269-276	VSHEDPEV	HC	
269-278	VSHEDPEVKF	HC	
269-280	VSHEDPEVKFNW	HC	



## Supplementary Information

281-296	YVDGVEVHNAKTKPRE	HC	
285-296	VEVHNAKTKPRE	HC	
294-305	PREEQYNSTYRV	HC	
304-313	RVVSVLTVLH	HC	
310-314	TVLHQ	HC	
310-316	TVLHQDW	HC	
310-317	TVLHQDWL	HC	
310-321	TVLHQDWLNGKE	HC	
312-321	LHQDWLNGKE	HC	
313-321	HQDWLNGKE	HC	
315-321	DWLNGKE	HC	
318-336	NGKEYKCKVSNKALPAPIE	HC	
322-336	YKCKVSNKALPAPIE	HC	1xDeamidated [N7]
322-336	YKCKVSNKALPAPIE	HC	
325-336	KVSNKALPAPIE	HC	
329-336	KALPAPIE	HC	
337-351	KTISKAKGQPREPQV	HC	
337-359	KTISKAKGQPREPQVYTLPPSRE	HC	
337-368	KTISKAKGQPREPQVYTLPPSREEMTKNQVSL	HC	
352-356	YTLPP	HC	
352-359	YTLPPSRE	HC	
359-367	EMTKNQVSL	HC	
359-368	EMTKNQVSLT	HC	
369-379	TCLVKGFYPSD	HC	
371-379	LVKGFYPSD	HC	
372-379	VKGFYPSD	HC	
372-380	VKGFYPSDI	HC	
372-381	VKGFYPSDIA	HC	
380-401	IAVEWESNGQPENNYKTTTPVL	HC	
380-401	IAVEWESNGQPENNYKTTTPVL	HC	1xDeamidated [N]
380-407	IAVEWESNGQPENNYKTTTPVLDSGFS	HC	
382-393	VEWESNGQPENN	HC	
384-393	WESNGQPENN	HC	
384-394	WESNGQPENNY	HC	
384-401	WESNGQPENNYKTTTPVL	HC	
394-401	YKTTTPVL	HC	
395-401	KTTTPVL	HC	
402-407	DSDGSF	HC	
414-425	TVDKSRWQQGNV	HC	
414-426	TVDKSRWQQGNVF	HC	
426-433	FSCVMHE	HC	
426-450	FSCVMHEALHNHYTQKSLSLSPGK	HC	1xLys-loss [C-Term]
427-433	SCSVMHE	HC	
427-439	SCSVMHEALHNHY	HC	
427-450	SCSVMHEALHNHYTQKSLSLSPGK	HC	1xLys-loss [C-Term]
432-439	HEALHNHY	HC	
432-443	HEALHNHYTQKS	HC	
432-444	HEALHNHYTQKSL	HC	
432-450	HEALHNHYTQKSLSLSPGK	HC	1xLys-loss [C-Term]
434-443	ALHNHYTQKS	HC	
434-450	ALHNHYTQKSLSLSPGK	HC	1xLys-loss [C-Term]
436-443	HNHYTQKS	HC	
436-450	HNHYTQKSLSLSPGK	HC	1xLys-loss [C-Term]
440-450	TQKSLSLSPGK	HC	1xLys-loss [C-Term]
444-450	LSLSPGK	HC	1xLys-loss [C-Term]
445-450	SLSPGK	HC	1xLys-loss [C-Term]

## 9.4 Documentation of contribution

### FORM 2

**Manuscript No. I**

**Short reference** [Schlecht et al. (2021), Anal. Chem.]

#### **Contribution of the doctoral candidate**

Contribution of the doctoral candidate to figures reflecting experimental data (only for original articles):

<b>Figure 1</b>	<input type="checkbox"/> 100% (the data presented in this figure come entirely from experimental work carried out by the candidate)
	<input type="checkbox"/> 0% (the data presented in this figure are based exclusively on the work of other co-authors)
	<input checked="" type="checkbox"/> Approximate contribution of the doctoral candidate to the figure: 50% Brief description of the contribution: development and design of the shown interface parts, interface setup and testing
<b>Figure 2</b>	<input type="checkbox"/> 100% (the data presented in this figure come entirely from experimental work carried out by the candidate)
	<input type="checkbox"/> 0% (the data presented in this figure are based exclusively on the work of other co-authors)
	<input checked="" type="checkbox"/> Approximate contribution of the doctoral candidate to the figure: 50% Brief description of the contribution: support of experimental part, data evaluation, creating figure

**FORM 2**

**Manuscript No. II**

**Short reference** [Schlecht et al. (2023), Electrophoresis]

**Contribution of the doctoral candidate**

Contribution of the doctoral candidate to figures reflecting experimental data (only for original articles):

<b>Figure 1-4</b>	<input checked="" type="checkbox"/>	100% (the data presented in this figure come entirely from experimental work carried out by the candidate)
	<input type="checkbox"/>	0% (the data presented in this figure are based exclusively on the work of other co-authors)
	<input type="checkbox"/>	Approximate contribution of the doctoral candidate to the figure: _____ % Brief description of the contribution: (e.g. "Figure parts a, d and f" or "Evaluation of the data" etc.)

**FORM 2**

**Manuscript No. III**

**Short reference** [Schlecht et al. (2018), Anal. Bioanal. Chem.]

**Contribution of the doctoral candidate**

Contribution of the doctoral candidate to figures reflecting experimental data (only for original articles):

<b>Figure 1-3</b>	<input type="checkbox"/>	100% (the data presented in this figure come entirely from experimental work carried out by the candidate)
	<input type="checkbox"/>	0% (the data presented in this figure are based exclusively on the work of other co-authors)
	<input checked="" type="checkbox"/>	Approximate contribution of the doctoral candidate to the figure: 20% Brief description of the contribution: concepts and integration of figures in the trend article, similar to review article

**FORM 2**

**Manuscript No. IV**

**Short reference** [Schlecht et al. (2023), Anal. Chem.]

**Contribution of the doctoral candidate**

Contribution of the doctoral candidate to figures reflecting experimental data (only for original articles):

<b>Figure 1-5</b>	<input checked="" type="checkbox"/>	100% (the data presented in this figure come entirely from experimental work carried out by the candidate)
	<input type="checkbox"/>	0% (the data presented in this figure are based exclusively on the work of other co-authors)
	<input type="checkbox"/>	Approximate contribution of the doctoral candidate to the figure: _____ % Brief description of the contribution: (e.g. "Figure parts a, d and f" or "Evaluation of the data" etc.)

## 9.5 List of publications and presentations

- 1) **Schlecht J**, Jooß K, Neusüß C (2018) Two-dimensional capillary electrophoresis-mass spectrometry (CE-CE-MS): coupling MS-interfering capillary electromigration methods with mass spectrometry. *Analytical and bioanalytical chemistry* 410(25):6353–6359. <https://doi.org/10.1007/s00216-018-1157-9>
- 2) Stolz A, Jooß K, Höcker O, Römer J, **Schlecht J**, Neusüß C (2019) Recent advances in capillary electrophoresis-mass spectrometry: Instrumentation, methodology and applications. *Electrophoresis* 40(1):79–112. <https://doi.org/10.1002/elps.201800331>
- 3) Römer J, Montealegre C, **Schlecht J**, Kiessig S, Moritz B, Neusüß C (2019) Online mass spectrometry of CE (SDS)-separated proteins by two-dimensional capillary electrophoresis. *Analytical and bioanalytical chemistry* 411(27): 7197–7206. <https://doi.org/10.1007/s00216-019-02102-8>
- 4) **Schlecht J**, Stolz A, Hofmann A, Gerstung L, Neusüß C (2021) nanoCEasy: An Easy, Flexible, and Robust Nanoflow Sheath Liquid Capillary Electrophoresis-Mass Spectrometry Interface Based on 3D Printed Parts. *Analytical chemistry* 93(44):14593–14598. <https://doi.org/10.1021/acs.analchem.1c03213>
- 5) **Schlecht J**, Moritz B, Kiessig S, Neusüß C, (2022) Characterization of Therapeutic mAb Charge Heterogeneity by iCIEF Coupled to Mass Spectrometry (iCIEF-MS). *Electrophoresis* 44(5-6):540-548. <https://doi.org/10.1002/elps.202200170>
- 6) **Schlecht J**, Jooß K, Moritz B, Kiessig S, Neusüß C (2023). Two-Dimensional Capillary Zone Electrophoresis-Mass Spectrometry: Intact mAb Charge Variant Separation Followed by Peptide Level Analysis Using In-Capillary Digestion. *Analytical chemistry* 95(8):4059-4066. <https://doi.org/10.1021/acs.analchem.2c04578>

## List of Publications and Presentations

- 7) Wiesner R, Zagst H, Lan W, Bigelow S, Holper P, Hübner G, Josefsson L, Lancaster C, Lo L, Lößner C, Lu H, Neusüß C, Rüttiger C, **Schlecht J**, Schürle P, Selsam A, van der Burg D, Wang S, Zhu Y, Wätzig H, Sängler-van de Griend C (2023). An interlaboratory capillary zone electrophoresis-UV study of various monoclonal antibodies, instruments, and  $\epsilon$ -aminocaproic acid lots. Electrophoresis. <https://doi.org/10.1002/elps.202200284>

- **International Symposium on Electroseparation and Liquid Phase-Separation Techniques (ITP) 2019**

Presentation title:

Imaged capillary isoelectric focusing coupled to mass spectrometry: online iCIEF-ESI-MS of monoclonal antibodies (mAb)

- **Analytical Technologies Europe (AT Europe) 2020**

Presentation title:

Mass Spectrometric Characterization of iCIEF-separated Antibody Charge Variants

- **International Symposium on Microscale Separations and Bioanalysis (MSB) 2021**

Presentation title:

Peptide Mapping of Charge-based Separated Biotherapeutics by CZE-CZE-MS/MS

- **CE Pharm 2021**

Presentation title:

Peptide Mapping of Charge-based separated Biotherapeutics by CZE-CZE-MS/MS